12-11-2015 12:00 AM

Investigation of Hybrid Foundation System for Offshore Wind Turbine

Ahmed Mohamed Reda Abdelkader, *The University of Western Ontario*

Supervisor: Hesham Elnaggar, *The University of Western Ontario*

A thesis submitted in partial fulfillment of the requirements for the Doctor of Philosophy degree in Civil and Environmental Engineering

INVESTIGATION OF HYBRID FOUNDATION SYSTEM FOR OFFSHORE WIND TURBINE

(Thesis format: Integrated Article)

By

Ahmed Reda Abdelkader

Graduate Program in
Engineering Science
Department of Civil and Environmental Engineering

A thesis submitted in partial fulfillment
of the requirements for the degree of

Doctor of Philosophy
The School of Graduate and Postdoctoral Studies
The University of Western Ontario
London, Ontario, Canada

Abstract

Green energy resources are essential to meet the growing energy demands in the near future while reducing the effects of global warming. Offshore wind energy is one of the main efficient renewable energy sources which drive the ever increasing expansion of offshore wind farms globally. Wind energy technologies are improving making energy production more affordable, which helped Denmark, for example, to produce about 25% of its energy. One of the main challenges for offshore wind projects is the cost of foundation construction, which represents about 40% of the total cost. The investigated hybrid foundation system has the potential to reduce the foundation cost, while meeting the demands for performance and capacity for large wind turbines. The hybrid foundation system comprises a steel pile attached to a concrete plate to increase its lateral and rotational stiffness and capacity.

The main objective of this thesis is to examine the performance of the proposed hybrid system subjected to the environmental loads expected to act on the 5 MW National Renewable Energy Laboratory (NREL) wind turbine. To achieve this objective, both physical and numerical investigations were conducted to address several aspects of the problem. First, wind tunnel tests were performed on a scaled model (with 1:150 ratio) of the 5 MW wind turbine at the Boundary Layer Wind Tunnel Laboratory in Western University. Force balance technique was applied to determine the different base load components under the ultimate wind loading considering different configurations and angles of attack.

A comprehensive parametric study was conducted employing three-dimensional nonlinear finite element models considering different foundations systems installed in sand and subjected to the measured wind loads, along with applicable wave loads for 20m deep water. The foundation

systems included: monopile with diameter of 4 and 6 m and a hybrid system with pile diameter of 4 m attached to a concrete plate with and without ribs and plate diameter was 12 m or 16 m. For all considered foundation systems, the pile embedded depth varied from 8 to 36 m long. Different load combinations were examined for ultimate and serviceability static load cases.

The axial and lateral stiffness and capacity of the different foundation systems were evaluated and compared to lineate the advantageous effect of adding the plate to the monopile. The results demonstrated the superior performance and the higher capacity of the hybrid system and the potential cost savings associated with reducing the required pile diameter to support the 5MW NREL wind turbine. In addition, some guidelines are offered to evaluate the capacity of the hybrid system.

Finally, laboratory tests were conducted on scaled down foundation models under 1 g. The tests were conducted to evaluate the long term performance of the hybrid system under monotonic and cyclic wind loading conditions. Both the lateral and rotational responses of the foundation systems were evaluated under monotonic loading and after 10,000 cycles of loading. The test were able to detect the effect of adding the plate in the hybrid system to study its effect and its increasing in the rocking and lateral capacity. The results from the model tests confirmed the superior performance of the hybrid foundation system in terms of increased lateral and rotational stiffnesses, which is important for performance of supported wind turbines, as well as lateral capacity, which increases the factor of safety against excessive lateral displacement. Furthermore, the results obtained from the tests were employed to develop equations to predict the stiffness of the proposed hybrid foundation system.

Co-Authorship Statement

This thesis has been prepared in accordance with the regulation of paper based format stipulated by the school of Graduate and Postdoctoral Studies at the University of Western Ontario. Some parts of Chapters 3, 4 and 5 of this thesis were published in two conferences and two (FOUR) journal papers. All modeling process, physical testing, data analysis, and writing of initial version of this thesis were carried out by the candidate himself under supervision of his research advisor, Professor Hesham El Naggar. Various version of Chapters 3 to 6 either submitted or will be submitted for possible publication in peer-reviewed journals.

In additions, the following papers have been published:

Abdelkader, A., Aly, Bitsuamlak, G., El Naggar, M.H.(2013)" Experimental Evaluation of Wind Loads for Wind Turbines' Foundation Design", Wind and Structres Journal, Submitted 2013.

A.M. Abdelkader, M. H. El Naggar,(2014)" Performance of Hybrid Foundation System for Offshore Wind Turbines", Geotechnical and Geological Engineering Journal , Submitted 2014.

A.M. Abdelkader, M. H. El Naggar,(2014) "Response of Hybrid Foundation System for Offshore Wind Turbines to the operating loads", EMI2014 Mini-Symposium: Computational Modeling in Civil Engineering, McMaster University, Canada.

A.M. Abdelkader, M. H. El Naggar,(2014) "Simulation of the 5 MW NREL Wind Turbine for Extreme Wind Loads Measurements", EMI2014 Mini-Symposium: Wind Engineering Issues for Low Buildings and Other Structures, McMaster University, Canada.

Ahmed Abdelkader, M. H. Elnaggar (2015)" Effects of Loading on Stiffness and Capacity of Wind Turbine Hybrid Foundation under 1 g Modeling", QeoQuebec 2015, Quebeccity, Canada.

Acknowledgments

The author would like to express his deep appreciation and gratitude to his supervisor, Professors Hesham El Naggar. The research presented in this thesis would not have been possible without his supervision, guidance and constructive advice. Professors Hesham El-Naggar sincere mentorship and friendship provided the author with an enriching personal and professional experience, which shall be acknowledged forever. The author would also like to express his gratitude to Prof. Girma Bitsuamalk for his guidance and support during the wind tunnel testing. His expertise and guidance were instrumental in accomplishing this novel study.

The author would like to thank all his colleagues for their friendship and enjoyable, stimulating discussions. The great assistance from the staff of the University Machine Services (UMS) is acknowledged. The author would like also to thank all the technical and administrative staff at the Department of Civil and Environmental Engineering, the University of Western Ontario, for their continuous help. The author is indebted to Professors Emad Abdel-Glil, Mohamed El Gendy, Hassan Ibrahim and all the civil engineering professors at Port Said University.

The great assistance of Dr. Aly Moussad from Louisiana State University and his help in the Boundary Layer wind tunnel test is appreciated, Dr. Ahmed Soliman from Western University to his great help in structural lab and advising. The author would like to thank the Egyptian people, the Ministry of Higher Education and the Bureau of culture and Educational affairs in Montreal for their financial support of this research during this hard time in our history.

Finally, and most important, the author would like to thank his dear family back home, his father, mother, and sisters for their understanding, continuous support and encouragement throughout the course of this research and through this long period of time.

Table of contents

LIST OF FIGURES

LIST OF TABLES

LIST OF SYMBOLS

wind tunnel parameters

ρ	air density
Area	wind turbine projection area in nature
area	wind turbine projection area in lab
C_D	force and moment coefficients
C_M	moment coefficients
$Force_{full\text{-}scale}$	tower base forces at full-scale
$Force_{lab}$	tower base forces at lab
F	represent frequency in nature
f	represent frequency in lab
L	length in nature
l	*l* are length in lab
$Moment_{full\text{-}scale}$	tower base moments at full-scale
$Moment_{lab}$	tower base moments at lab
T	*T* time in nature
t	time in lab
U	wind speed in nature
u	wind speed in lab
NREL	National Renewable Energy Lablatory

Foundation Parameters

η	Aspect ratio
γ	Soil Unit weight
σ	Vertical stresses
σ'	Effective vertical stresses
v	Poisson's ratio

ϕ	Friction angle of sand
ϕ_{cr}	Critical friction angle
ψ	Angle of dilation
δ	Interface friction angle
a	Dimension less constant
c	Dimension less constant
C	Cohesion of soil
$C1$	Dimension less constant
$C2$	Dimension less constant
α	Empirically determined degradation parameter
$D_{plate}/D_{pl}/B$	Plate diameter
$D_{pile}/Dp/D$	Pile diameter
D_t	Pipe diameter (top part)
E_{pile}/E_p	Pile modules of elasticity
E_{pl}	Plate modules of elasticity
E_s	Soil modules of elasticity
e_{max}	Maximum voids ratio
e_{min}	Minimum voids ratio
e	Eccentricity of moment load
F_y	Steel yield strength
F_c	Concrete strength
G_s	Specific gravity
G	Shear modulus
g	Acceleration
H	Horizontal load
H'	Non dimensional horizontal load
I_{pile} / I_p	Pile moment of inertia

K_s	Lateral earth pressure coefficient
K	System stiffness
K_R	Flexibility factor
K_1	Dimension less constant
K_2	Dimension less constant
K_3	Dimension less constant
L	Pile Length
M	Moment on pile head
N	Number of cycles
N_γ	Bearing capacity factor self weight
N_c	Bearing capacity factor cohesion
N_q	Bearing capacity factor overburden
P_a	Atmospheric pressure
Q	the axial load on the pile
Q_{HSy}	Vertical capacity of hybrid system
$Q_{monoiple}$	Vertical capacity of monopile
Q_{Plate}	Vertical capacity of plate
R_N	Soil reaction modulus in the first cycle
R_0	Soil reaction modulus in the N cycle
u_N	Pile head displacement in the Nth cycle
u_0	Pile head displacement in the first cycle
u	Pile head displacement
θ	Pile head rotation
β	Empirical degradation parameter

CHAPTER ONE

INTRODUCTION

1.1 Background

The increasing energy demands fuels the search for new green energy sources (Lozano-Minguez *et al.*, 2011; Hameed et al., 2011). Wind Energy is one of the widely pursued green and renewable energy sources. In particular, offshore wind farms represent the preferred options in so many places around the world in order to take advantage of high wind intensity and to overcome community problems associated with onshore wind farms. In Europe alone, there are more than 20 major offshore wind farms, with Denmark leading the world with the largest wind energy productivity. In recent years, China has made significant investment in several offshore wind farms. On the other hand, till now there are no major offshore wind farms in North America, especially after the cancellation of several wind farms projects that were planned in Ontario, Canada. Nonetheless, the great lakes location can be considered suitable for offshore wind farms, which should be taken advantage of as it is the case in the Trillium wind power 1 project (Trillium power).

For reliable and efficient design of offshore wind turbines, all environmental loads should be properly evaluated and considered in the design. In addition to wind loads, offshore wind turbines are subjected to additional loads due to waves and currents. Theses loads must be considered when selecting and sizing a suitable foundation system for wind turbines. Usually, sites proposed for

offshore wind farms are located in shallow water to reduce the challenges associated with the design of the turbines foundation system. As the water depth increases, environmental loads acting on the offshore wind turbine increase, and consequently, the cost of the foundation system. The cost of offshore foundations for these developments is a significant ratio of the overall installed costs, amounting to about 35% to 40% (Byrne and Houlsby, 2003; Andrews, 1998). Thus, developing suitable efficient foundation designs is so important to ensure the economic viability of offshore wind turbines.

The engineering expertise in the design and construction of marine structures came mainly from platforms serving in the oil industry. However, there is a major difference between the oil platforms and wind turbines in terms of vertical to horizontal load ratios. This ratio is high for platforms employed in offshore oil production, while it is low in wind turbines foundations, which imposes different demands in their design.

Generally, the preferred foundation type depends on the water depth and the experience of the design engineer with offshore foundations. The most common foundation type for shallow water is the Gravity Base Foundation, which depends on its high own weight (up to 2000 tons) to overcome the lateral loads. These foundations are usually precast concrete constructed onshore then moved to be installed in offshore locations in order to minimize the construction cost. A novel systems for gravity base was presented in Nysted and Thornton bank offshore wind farm (Thomesn et al, 2007) where large hollow gravity bases were casted onshore then moved to offshore to be erected and then filled with backfill material from the site.

Monopile (monopole) foundations are widely used to support offshore wind turbines, e.g. were used in Horns Rev, Denmark, to support 2.3 MW turbines. The monopiles are typically 4 m or

more in diameter and 20 m to 40 m long. The piles are usually hollow steel driven piles connected to the tower by transitional part (Bransby and Randolph, 1998). Suction caissons are another foundation type, which resembles a large upturned bucket. To install a suction caisson, it is lowered to sea bed level, and then the trapped water under it will be sucked by pumps to install the foundation to its final position (Houlsby et al., 2001). Ibsen et al. (2004) presented a new bucket system for 3 MW turbines, which includes rips.

A new hybrid foundation system was proposed as an efficient, economic system that satisfies the requirements of wind turbines under the specified loads (Stone et al., 2007; Newson et al., 2007). El-Marassi *et al* (2008) indicated that the hybrid (caped pile) foundation system enhanced the lateral and axial load capacities and increased lateral stiffness, compared to monopole foundation. They conducted a parametric study covering a range of pile and plate diameter to pile length ratios using 2D and 3D finite element models, and used the results to develop closed form solutions for the capacity of the hybrid foundation using limit equilibrium.

The present study further investigates the performance and capacity of the hybrid foundation system constructed by combining a monopole with a concrete plate. Different configurations of the hybrid system are proposed and investigated in order to provide optimized design to enable reducing the construction and material cost of a new offshore wind turbine foundation. The proposed hybrid system is believed to lower construction cost, while ensuring the same performance of monopiles with larger diameters. It can also be used in upgrading the capacity of existing wind turbines foundations.

1.2 Research Objectives

The aim of this study is to evaluate the performance of the innovative hybrid foundation system that can support 5MW offshore wind turbines considering both the capacity and serviceability requirements. This proposed system combines a steel pile and a concrete plate in order to increase its capacity, especially in lateral and rocking modes. In order to achieve this objective, model 5 MW wind turbine was tested in boundary layer wind tunnel to establish the applicable wind loads. These loads were then applied in numerical and small-scale laboratory investigations to evaluate the performance of different foundation system of 5 MW wind turbines.

The measurable objectives associated with the proposed study program are as follows:

- Provide detailed base loads based on 5 MW NREL wind turbine to be used in the study of offshore wind turbine foundations.
- Undertake a ‘proof of concept’ or feasibility study of a novel foundation system to support laterally loaded structures.
- Evaluate the performance of the proposed 'hybrid' systems under different loading conditions.
- Develop guidelines for the design of hybrid foundation systems at different variables, while taking account of the influence of the relative geometry of the constituent.

1.3 Methodology and Novelty of Approach

In this thesis, numerical and experimental investigations are conducted to evaluate the performance of the hybrid foundation system under various vertical, horizontal and moment loading combinations. Wind tunnel tests have been conducted to determine the different base loading components of offshore wind turbine base loads in the Boundary Layer Wind Tunnel at Western University, Canada, based on 5 MW NREL (National Renewable Energy Laboratory) wind turbine. Extensive finite element analyses were performed using the commercial software package ABAQUS (Hibbitt et al., 2008) are used to provide interpretation of the behavior of the hybrid foundation system and to further elucidate the findings through parametric analysis. Furthermore, the numerical results are backed up by the results of experimental testing on scaled physical model foundations under 1 g conditions.

1.4 Thesis Outline

The remainder of this thesis is divided into five main chapters.

Chapter 2 comprises a comprehensive literature review on the behavior of conventional onshore and offshore shallow and deep foundations under combined vertical, horizontal and moment loading.

Chapter 3 discusses the loads that act on the foundation from both the wind and the waves. It presents the wind tunnel tests conducted to determine the foundation loads at the base of a 5MW NREL (National Renewable Energy Laboratory) by using force balance techniques.

Chapter 4 presents a parametric study using three-dimensional nonlinear finite element models employing the computer program ABAQUS to investigate the performance of hybrid foundation systems as well conventional foundations subjected to static loads representing the operational loads level. It investigates the foundations responses including lateral and vertical displacements and rotation considering different load combinations. The foundation systems considered in the analysis include monopoles with 4 and 6 m diameter and the hybrid system with monopole of 4 m diameter and concrete plate with and without ribs with diameter of 12 and 16 m. The parametric study examined the effect of the pile length on the serviceability of both monopoles and hybrid foundations.

Chapter 5 evaluates the ultimate capacity of the considered foundation systems and the maximum stresses in their structural components. The ultimate wind loads established from the wind tunnel tests were used to represent the extreme loading conditions acting on the foundation system. Diffenet load combinations were considered in the analysis.

Chapter 6 describes the monotonic and cyclic load tests conducted in the laboratory investigation to examine the comparative performance of the hybrid systems and monopoles. The test was carried out under 1 g with scaling laws to study the effect of stiffness change under long term cyclic loads. The results from the study demonstrate the relative advantage of the hybrid system over the monopoles in terms of lateral displacement and rotation.

Chapter 7 summarizes the main findings of this research and provides recommendations for future studies and research.

1.5 References

Andrews, R. N. L. (1998). Environmental Regulation and Business "Self-Regulation." Policy Sciences, 31(3): 177-197

Byrne, B.W. and Houlsby, G.T. (2003), “Foundations for Offshore Wind Turbines”, Philosophical Transactions of the Royal Society of London, **A**(361), 2909-2930.

El-Marassi M, Newson T, El-Naggar H and Stone KJL. (2008). Numerical modelling of the performance of a hybrid monopiled-footing foundation. Proceedings of the 61st Canadian Geotechnical Conference, GeoEdmonton 2008. Edmonton, (Paper No. 480), 97 – 104.

Hameed, Z., Vatn, J. and Heggset, J. (2011), “Challenges in the reliability and maintainability data collection for offshore wind turbines“, Renewable Energy, **36**(8), 2154-2165.

Hibbitt, Karlsson, and Sorensen, Inc. (2008), “ABAQUS/Standard User’s Manual”. Hibbitt, Karlsson, and Sorensen, Inc., Pawtucket, RI.

Houlsby G.T. and Byrne B.W. (2001) "Novel Foundations for Offshore Wind Farms", Research Proposal to EPSRC (August 2001), Department of Engineering Science, Oxford University.

Houlsby G.T. and Byrne B.W. (2001) “Assessing Novel Foundation Options for Offshore Wind Turbines", Department of Engineering Science, Oxford University.

Houlsby, G.T. and Byrne, B.W. (2000) “Suction Caisson Foundations for Offshore Wind Turbines and Anemometer Masts”, Wind Engineering, Vol. 24, No. 4, pp 249-255.

Ibsen, L.B. and Brincker, R. (2004) “Design of New Foundation for Offshore Wind Turbines”, Proceedings of the 22nd International Modal Analysis Conference (IMAC), Detroit, Michigan, 2004

Lozano-Minguez, E., Kolios, A.J., Brennan, F.P. (2011), "Multi-criteria assessment of offshore wind turbine support structures", Renewable Energy, 36(11), 2831-2837

Stone, K., Newson, T. and Sandon, J. (2007). An Investigation of the Performance of a 'Hybrid' Monopile-Footing Foundation for Offshore Structures. In Proceedings of the 6th International Offshore Site Investigation and Geotechnics Conference, London, UK, 391-396.

Jorn H. Thomsen, Torben Forsberg, Robert Bittner (2007) " Offshore Wind Turbine Foundations - The COWI Experience", Proceedings of the 26th International Conference on Offshore Mechanics and Arctic Engineering, San Diego, California, USA.

CHAPTER TWO

LITERATURE REVIEW

The increasing demands on energy combined with the stringent environmental requirements drive the pursuit to new green energy technology. Wind energy is one of the proposed green energy sources, especially through mega offshore wind farms. With the trend of more powerful wind turbines in offshore environment, the foundation are subjected to a complex load combination including large horizontal forces and moments including the torque moment due to the 3D twisting in the blade of the wind turbine. In addition, they are subject to wave, current and accidental loads.

Engineering experience with foundations for the offshore structures was derived mainly from the oil industry. However, there is a major difference between foundations supporting oil platforms and wind turbines due to the difference in horizontal to vertical loads ratio. For wind turbine foundations, this ratio is much higher, which requires different foundation systems to support the large horizontal forces and associated large moments. On the other hand, for more than two decades of offshore wind turbines farms, the available experience and expertise and advent of innovative powerful equipment enabled the installation of suitable foundations for the proposed area. Considering the wind loads from the turbine and the water level at the installation site, different foundations options become more economically viable. Generally, shallow foundations are considered first as gravity base with small water depth (Fig. 2-1a). For larger water depth, deep foundation systems are used involving large diameter steel piles (Fig. 2-1b). For deep waters, suction caissons and tetrapod foundations or even floating foundation systems are used (Fig. 2-1c).

New techniques in offshore wind turbines foundations are required to reduce the high construction cost that is up to 40% of the total cost (*Houlsby et al.,* 2001**).** Wind turbine foundations for onshore or offshore structures received comprehensive attention recently in an effort to develop more economical and reliable solutions for this complicated engineering problem. Offshore foundation systems in particular are subject to additional forces and installation cost due to their marine environment.

Hybrid foundation is an innovative system, which comprises a combination of shallow foundation and pile. Initial investigations of hybrid foundations were conducted by *Carder* and *Brooks* (1993) and *Carder et al.* (1999). The concept in such system is to strengthen the pile by attaching a plate at its head to enhance its lateral and rotational resistance. Thus, the system performs similar to a retaining wall with stabilizing base (*Carder* and *Brooks,* 1993; *Carder et al.,* 1999). *Powrie* and *Daly* (2007), *Poulos* and *Randolph* (1983) studied the effect of the pile cap under vertical loads while Kim et al. (1979), *Mokwa* (1999) and *Maharaj* (2003) studied its effect under lateral loads.

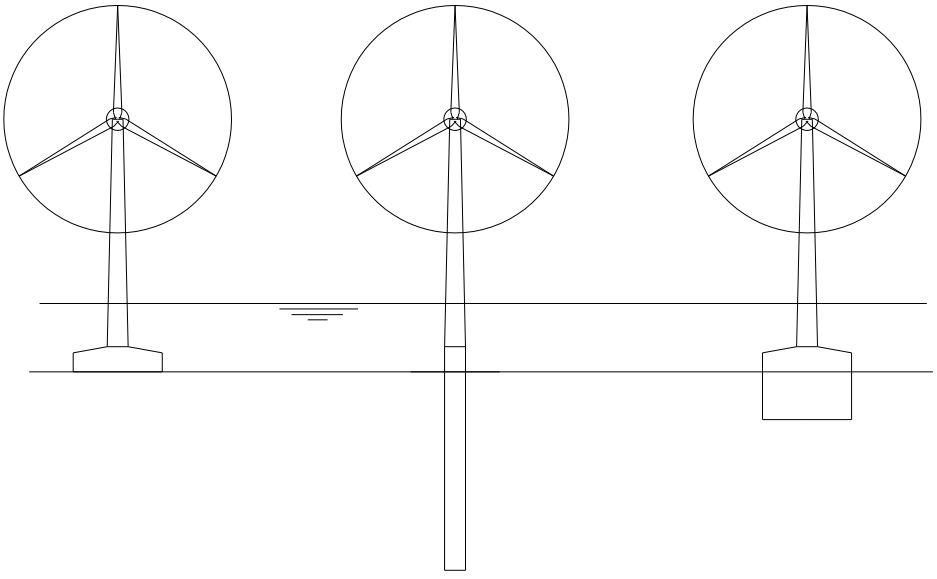

Fig. 2.1 Offshore foundations

2.1. OFFSHORE FOUNDATIONS

Offshore foundations experience was derived mainly from more than a century of developments in offshore oil and gas industry. Most of these projects entail high initial cost invested in the oil production tower, including its foundation. This is different than the case in wind farms, where the cost of the wind turbine itself is relatively not high. Additionally, the difference in the load combinations considered for both types of projects are different, which require different concept, i.e., maximizing lateral and rotational stiffness in case of wind turbine foundations as opposed to maximizing axial capacity for oil production towers. Even though wind energy sector is growing fast in North America, experience with major offshore wind power just started with the construction of Block Island Wind Farm in 2015 for five 6 MW turbines.

Therefore, there is a need to develop innovative and economically viable foundation option to sustain the expected growth in offshore wind projects in North America. A recent study by the National Renewable Energy Laboratory (NREL, 2010) indicated that the cost per MW of power from wind turbines decreases as the size of the turbine rotor increases (Fig. 2-2). This finding promotes the development of larger wind turbines, which means growing demands on foundation systems to meet the increased wind loads at an acceptable cost level. At the same time, the cost of the conventional foundations (gravity base and monopoles) increases substantially as the water depth increases (Fig. 2-3). The work presented here is focussed on a foundation system that is safe and economic for large wind turbines. The hybrid foundation system was examined by *El Marassi* (2011), which involved the development of limit equilibrium solutions for its capacity. He conducted 2D and 3D finite element models for the hybrid system, but considered the concrete plate to be rigid.

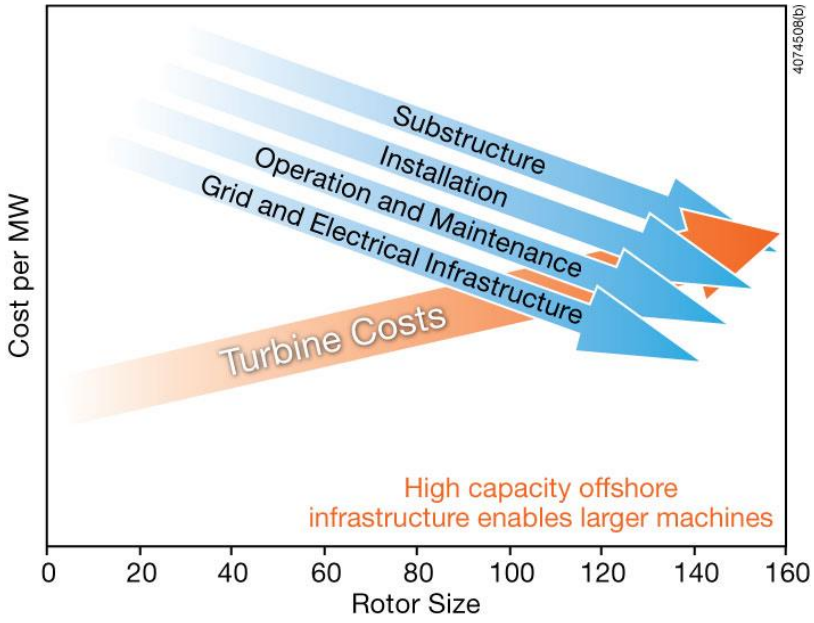

Fig. 2.2 Relation between turbine size and the cost (NREL report September 2010)

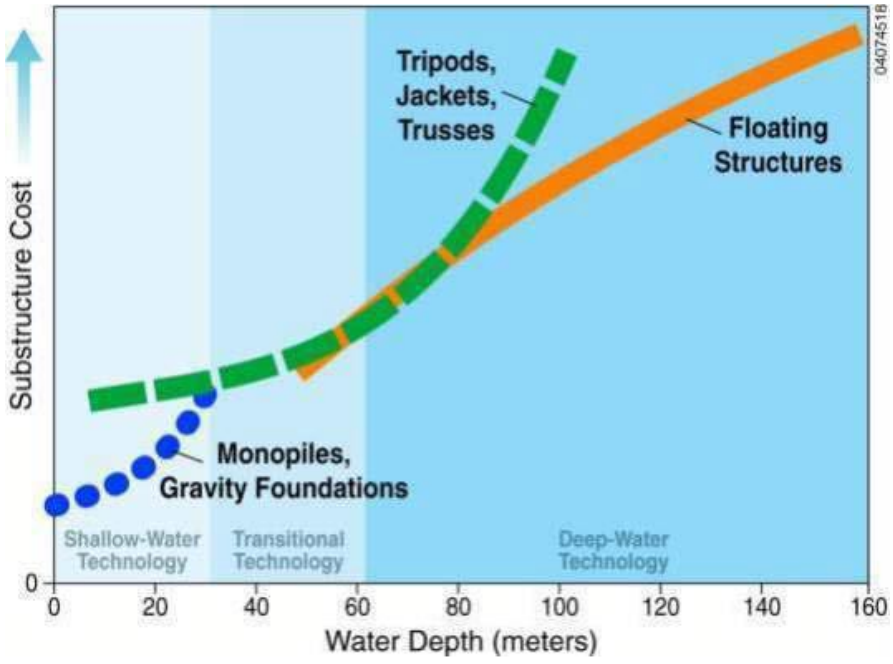

Fig. 2.3 Cost of offshore wind turbine substructures with water depth (NREL report September 2010, Dolan 2004)

2.1.1. *Gravity Base Foundations*

The gravity base foundation is the most common foundation type for shallow water (*Malhotra*, 2007) and is widely used in the Baltic and North Sea in Europe. These foundations resist lateral and overturning forces by the action of its own weight. They are usually constructed onshore then removed to be installed in offshore locations in order to minimize the high cost of offshore construction. On the other hand, they require a large barge system for its transportation, which increases the construction cost. With the increase of water depth, the use of gravity base foundations will not be sufficient due to the need for more weight to resist the lateral forces. An example for such large gravity base is the foundations employed at a depth of over 27 meters at The Thornton Bank Wind Farm, Belgium, as reported by *Houlsby et al.* (2001). The typical configuration of the Gravity base foundation can be seen in **Figure 2.4.**

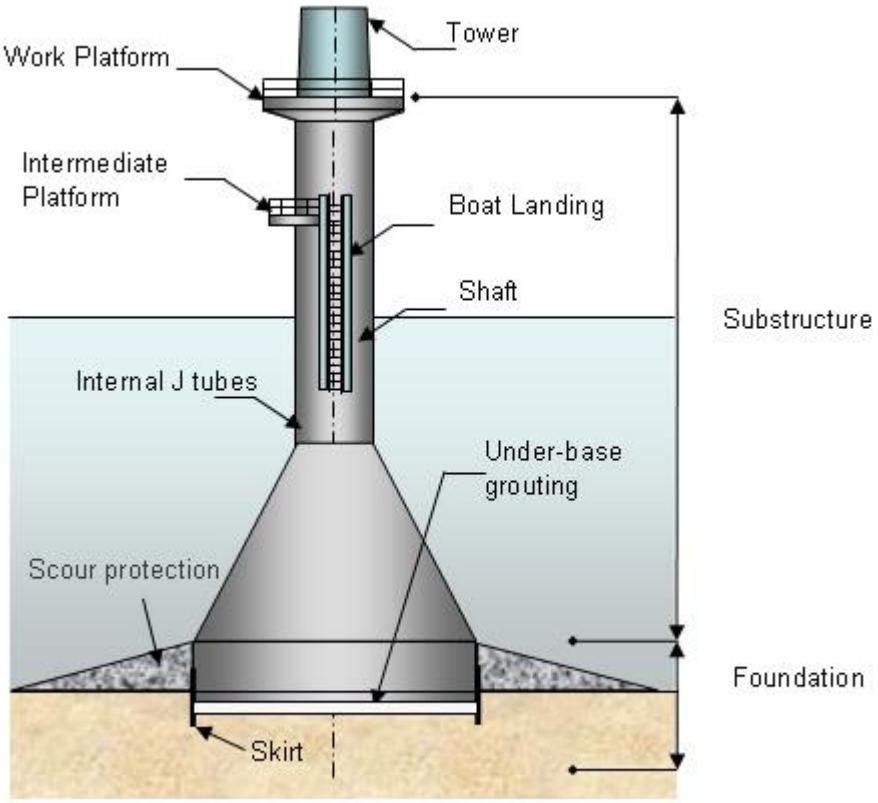

Fig. 2.4 Typical Gravity base foundation (Garrad Hassan And Partners LTD).

The main parameters involved in the design of gravity base foundations design are its diameter and height. The performance of the foundation may be improved by adding ballast after the construction. With increasing water depth, it is not practical to use gravity base due to the high construction cost associated with the higher overturning moments it experiences, which require special construction preparation such as replacement of the bed soil with coarse material. *Zaaijer (2003)* indicated that the gravity base itself can be under massive heave forces.

2.1.2. *Monopile Foundations*

Monopile foundations are widely used for shallow water. Monopiles were used in both the Horns Rev, Denmark, and London Array wind farm, United Kingdom. The piles are typically 4 m in diameter or more (up to 6 m) and 20 m to 40 m long. A typical configuration of monopole foundation is shown in **Figure 2.5**. The piles are usually hollow steel piles that will be driven by a specialized barge with upending and pile driver tools, which leads to high construction cost. In addition, the increase in pile length will cause substantial increase in the installation cost which is already high (*Houlsby et al.*, 2001). **Figure 2.6** shows the transportation process of the pile foundation and the installation method as driven pile.

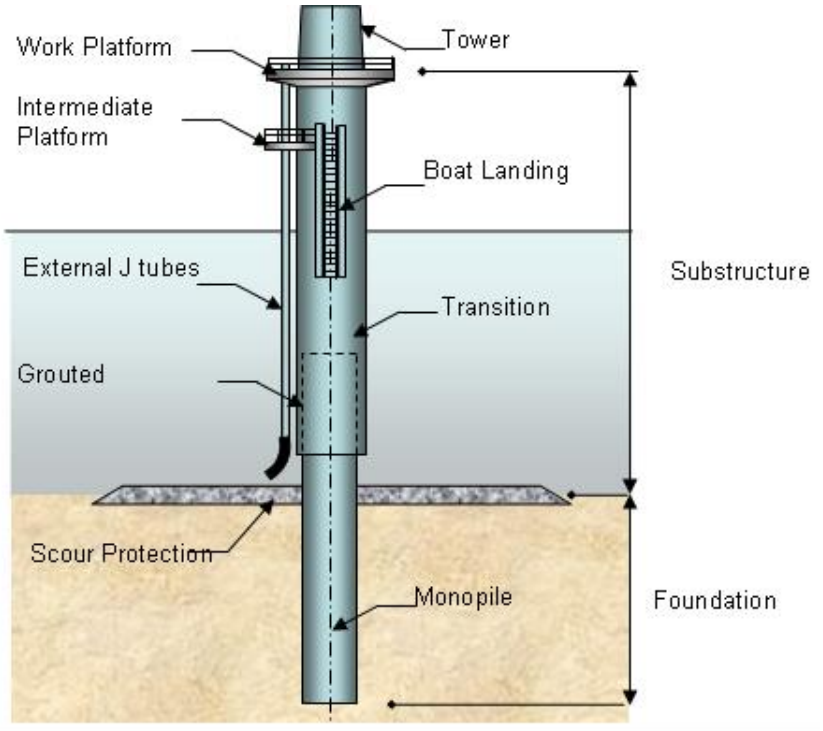

Fig. 2.5 Typical Monopile foundation (Garrad Hassan And Partners LTD).

(a) Monopile installation

(b) Piles transportation.

(c) Pile connections

Fig. 2.6 Monopile installation method (Donde Energy).

The ductility of monopile systems can affect the serviceability limits of the wind turbines, but at the same time dampens the wind loads (*Malhotra*, 2007). Under cyclic loading, pore water pressure can be generated around the pile, which can reduce the effective confining pressure and the shear force around the pile causing increasing in the vertical settlement of the system (*Malhotra*, 2007).

2.1.3. Suction Caissons

Suction caissons are gaining popularity as a foundation system for offshore wind turbines, especially in intermediate deep water installations. It is a large upturned bucket, which will be

lowered to sea bed level in intermediate depth water, and then the trapped water beneath it will be sucked by pumps to install the foundation to its final position. The advantages of this method are saving material and simple installation procedure. However, with the increase of water depth it loses its advantages. This system was used at the Frederikhavn project, Denmark (*Houlsby et al.*, 2001).

2.1.4. Overview and Comparison of Foundations

It is important to study different types of offshore foundations before choosing the suitable one. Generally there are some of major factors control this such as the water depth that lead to starting with gravity base then the monopile. And method of construction, finally the most important factor is the cost. Table 2.1 shows a comparison between different types of offshore foundations.

Table 2.1: Investigation of Offshore Foundations types (after *Bryne* and *Houlsby*, 2006)

Type of Foundation	Size (m)	Weight (ton)	Typical water depth (m)
Gravity Base	12-15	500-1000	0-15
Monopile	3-6	175-350	0-30
Monopile with Guy Wires	3-6	175-350	20-40
Tripod	15-20	125-150	20-40
Braced frame with Multiple Piles	15-20	200-400	20-50
Suction Buckets	10-20	150-400	0-30
Tension leg Platform	10-20	100-400	>50

2.2. BEHAVIOR OF SINGLE PILES UNDER LATERAL LOADS

Offshore pile foundations are usually subjected to lateral loads combined with moment. Under extreme wind loading conditions, the offshore foundation experience large lateral displacement, which can impact the performance of the wind turbine. Both the ultimate capacity and serviceability of the pile foundation must be studied to ensure satisfactory performance of the wind turbine.

2.2.1. Nonlinear Response of Piles

For large displacements, piles behave in a nonlinear fashion. The finite element method can handle nonlinearity but the solution is very costly and can be inaccurate (Trochanis et al., 1988; Maheshwari et al., 2004; Bentley and El Naggar, 2000). A practical model for nonlinear analysis is the lumped mass model in which the soil stiffness and damping are discretized and represented by isolated springs and dashpots. Such models are popular in offshore technology where large displacements are expected. El Naggar and Novak (1995b, 1996) developed a nonlinear lumped mass analysis and used it to model the piled foundations of offshore towers, and El Naggar and Bentley (2000) further developed it by incorporating dynamic p-y curves. Mostafa and El Naggar (2002) developed a model for the nonlinear analysis of the lateral response of piles and Mostafa and El Naggar (2004) used it to analyze the response of offshore towers wave and current loads. El Naggar et al. (2005) extended the approach for the analysis of the seismic response of offshore towers.

2.2.1.1. Analytical methods of predicting lateral deflection of single pile

For predicting the lateral displacement of the pile (*p-y*) curves can be used it was presented by API (American Petroleum Institute) and DNV as the pile is analyzed as an elastic beam that transfer the load by linear and nonlinear springs along the pile. Winkler approach as subgrade reaction method for solving the p-y curve where the soil is modeled as springs. *Matlock and Reese* (1960) defined the spring stiffness E_s as

$$E_s = \frac{-p}{y} \qquad \textbf{Eq. 2.1}$$

For beam on elastic foundation *Hetenyi* (1946) proposed solution as:

$$E_{pile} I_{pile} \frac{d^4 y}{dx^4} + Q \frac{d^2 y}{dx^2} + E_s y = 0 \qquad \textbf{Eq. 2.2}$$

Where E_{pile} is the modules of elasticity of the pile, I_{pile} is the moment of inertia of the pile cross section, Q is the axial load on the pile, x is the pile depth, E_s is is the modules of elasticity of the soil and y is the lateral displacement of the pile. Based on this solution *Reddy* (1993) presented the following equation for piles under lateral loads.

$$\frac{d^4 y}{dx^4} + \frac{E_s}{E_{pile} I_{pile}} = 0 \qquad \textbf{Eq. 2.3}$$

2.2.2. Ultimate Lateral Load Resistance of Single Piles

For piles under lateral loads the calculation of ultimate loads were studied by different methods such as *Broms* (1964) where a disruption of soil resistance was used to calculate ultimate lateral loads by static equilibrium equations. *Poulos* and *Davis* (1980) studied the behavior of piles under lateral loads. *Hansen* (1961), *Felming et al.* (1992) studied nonlinear behavior of piles installed in

cohesionless soil. *Zamri et al* (2009) investigated numerically the behavior of single pile under pure lateral and combined loadings by using 3D finite element analysis. *Phanikanth et al* (2010) examined the failure mechanisms and behavior of lateral loaded pile foundations found that the pile behavior depends on its characteristic length. *Zadeh et al* (2011) presented two case studies: the first involves the behavior of piles under lateral load on sand and clay soils and soil layered system; and the second case examines the behavior of piles under vertical and lateral loading.

2.2.3. Ultimate Lateral Load Resistance of Hybrid Foundation

El Marassi et al (2008) proposed a hybrid foundation system composed of gravity base with central monopile. Their finite element analysis showed that the interaction between the two foundation components results in high lateral load resistance as well as enhanced rocking capacity. Based on the results of the finite element analysis, they developed a limit equilibrium solution for predicting the capacity of the hybrid foundation.

2.3. EXPERIMENTAL STUDIES ON RESPONSE OF PILES

Various types of pile tests piles are conducted to validate and calibrate the available methods of analysis. They differ according to the size of the piles and the test medium and technique employed. The main types are described below.

2.3.1. FULL SCALE LOAD TEST

In these tests, full scale piles are installed in the natural deposit. The main advantages of this technique are that natural soil response is examined and unobstructed wave propagation is allowed.

However, the cost of carrying this type of tests is substantial. Experimental studies that fall in this category include Tuzuki et al. (1992), Mizuno and Iiba(1992), Hakulinen (1991), Kobayashi et al. (1991), Musser (1996), Masuda et al. (1986), Kobori et al. (1991), Crouse and Cheang (1987) and El-Marsafawi et al. (1992), Elkasabgy and El Naggar ( ) and Elsharnouby and El Naggar (). In addition, the different methods available in the literature to establish the *p-y* curves for piles installed in saturated and unsaturated sand (*Bhushan et al.*, 1981; *Bhushan and Askari*, 1984) are based on full-scale load test results.

2.3.2. Prototype Field Tests

Field experiments with small prototype pile are easier and less expensive to conduct while still allow for unobstructed wave propagation. The work by Novak and Grigg (1976), Novak and El-Sharnouby (1984), El-Marsafawi et al. (1992) and Burr et al. (1997) fall in this category. Even though field testing of large piles is more costly and challenging to conduct, it provides more valuable and relevant data.

2.3.3. Centrifugal Modelling

In this technique, a small scale model of the pile is installed in a small container filled with sand or remolded clay, which would be mounted on a centrifuge. At the operating speed, the model is exposed to centrifugal forces far in excess of the gravity force, making it possible to reproduce prototype gravity-induced stresses in soil in the small scale model. Thus, confining stress is identical in both the prototype and model soils, and consequently the stress-strain relation is the same in both the prototype and the model. *Scott et al*. (1977, 1982), Prevost and *Scanlan* (1983) and *Ting and Scott* (1984) described experimental studies using this technique.

2.3.3. Small Scale Laboratory Tests

These tests are conducted with very small model piles in test bins or tanks. The small scale laboratory tests are popular because they are inexpensive, easy to organize and independent of the weather. There deficiencies are the difficulty in modelling an undisturbed natural deposit, and achieving meaningful confining pressure. Different solutions were proposed and implemented to alleviate these difficulties; however, they cannot be eliminated. Experiments reported by *Kana et al.* (1986) fall in this category.

Soil liquefaction in offshore wind turbine foundation was studied by *Stahlmann* et al. (2005). L *Le Blanc* (2010) investigated the long term cyclic loading for monopiles using 1 g test to examine the stiffness change with number of loadings. *Hellmigk* (2012) modeled monopile behaviour in Ottawa sand, in attempt to simulate offshore wind turbine foundation. *Joonyong et al.* (2012) presented test setup that was used successfully to evaluate the lateral behaviour for offshore wind turbine foundations, which involved a steel container with 1.20×1.00×1.00 m internal dimensions. Another technique for 1-g modeling was presented by *Altee et al. (*1994), which involves calculating stress and strain within the soil by considering rigid pile behaviour.

2.4. REFERENCES

DNV-OS-J101, "Design of Offshore Wind Turbine Structures" technical report. SEPTEMBER 2011.

DNV-OS-J101, Offshore Standard, (2011), "Design of Offshore Wind Turbine Structures", Electronic Version available at http://www.dnv.com/ (On Jan. 25, 2013).

IEC 61400-3, "International Standard**",** Edition 1.0 2009-02.

API RP2A. (2000). Recommended Practice for Planning, Designing, and Construction Fixed Offshore Platforms-Working Stress Design. Washigton D.C. :American Petroleum Institute.

Ahmed Yehia Abd Elaziz" Performance Of Hollow Bar Micropiles Under Axial And Lateral Loads In Cohesive Soils", 2012.

El Sharnouby, M. 2012. " Monotonic And Cyclic Behaviour Of Steel Fibre-Reinforced And Frp-Steel Fibre-Reinforced Helical Pulldown Micropiles", Ph.D thesis, University of Western Ontario.

Bentley, K.J. and El Naggar, M.H., 2000. Numerical analysis of kinematic response of piles. Canadian Geotechnical Journal, Vol. 37, No. 6, pp. 1368-1382

Broms, b. B. (1964a). Lateral Resistance of Piles in Cohesive Soils. ASCE Journal of the soil Mechanics and foundation Division Proceedings (JSMFD), 90 SM2, 24-63

Broms, b. B. (1964b). Lateral Resistance of Piles in Cohesionless Soils. ASCE Journal of the soil Mechanics and foundation Division Proceedings (JSMFD), 90 SM3, 123-156.

Brinch Hansen, J. (1961). The ultimate resistance of rigid piles against transversal forces. The Danish Geotechnical Institute Bulletin 12, 5-9.

Bhushan K., and Haley, S. C., (1980)."Development of Computer Program Using P-Y Data from Load Test Results for Lateral Load Design of Drilled Piers" a research report prepared for Woodward-Clyde Consultants Professional Development Committee, San Francisco, California.

Bhushan, K., and Askari, S., (1984). "Lateral Load Tests on Drilled Pier Foundations for Solar Plant Heliostats" Laterally Loaded Piles, ASTM STP 835, James A. Langer, Ed., American Society of Testing and Materials, pp. 141-155.

Bhushan, K., Lee, L. J., and Grime, D. B., (1981). "Lateral Load Tests on Drilled Piers in Sand" Proceedings of a Session on Drilled Piers and Caissons, sponsored by the Geotechnical Engineering Division at the ASCE National Convention, St. Louis, Missouri, pp. 131-143.

Bhushan, K., Haley, S. C., and Fong, P. T., (1979). "Lateral Load Tests on Drilled Piers in Stiff Clays" Journal of the Geotechnical Engineering Division, ASCE, Vol. 105, No. GT8, Proc. Paper 14789, pp. 969-985.

Byrne, B.W. and Houlsby, G.T. (2003) "Foundations for Offshore Wind Turbines", Philosophical Transactions of the Royal Society of London, Series A, Vol. 361, December, pp 2909-2930.

Carder, D. R. and Brookes, N. J. (1993). Discussion in the Retaining structures (ed.C. R. I. Clsyton), pp.498-501. London: Thomas Telford.

Crouse, C.B. and Cheang, L., 1987. Dynamic testing and analysis of pile-group foundation. Geotechnical Special Publication No. 11, ASCE, pp. 79-98.

El Marassi, M. (2011). Investigation of Hybrid Monopile Foundation system. PhD thesis, University of Western Ontario. Canada.

El Marassi et al, "An investigation of the use of a bearing plate to enhance the lateral capacity of monopile foundation", Frontiers in offshore Geotechnics II- Gourvenec & White (eds), pp 623-628, 2011.

El Marassi et al, "Numerical modeling of the performance of a hybrid monopiled-footing foundation", GeoEdmonton, pp97-104, 2008.

El Naggar, M.H. and Bentley, K.J., 2000. Dynamic analysis for laterally loaded piles and dynamic p-y

curves. Canadian Geotechnical Journal, Vol. 37, No. 6, pp. 1166-1183.

Elkasabgy, M. and El Naggar, M.H. 2015. Axial compressive response of large-capacity helical and driven steel piles in cohesive soil. Canadian Geotechnical Journal, Vol. 52, No. 2, pp. 224-243.

El Sharnouby, M.M. and El Naggar, M.H. 2012. Field investigation of axial monotonic and cyclic performance of reinforced helical pulldown micropiles. Canadian Geotechnical Journal, Vol 49, No. 5, pp. 560-573.

El Naggar, M.H., Shayanfar, M.A., Kimiaei, M., and Aghakouchak, A.A. 2005. Simplified BNWF model for nonlinear seismic response analysis of offshore piles. Canadian Geotechnical Journal, Vol. 42, No. 2, pp. 365-380.

Fleming, W. G. K., Weltman, A. J., Randolph, M. F., and Elson, W. K. (1992). Piling engineering. Surrey University Press, London.

Hakulinen, M. 1991. Measured full-scale dynamic lateral pile responses in clay and in sand. Proceedings of 2nd International Conference on Recent Advances in Geotechnical Earthquake Engineering and Soil Dynamics, University of Missouri at Rolla, Rolla, MO, pp. 201-206.

Hellmigk, K., (2012), "development of a 1g model pile test facility for offshore wind turbines". Master thesis, University of Rhode Island.

Hetenyi, M. (1946). Beams on Elastic Foundation. Ann Arbor, The University of Michigan Press.

Houlsby G.T. and Byrne B.W. (2001) "Novel Foundations for Offshore Wind Farms", Research Proposal to EPSRC (August 2001), Department of Engineering Science, Oxford University.

Houlsby G.T. and Byrne B.W. (2001) " Assessing Novel Foundation Options for Offshore Wind Turbines", Department of Engineering Science, Oxford University.

Houlsby, G.T. and Byrne, B.W. (2000) "Suction Caisson Foundations for Offshore Wind Turbines and Anemometer Masts", Wind Engineering, Vol. 24, No. 4, pp 249-255.

Heidari, M, El Naggar, M. H., Jahanandish, M., and Ghahramani, A. 2014. Generalized cyclic p-y curve modeling for analysis of laterally loaded piles. Journal of Soil Dynamics and Earthquake Engineering. Vol. 63 (1), pp. 138-149.

Houlsby, G.T. (2003) "Modelling of Shallow Foundations for Offshore Structures", Invited Theme Lecture, Proc. International Conference on Foundations, Dundee, 2-5 September, Thomas Telford, pp 11-26.

Kana, D. D., Boyce, L. and Blayney, G. W., 1986. Development of a scale model for the dynamic interaction of a pile in clay. Journal of Energy Resources Technology, ASME, Vol. 108, pp. 254-261.

Kim, J. B., Singh, L. P., and Brungraber, R. J. (1979). Pile Cap Soil Interaction from Full Scale Load Tests. ASCE Journal of geotechnical and Enviromental Engineering, 105 (5):643-653.

Kobayashi, K.Yao, S. and Yoshiada, N., 1991. Dynamic compliance of pile group considering nonlinear behaviour around piles. Proceedings of 2nd International Conference on Recent Advances in Geotechnical Earthquake Engineering and Soil Dynamics, University of Missouri at Rolla, Rolla, MO, pp. 785-792.

Kobayashi, K.Yao, S. and Yoshiada, N., 1991. Dynamic compliance of pile group considering nonlinear behaviour around piles. Proceedings of 2nd International Conference on Recent Advances in Geotechnical Earthquake Engineering and Soil Dynamics, University of Missouri at Rolla, Rolla, MO, pp. 785-792.

Gadre, A. and Dorby, R. (1998). Laateral Cyclic Loading Centrefuge Tests on Square Embedded Footing, ASCE Journal of geotechnical and Enviromental Engineering, 124 (11): 1128-1138.

Maharaj, D. K. (2003). Load-Deflection Response of Laterally Single Pile by Nonlinear Finite Element Analysis. EJEC.

Maheshwari, B.K., Truman, K.Z., El Naggar, M.H. and Gould, P.L. 2004. 3D nonlinear analysis for seismic soil-pile-structure interaction. Soil Dynamics and Earthquake Engineering, vol. 24, No. 4, pp. 343-356.

Masuda, K., Saseki, F., Urao, K. Veno, K. and Miyamoto, Y. 1986. Simulation analysis of forced vibration test of actual pile foundation by thin layer method. Proceedings of Annual Meeting of Arch. Inst. Of Japan, Architectural Institute of Japan.

Matlock, H., and Reese, L. C. (1960). Generalized solutions for laterally loaded piles. ASCE Journal of Soil Mechanics and Foundations Division, 86(SM5), 63-91.

Malhotra, S. (2007). Design and Construction Considerations for Offshore Wind Turbine Foundations. In proceedings of the 26th International Conference on Offshore Mechanics and Arctic Engineering, San Diego, California.

Mizuno, H. and Iiba, M., 1992. Dynamic effects of backfill and piles on foundation impedance. Proceedings of 10th World Conference on Earthquake Engineering, Madrid, Spain, Vol. 3, pp. 1823-1828.

Mokwa, R. L. (1999). Investigation of the Resistance of Pile Caps to Lateral Loading. PhD thesis, Virginia Polytechnic Institute, Blacksburg, Virginia.

Mostafa, Y.E. and El Naggar, M.H. 2002. Dynamic analysis of laterally loaded pile groups in sand and clay. Canadian Geotechnical Journal, Vol. 39, No. 6, pp. 1358-1383.

Mostafa, Y.E. and El Naggar, 2004. Response of fixed offshore platforms to wave and current loading including soil-structure interaction. Soil Dynamics and Earthquake Engineering, Vol. 24, No. 4, pp. 357-368.

Musser, S.C., 1996. Utah DOT's testing program to determine the soil-structure interaction of pile groups under lateral loads. Proceedings of 4th Caltrans Seismic Research Workshop, California Department of Transportation, Sacramento, 1996

Powrie, W. and Daly, M. P. (2007). Centrifuge Modeling of embedded Retaining Wall with Stabalizing bases. Geotechnique, 57(6), 485-497.

Poulos, H. G. and Randolph, M. F. (1983). Pile Group Analysis: A Study of Two Mehtods. ASCE Journal of Geothechnical Engineering, 109 (3): 355-372.

Prevost, J. H. and Scanlan, R. H. 1983. Dynamic soil-structure interaction: centrifugal modelling. Journal of Soil Dynamics and Earthquake Engineering, Vol. 2, No. 4, pp. 212-221.

Poulos, H.G. and Davis, E.H., (1974). Elastic Solutions for Soil and Rock Mechanics. John Wiley and Sons, New York.

Poulos, H.G. and Davis, E.H., (1980). Pile Foundation Analysis and Design. John Wiley and Sons, New York.

Reddy, J. N. (1993). An Introduction to the Finite Element Method. 2nd edition, McGraw-Hill. Inc., NY.

Scott, R. F., Ting, J. and Lee, J., 1982. Comparison of centrifuge and full-scale dynamic pile tests. Proceedings of International Conference on Soil Dynamics and Earthquake Engineering, Southampton, Vol. 1, pp. 299-309.

Sheta, M. and Novak, M., 1982. Vertical vibration of pile groups. Journal of the Geotechnical Engineering Division, ASCE, 108 (GT4), 570-590.

Tuzuki, M., Inada, O. and Yamagishi, M., 1992. Field testing and analysis of dynamic loaded pile group. Proceedings of 10th World Conference on Earthquake Engineering, Madrid, Spain, Vol. 3, pp. 1787-1790.

Ting, J. M. and Scott, R. F., 1984. Static and dynamic lateral pile group action. Proceedings of 8th World Conference on Earthquake Engineering, San Francisco, Vol. III, pp. 641-648.

Zaaijer, M.B. (2003). Comparison of monopile, tripod, suction bucket and gravity base design for a 6 MW turbine. In Proceedings of the European Seminar on Offshore Wind energy in Mediterranean and Other European Seas, OWEMES-2003, Naples, Italy.

Zamri et al (2009), “Lateral Behavior of Single Pile in Cohesionless Soil Subjected to Both Vertical and Horizontal Loads”, European Journal of Scientific Research, ISSN 1450-216X Vol.29 No.2 (2009), pp.194-20

CHAPTER THREE

FOUNDATION DESIGN LOADS FOR 5 MW NREL OFFSHORE WIND TURBINE

This chapter attempts to overcome the lack of existing a guideline for loads calculation on offshore wind turbine for foundation design. Extreme wind loads for the foundation design based on a 5 MW NREL (National Renewable Energy Laboratory) offshore wind turbine were estimated at tower's base as shear and moments by using wind tunnel test. The results were compared with limited NREL results which were achieved by FAST (Fatigue, Aerodynamics, Structures, and Turbulence) program. Wave loads for this foundation were taken from NREL/TP-5000-48191 Technical report for 20 [m] water depth. In addition, the results presented in the current work provide useful information for the design of offshore wind turbine foundations.

3.1. INTRODUCTION

Offshore wind power industry is growing fast (Lozano-Minguez, 2011; Hameed *et al.*, 2011; Oh *et al.*, 2012). Initial sites proposed for offshore wind farms are usually located in shallow water which raises interests about the design of the turbines foundation system. The cost of offshore foundations for these developments is a significant ratio of the overall installation cost, it is about 35% (Byrne *et al*., 2003), and so the development of suitable designs for the foundations is essential. The engineering expertise in the design and construction of marine structures came mainly from platforms in the oil industry, but generally there is a major difference between the platforms and wind turbines in vertical to horizontal load ratio. As in oil platforms the vertical

loads are much bigger. The literature has less guidance for the evaluation of wind-induced loads that can be used for the design of the offshore wind turbines foundation system. Basically, there are three sources of information: (1) small-scale experimental studies, (2) theoretical/numerical studies and (3) field and full-scale measurements.

Small-scale experimental studies: Experimental studies for wind load estimation at the base of wind turbines were carried out on a 1:50 scale model for several 5 MW floating offshore wind turbines (FOWT) in a wave tank under combined wind and wave loading at the Maritime Research Institute Netherlands (MARIN) (De Ridder *et al.*, 2011). Model scale experiments at the Ocean Basin Laboratory in Trondheim in order to validate the motion characteristics of the HYWIND concept (the world's first full-scale floating wind turbine, Hywind being assembled in the Åmøy Fjord near Stavanger, Norway in 2009, before deployment in the North Sea) under coupled wave and wind loads for a floating wind turbine was conducted by (Skaare *et al.*,2007).

Theoretical/numerical studies: A typical turbine loading on the mast as a function of wind speed is given by (Dominique *et al.*, 2009). This information is used to understand the force and moment the turbine will exert on the top of the foundation column. In a report published by NREL/TP-500-38060 (2009) all load data for 5 MW NREL (National Renewable Energy Laboratory), as a reference wind turbine, were presented. The report includes rotor thrust and torque for different wind speeds. Jonkman and Musial (2010) presented foundation shear and moment loads for both rigid and flexible pile foundation systems. NREL/CP-5000-54221 (2012) presented wind turbine loads as shear and moment for floating 5 MW NREL wind turbine to verify the scaling laws.

NREL/CP-500-47536 (2010) provides an estimation of seismic load demand for a wind turbine in the time domain. LeBlanc (2008) presented typical loads for 2 MW wind turbine where it was applied on a mono pile to study the response of stiff piles in sand to long-term cyclic lateral loading. LeBlanc (2010) used wind turbine loads to study the response of stiff piles to random two-way lateral loading. Ragan and Manuel (2007) presented statistical extrapolation methods for estimating wind turbine extreme loads for a utility-scale 1.5 MW turbine sited in Colorado to compare the performance of several alternative techniques for statistical extrapolation of rotor and tower loads. Loads of 450 kW wind turbine to study the load bearing capacity and the seismic behavior of a prototype steel tower were presented by (Bazeos *et al.*, 2002). Henrik Svensson (2010) presented typical wind loads for wind turbines situated on the west coast of Sweden. DNV (2011) and IEC(2009) codes present guide lines for calculating wind climate parameters, loads, load effects and load factors for offshore wind turbines.

Field study: Full-scale data on two blades were collected by NREL/TP-500-29955 (2001) to provide information needed to quantify the full-scale three-dimensional (3-D) aerodynamic behavior of horizontal-axis wind turbines (HAWT's). In addition, aerodynamic responses in field tests were carried out by Schepers et al. (1997).

In this work, a wind tunnel study was carried out to estimate the wind-induced loads for the foundation of a 5 MW offshore wind turbine. An experimental study was carried out by using force balance technique at the boundary layer wind tunnel of Western University on a scaled 1:150 model. The results were compared with limited NREL results which were achieved by FAST (Fatigue, Aerodynamics, Structures, and Turbulence) program.

3.2. ESTIMATION OF WIND LOADS FOR PARKED POSITION

Offshore wind turbines in a parked position can experience extremely high wind loads, depending on the direction of the incoming wind. Under parked position, the blades and the tower behave more like a bluff body rather than streamline objects. The flow is massively separated over the entire blade span and can significantly contribute to the design loads. While the drag wind loads on isolated parked blades (excluding the tower) are provided by FAST for a particular configuration, a wind tunnel study was carried out for the estimation of the base shear and moment loads for many blade configuration scenarios with wind coming from all possible directions.

3.2.1. FAST modeling

FAST is NREL's primary aero-elastic wind turbine simulator that models HAWTs with two or three blades and allows computing the aerodynamic forces on the turbine blades (Buhl Jr and Manjock, 2006). Generally, the software is an analysis tool and not a design tool, but one can use it to check experimental concepts during the design phase.

IEC load case 6.2 was used with FAST program on the NREL 5 MW wind turbine, which involves parking the rotor with all the blades feathered to 90°and sweeping 360° of yaw error for sustained winds at a 50-year return wind speed. These simulations were run in turbulent wind, not steady wind. The mean hub-height wind speed for each 1-hr simulation was 47.5 m/s. This is 95% of the value of the 10-minute extreme wind speed with a recurrence period of 50 years.

In FAST, the rotor thrust (RotThrust) is defined as the axial force along the shaft. However, FAST not only includes the aerodynamic (applied) loads in this value, but also the mass/inertia terms. That is, the rotor thrust in FAST includes all of the loads (aero and structural) that are transmitted between the rotor and nacelle. The weight of the rotor will lead to a mean offset of this load from the true aerodynamic thrust (Jain *et al.*, 2012)

The FAST data presented in the current study do not account for tower loads. The tower drag force was calculated by dividing the tower for nine parts each one is 10 m height. Wind speed was calculated at the center of each part. An average value for the drag coefficient of 1.2 was used based on an average Reynolds number of 1.7e7. The peak tower loads are obtained from the mean values using peak factors of 2.5, 3.0 and 3.5.

3.2.2. Wind tunnel modeling

Three dimensional model based on the 5 MW NREL wind turbine was created by SolidWorks program (**Fig. 3.1**) based on data of NREL (TP-500-38060) report and air foil from TU Delft University. In these two sources most of data for tower, nacelle, hub and blades were given. A model scaled 1:150 was fabricated and tested in a boundary layer wind tunnel at Western University, Canada. The model consists of aluminum tubes representing the tower and the rotor. The hub and nacelles were fabricated from a rapid prototyping material. Estimated masses for the 1:150 scaled model are: rotor hub - 12.6g, turbine blade - 64.2g, Nacelle - 184.5g (various materials), main aluminum tube (skeleton for post) - 16.4g in addition to cladding for the post (to produce the taper by rohacell).

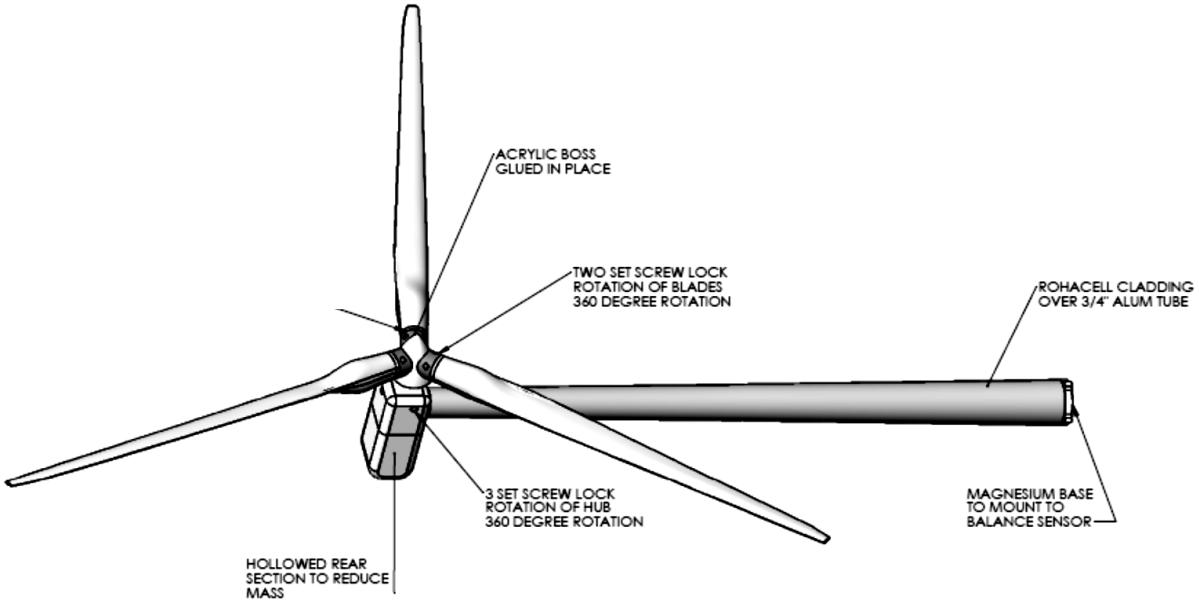

Fig. 3.1: Modeling based on 5 MW NREL wind turbine details and materials.

The wind tunnel experiment was carried out in an open water profile which entails to simulating the atmospheric flows of open water exposure. The mean wind speed, turbulence intensity and integral length scales of the along-wind velocity component are shown in **Fig. 3.2**:.

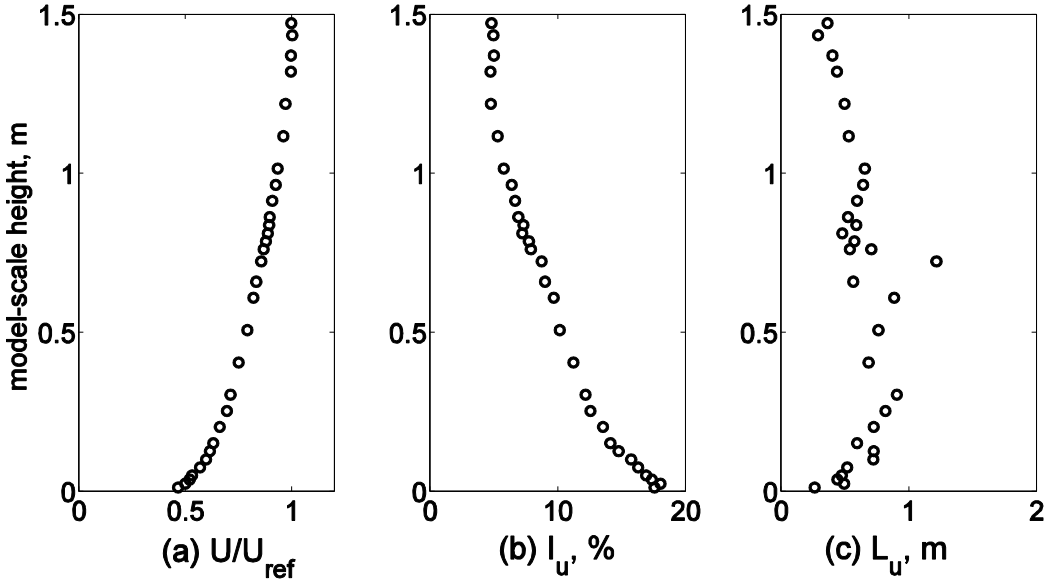

Fig. 3.2: Wind tunnel velocity profiles: (a) mean wind speed profile, (b) turbulence intensity profile and (c) integral length scale profile. U is the along-wind velocity component

The generated wind spectrum for the along-wind velocity component is plotted in **Fig. 3.2**: in comparison with the von Karaman spectra taken from the literature (Holmes, 2007). The reference mean hourly wind speed measured at the mean hub-height was about 3.6 m/s while the full-scale design wind speed is 47.5 m/s.

A force balance system was used to measure the overall shear and moments at the base of the light weight and stiff wind turbine tower model. The base loads and moments are useful for the design of the pile system and can be used in the estimation of the generalized forces for further dynamic analysis. This method was used to take advantages of its benefits as: (1) it just requires the system to be light weight and stiff with suitable scaled geometry, (2) the model can be constructed quickly and (3) the measurements of the base moments include correlations with wind forces in several geometrically complex parts of the wind turbine structure (w.r.t. the pressure integration technique). Several cases of loading were considered in the wind tunnel tests as shown in **Table 3.1**.

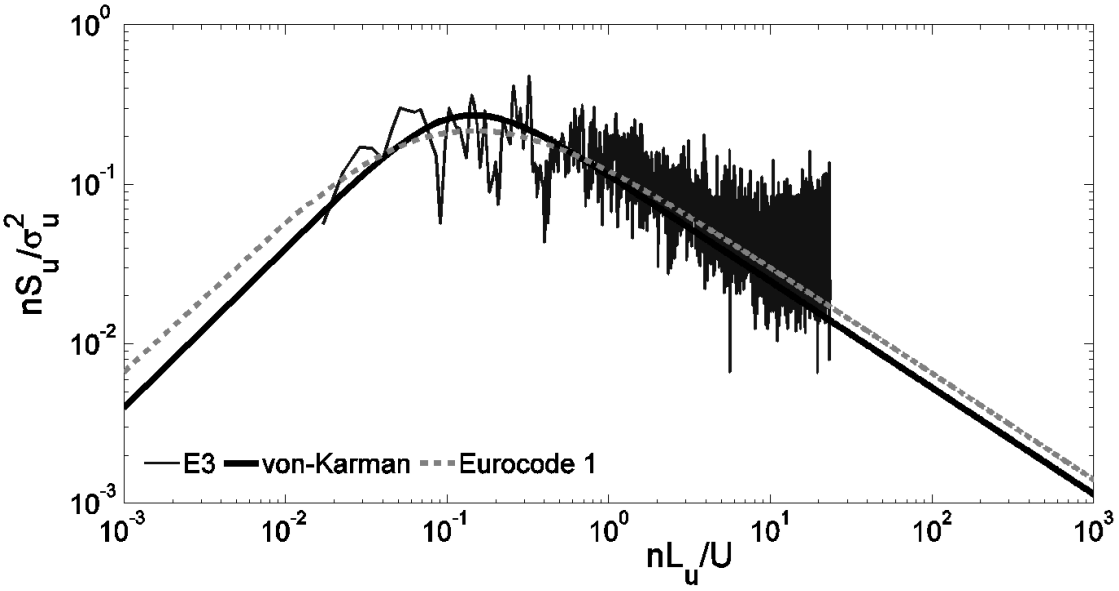

Fig. 3.3: Wind spectra of the along-wind velocity component (U): (a) non-dimensional spectra and (b) normalized spectra along with the von-Karman spectra

Table 3.3: Load cases considered in the boundary layer wind tunnel tests

Angle of attack (0°-180°)			
Rotor Configuration-CASE A (0°-120°-240°)		Rotor Configuration-CASE B (60°-180°-300°)	
Blade Angle-90°	Blade Angle-15°	Blade Angle-90°	Blade Angle-15°

Fig. 3.4 shows the wind tunnel test configurations used in the current study. A force balance calibration procedure was first carried out once the test model was mounted and before running any wind tunnel tests (see **Fig. 3.4b**). The calibration procedure consisted of applying a known horizontal load at the location of the hub both in the along-wind and cross-wind directions and immediately acquiring the base shear and moment loads. That was carried out to ensure accuracy and precession of the measuring and acquisition system. Basically two arrangements of testing were used: (1) case A in which the rotor was locked and one of the blades was located vertically in its extreme upper position (see **Fig. 3.4c**) and (2) case B in which the rotor was locked and one of the blades was located vertically in its extreme bottom position (see **Fig. 3.4d**).

(a) (b)

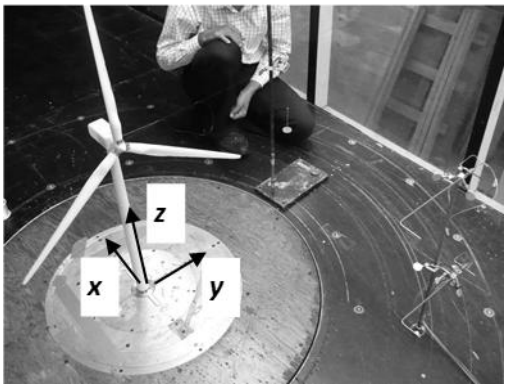

(c) (d)

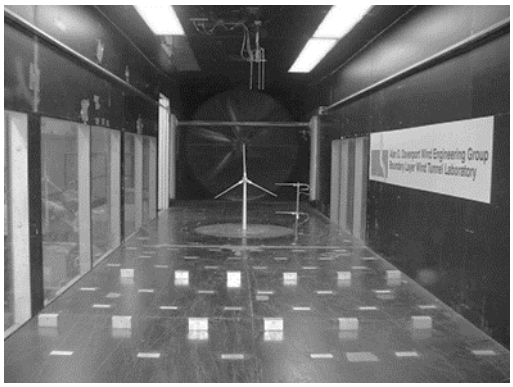

Fig. 3.4: Wind Tunnel test configurations: (a) 1:150 5 MW scaled model, (b) force balance calibration with the coordinate system, (c) case A with blade angle 90° and (d) case B with rotor angle 90°

The following laws of similitude were used to predict the full-scale wind loads on the wind turbine-tower structure from the wind tunnel measurements:

$$Force_{full-scale} = \frac{1}{2}\rho U^2 Area\, C_D \;,\; Force_{lab} = \frac{1}{2}\rho u^2 area\, C_D \qquad \textbf{Eq. 3.1}$$

$$Force_{full-scale} = Force_{lab}\,\frac{U^2}{u^2}(150)^2 \qquad \textbf{Eq. 3.2}$$

$$Moment_{full-scale} = \frac{1}{2}\rho U^2 Area * L * C_M,\; Moment_{lab} = \frac{1}{2}\rho U^2 area * l * C_M \qquad \textbf{Eq. 3.3}$$

$$Moment_{full-scale} = Moment_{lab}\,\frac{U^2}{u^2}(150)^3 \qquad \textbf{Eq. 3.4}$$

$$\frac{u}{f*l} = \frac{U}{F*L} \qquad \textbf{Eq. 3.5}$$

$$\frac{t*u}{l} = \frac{T*U}{L} \quad \textbf{Eq. 3.6}$$

$$T = \frac{L}{l} * \frac{u}{U} * t \quad \textbf{Eq. 3.7}$$

$$T = 150 * \frac{u}{U} * t \quad \textbf{Eq. 3.8}$$

Where: $Force_{full\text{-}scale}$ and $Force_{lab}$ are tower base forces at full-scale and lab respectively [kN]; $Moment_{full\text{-}scale}$, $Moment_{lab}$ are tower base moments at full-scale and lab respectively [kN.m]; ρ is the air density [kg/m^3]; *U* and *u* are wind speed in nature and lab respectively [m/s]; *Area*, *area* are wind turbine projection area in nature and lab respectively [m^2]; C_D and C_M are the force and moment coefficients; *L* and *l* are length in nature and lab respectively [m]; F and f represent frequency in nature and lab respectively; *T* and *t* are time in nature and lab, respectively [s].

3.3. RESULTS AND DISCUSSION

The first step carried out on the measured wind tunnel data, after scaling the loads using the laws of similitude discussed previously, was to remove the resonance components from the measurements. After the resonance peaks where removed (see **Figs. 3.5 and 3.6**), the load data in the time domain (see **Figs. 3.7 and 3.8**) are used to obtain the total wind load at the base of the turbine taking into account the flexibility of the wind turbine and the tower. The first three natural frequencies of the full-scale system are 0.322 Hz (fore-aft), 0.314 Hz (side to side) and 0.615 Hz (torsion). The overall integrated mass of the tower is 347,460 kg located at 38.234 m (w.r.t. ground along tower centerline). The base diameter is 6 m, the base thickness is 0.027 m, the top diameter

is 3.87 m and top thickness is 0.019 m. The shear modulus is 80.8 GPa. The structural damping ratio for all modes is 1 %. More details about the 5 MW wind turbine used in the current study are given in (Jonkman *et al.*, 2009) (**Table 3.2**). It is worth noting that these dynamic properties will depend on the type support structure, the installation site, differences in water depth, soil type, wind and wave severity and other factors. The tower properties for the equivalent land-based version of the NREL 5-MW baseline wind turbine were used. These properties provide a basis with which to design towers for site-specific offshore support structures.

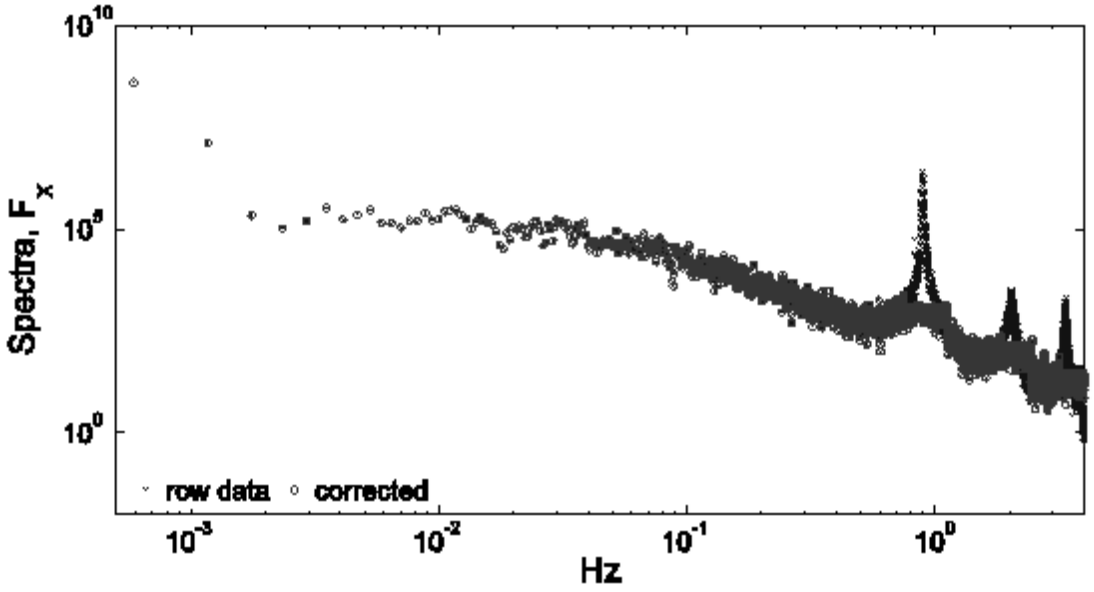

Fig. 3.5: Power spectra of the overall wind loads at the base of the wind turbine tower (row and corrected loads)

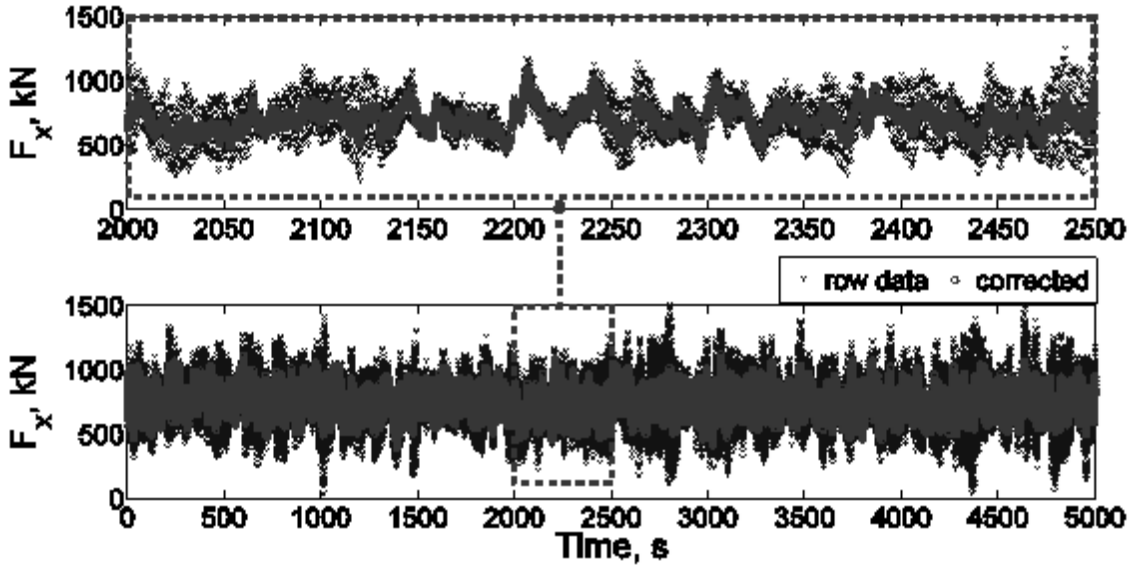

Fig. 3.6: Time history of the overall wind loads at the base of the wind turbine tower (row and corrected loads)

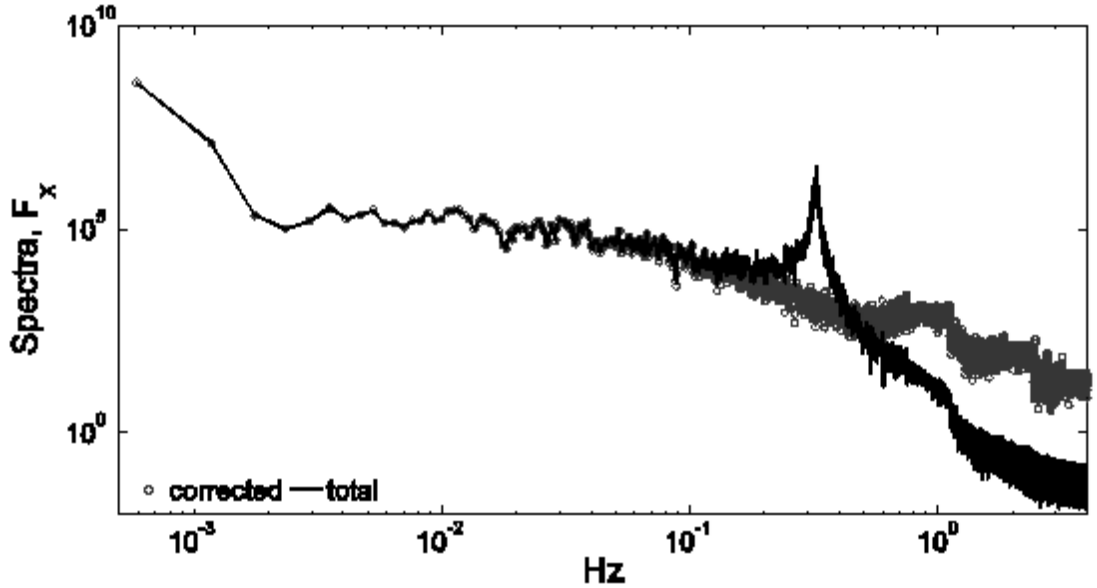

Fig. 3.7: Power spectra of the overall wind loads at the base of the wind turbine tower (corrected and total loads)

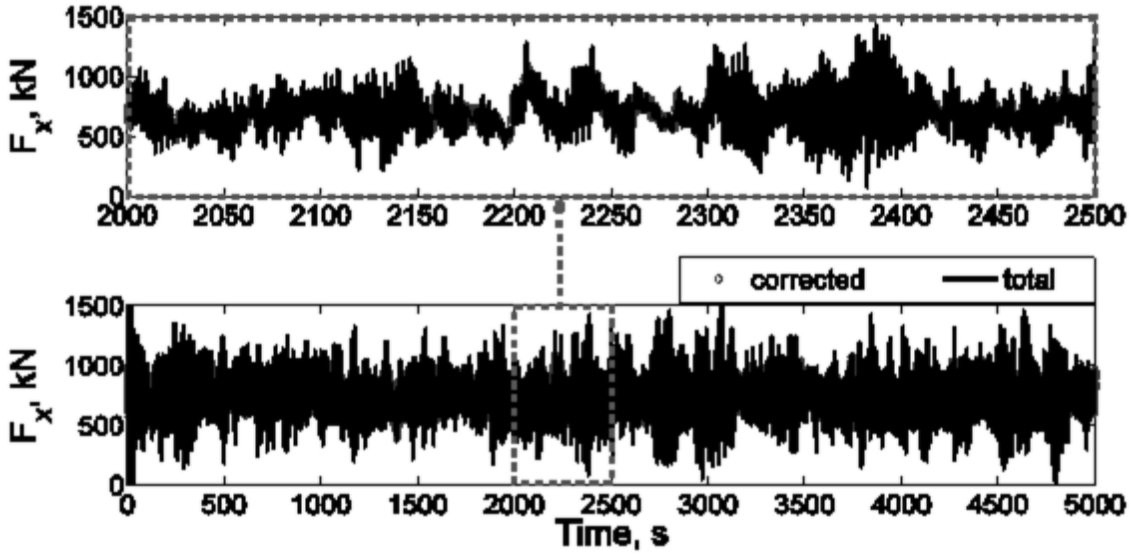

Fig. 3.8: Time history of the overall wind loads at the base of wind turbine tower (corrected and total loads)

Table 3.4: NREL reference wind turbine properties

Parameter	Value
Rating	5 MW
Rotor Orientation, Configuration	Upwind, 3 Blades
Control	Variable Speed, Collective Pitch
Drivetrain	High Speed, Multiple-Stage Gearbox
Rotor, Hub Diameter	126 m, 3 m
Hub Height	90 m
Cut-In, Rated, Cut-Out Wind Speed	3 m/s, 11.4 m/s, 25 m/s
Cut-In, Rated Rotor Speed	6.9 rpm, 12.1 rpm
Rated Tip Speed	80 m/s
Overhang, Shaft Tilt, Precone	5 m, 5º, 2.5º
Rotor Mass	110,000 kg
Nacelle Mass	240,000 kg
Tower Mass	347,460 kg

A plot of the drag loading (along-wind component of load) at the base of tower (taking into account tower loads) from FAST for the same load case is shown in **Fig. 3.9**: and referred to in the legend by 'nrel'. For the three peak factors assumed in the calculations of the tower's loads, the overall peak wind loads at the base of the NREL turbine are obtained by adding the tower peak loads to the peak loads obtained from FAST simulations. This force is shown in the direction of the mean wind. The peak values include structural oscillations of the rotor-nacelle weight/inertia, but the weight/inertia shouldn't impact the mean values.

The mean and peak drag loads obtained from the proposed wind tunnel based approach are also shown in **Fig. 3.9**: and referred to in the legend by 'wt'. The figure shows good agreement between the proposed approach and the FAST simulations in terms of mean drag values. However, the peak drag values are dependent on the peak factor used to calculate drag on the tower and to amend the FAST results. The trend of the peak values is in agreement with the FAST results with a peak factor ranging between 2.5 and 3.5.

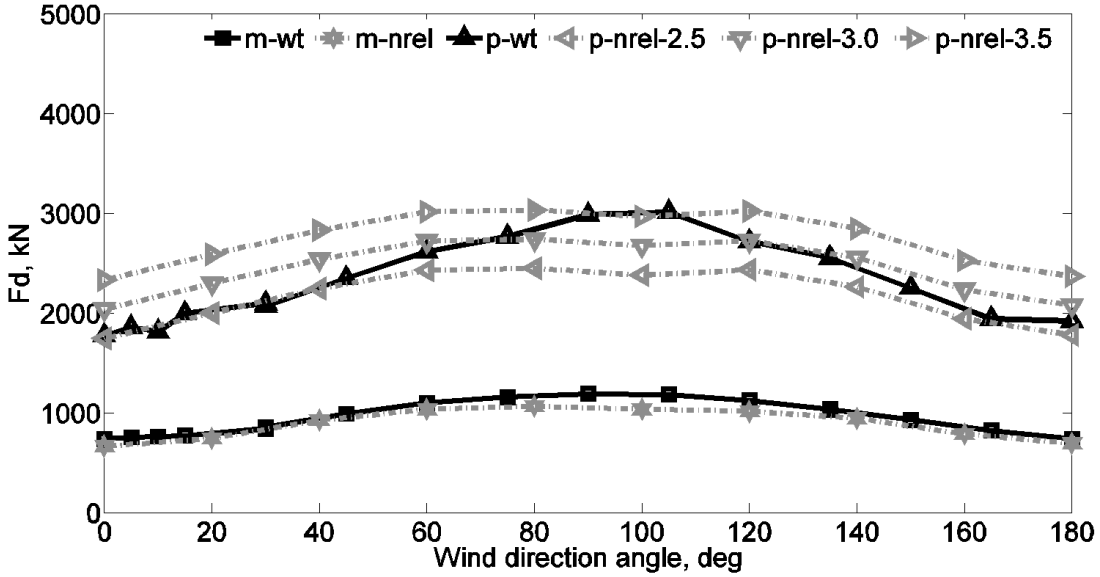

Fig. 3.9: Comparison between wind tunnel results and average FAST results

Design wind loads at the base of the tower are shown in **Figs 3.10** to **3.12**. The trend shows the influence of the wind direction angle on the three components of forces and the three components of moments at the base of the tower. While the 90^{o} direction angle is associated with maximum shear loads, the maximum torsion occurs at a 75^{o}. This reveals the importance of the wind direction angle as a key parameter in the evaluation of the foundation design loads of wind turbine-tower structures. It is worth noting that the wind tunnel based approach used allowed generating time history of six component load data (three forces and three moments) useful for the foundation design for several configurations.

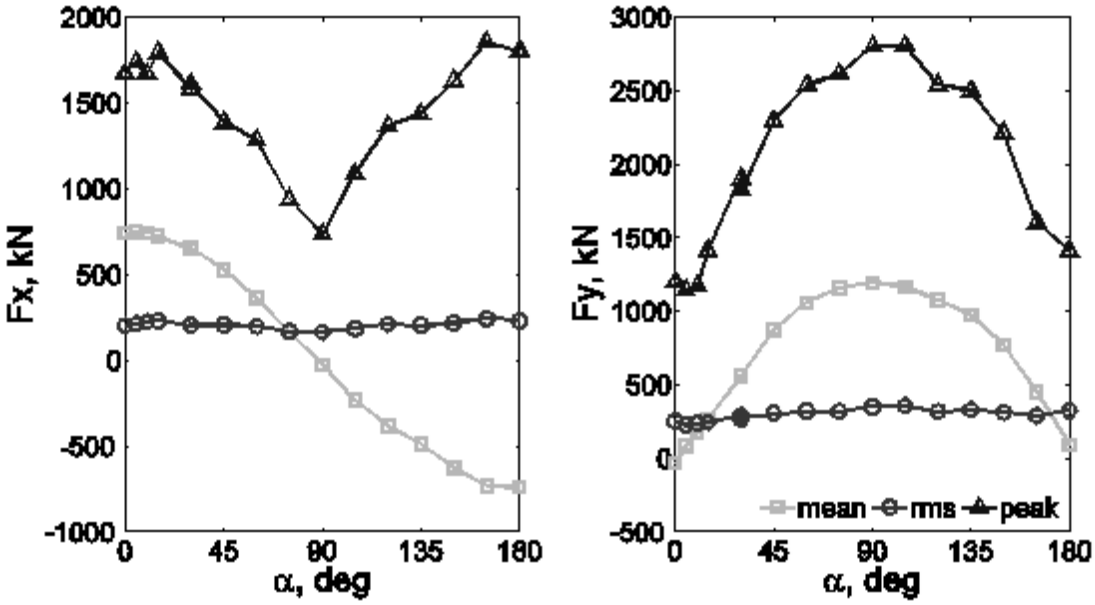

Fig. 3.10: Base shear loads Fx and Fy as function of the wind direction angle α

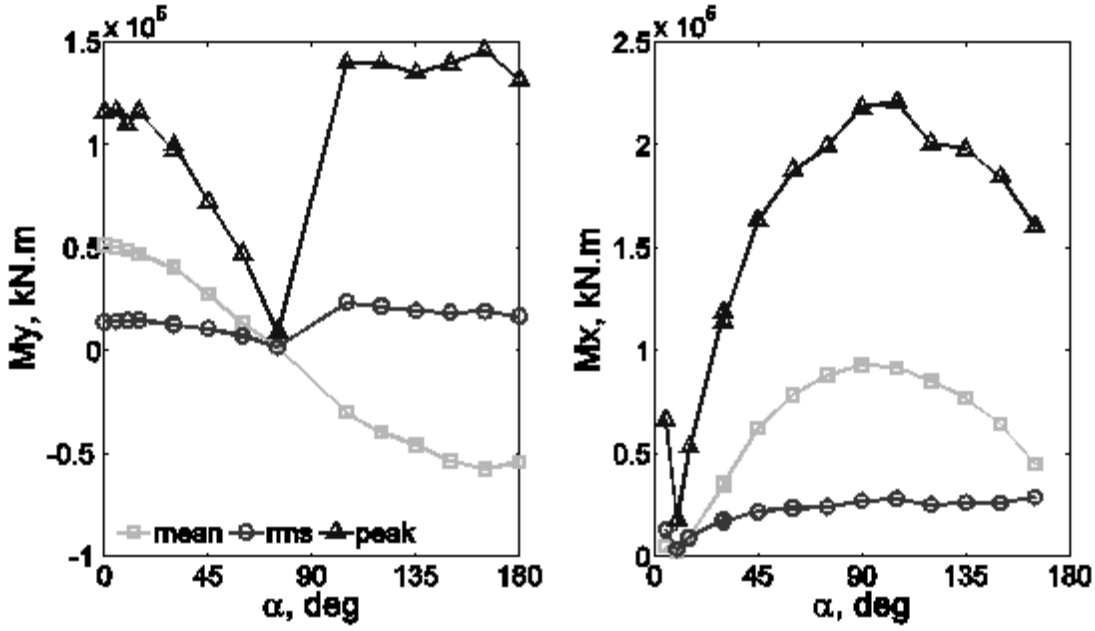

Fig. 3.11: Base bending moments My and Mx as function of the wind direction angle α

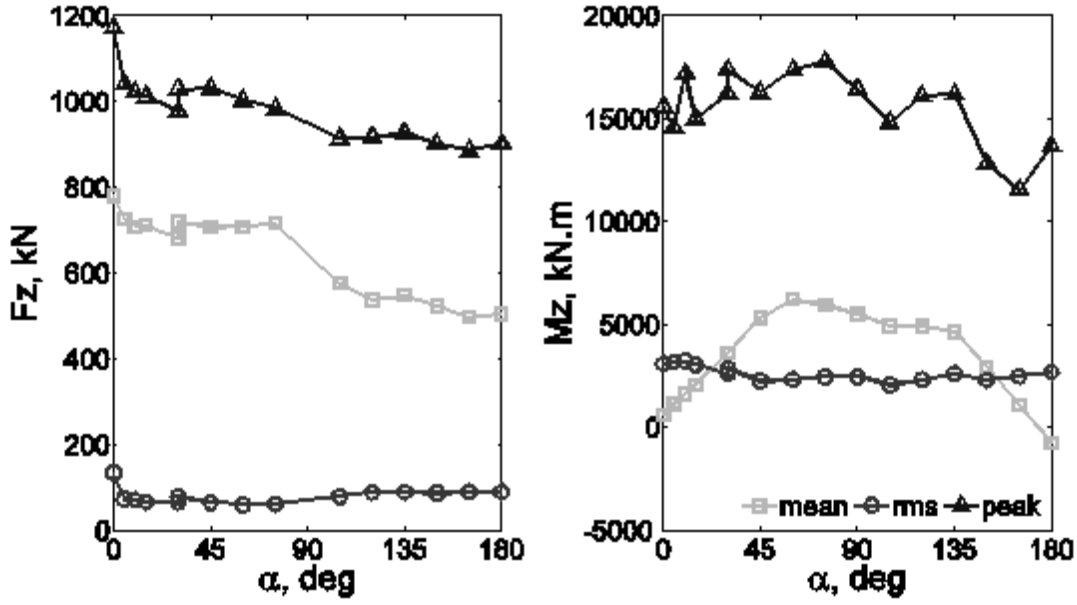

Fig. 3.12: Base normal wind load (Fz) and torque (Mz) as function of the wind direction angle α

Figures 3.13 and **3.14** show that there is no significant correlation between the along wind loads and other components of loads. This is due to the fact that cross-wind and torsional loads result

mainly from the aerodynamic pressure fluctuations in the separated shear layers and the wake flow fields, i.e. there is no direct relation to the oncoming velocity fluctuations.

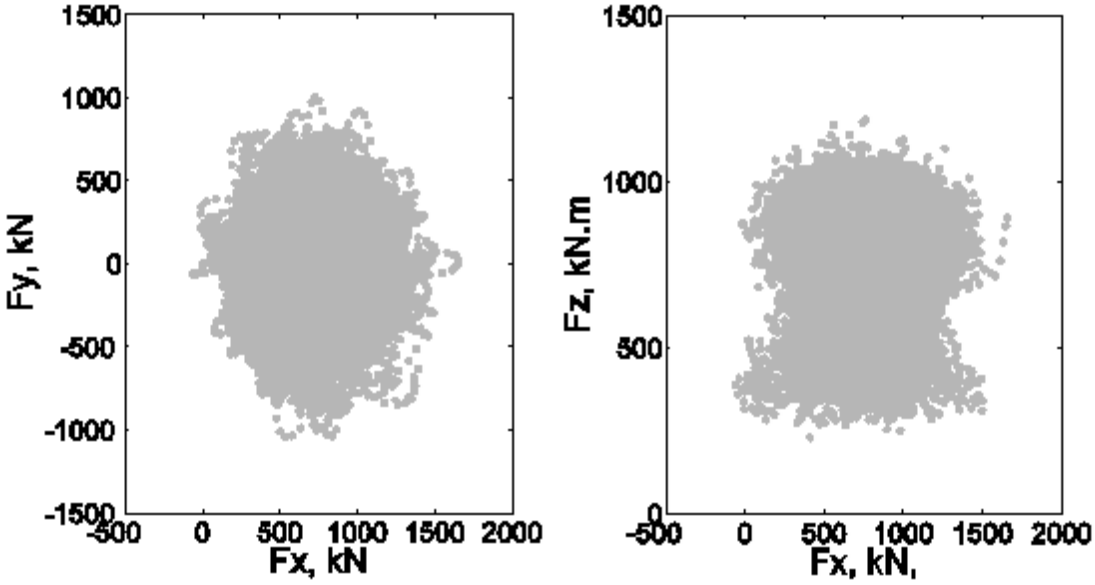

Fig. 3.13: Cross wind shear force Fy and normal wind load Fz versus along-wind shear Fx

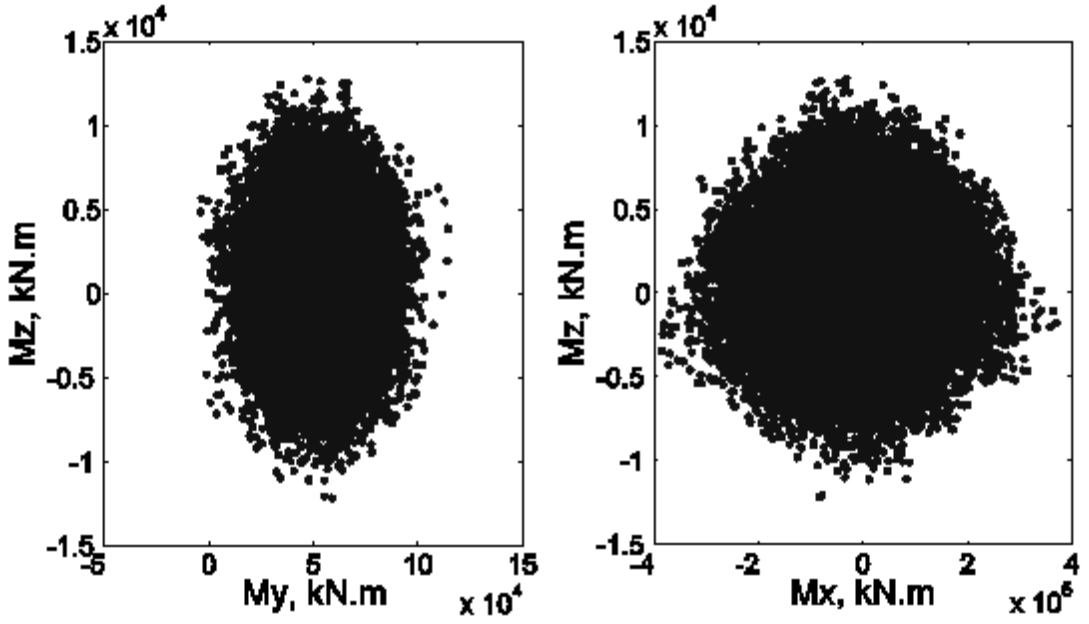

Fig. 3.2: Torsion (Mz) versus bending moments My and Mx

3.4. CONCLUSIONS

The work presents a procedure for evaluating foundation design loads for a 5 MW wind turbine based on wind tunnel testing. First, the overall base loads were obtained experimentally using the force balance technique and a rigid model of the turbine-tower structure. Second, the measured data were processed to remove resonance effects. Third, the base loads were obtained considering the structural response. Comparison between the along-wind base shear obtained from the proposed procedure and limited FAST simulations shows good agreement. The agreements in the comparison between the numerical and the wind tunnel test results give creditability for the proposed approach and the data presented to be used in offshore wind turbines foundations' design.

3.5 REFERENCES

Alan G. Davenport Wind Tunnel Group, (2007), "WIND TUNNEL TESTING:

A GENERAL OUTLINE", Technical Report, May 2007.

Bazeos, N., et al. (20020 "Static, seismic and stability analyses of a prototype wind turbine steel tower." *Engineering structures* **24**(8), 1015-1025.

Bazeos N, Hatzigeorgiou GD, Hondros ID, Karamaneas H, Karabalis DL, Beskos DE. (2002), "Static, seismic and stability analyses of a prototype wind turbine steel tower", Engineering Structures, **24**, 1015-1025.

Buhl Jr, M. L., Manjock, A. (2006), "A comparison of wind turbine aeroelastic codes used for certification", In 44th AIAA Aerospace Sciences Meeting and Exhibit, Reno, NV, January.

Buliga, A., (2011), "Aeroelastic comparison of a two and three bladed wind turbine rotors", Master Thesis, Technical University of Denmark

De Ridder, E. J., Koop, A., Doeveren, B. (2011). *DeepCwind Floating Wind Turbine Model Tests,* Maritime Research Institute, The Netherlands, Report No. : 24602-1-OB, Vol. 1.

DNV-OS-J101, Offshore Standard, (2011), "Design of Offshore Wind Turbine Structures", Electronic Version available at http://www.dnv.com/ (On Jan. 25, 2013)

Dominique, R., Cermelli, C., and Weinstein, A., (2009), "Wind float: A floating foundation for offshore wind turbines part i: design basis and qualification process", ASME 2009 28th International Conference on Ocean, Offshore and Arctic Engineering (OMAE2009), Honolulu, Hawaii, USA, May 31-June 5.

Byrne, B.W. and Houlsby, G.T. (2003), "Foundations for Offshore Wind Turbines", Philosophical Transactions of the Royal Society of London, **A** (361), 2909-2930.

IEC 61400-3, International Standard, (2009),"Wind turbines – Part 3: Design requirements for offshore wind turbines", Edition 1.0 2009-02.

Hameed, Z., Vatn, J. and Heggset, J. (2011), "Challenges in the reliability and maintainability data collection for offshore wind turbines", Renewable Energy, **36**(8), 2154-2165.

Hand, M.M., Simms, D.A., Fingersh, L.J., Jager, D.W., Cotrell, J.R., Schreck, S., and S.M. Larwood, (2001), "Unsteady Aerodynamics Experiment Phase VI: Wind Tunnel Test Configurations and Available Data Campaigns", Technical Report, National Renewable Energy Laboratory, NREL/TP-500-29955.

Holmes, D.J. (2007), *Wind Loading of Structures*, Taylor and Francis, New York, NY.

Houlsby, G.T. and Byrne B.W., (2001a), "Novel Foundations for Offshore Wind Farms", Research Proposal to EPSRC, Department of Engineering Science, Oxford University, August.

Houlsby, G.T. and Byrne B.W. (2001b), "Assessing Novel Foundation Options for Offshore Wind Turbines", Department of Engineering Science, Oxford University.

Houlsby, G.T. and Byrne, B.W. (2000), "Suction Caisson Foundations for Offshore Wind Turbines and Anemometer Masts", Wind Engineering, **24**(4), 249-255.

Jain, A., Robertson, A.N., Jonkman, A.M., Goupee, A.J., Kimball, R.W., Swift, A. (2012), "FAST Code Verification of Scaling Laws for DeepCwind Floating Wind System Tests", 22nd International Offshore and Polar Engineering Conference, Rhodes, Greece, June.

Jonkman, J., Butterfield, S., Musial, W., and Scott, G., (2009), "Definition of a 5-MW Reference Wind Turbine for Offshore System Development", National Renewable Energy Laboratory, Golden, CO, Technical Report, NREL/TP-500-38060, February.

Jonkman, J., and Musial, W., (2010), "Offshore Code Comparison Collaboration (OC3) for IEA Task 23 Offshore Wind Technology and Deployment", Technical Report, NREL/TP-5000-48191, December.

LeBlanc, C., (2009), "Design of Offshore Wind Turbine Support Structures", PhD Thesis, Department of Civil Engineering, Aalborg University, Denmark.

LeBlanc, C., Houlsby, G. T. & Byrne, B. W. , (2008), "Response of stiff piles in sand to long-term cyclic lateral loading", Geotechniqué..

LeBlanc, C., B. W. Byrne, and G. T. Houlsby. (2010), "Response of stiff piles to random two-way lateral loading." *Geotechnique* 60(9),715-721.

"Case Study: European Offshore Wind Farms - A Survey for the Analysis of the Experiences and Lessons Learnt by Developers of Offshore Wind Farms", Final Report, Deutsche WindGuard GmbH, Deutsche Energie-Agentur GmbH (dena), University of Groningen

Lozano-Minguez, E., Kolios, A.J., Brennan, F.P. (2011), "Multi-criteria assessment of offshore wind turbine support structures", Renewable Energy, 36(11), 2831-2837

Oh, K.Y, Kim, J.Y., and Lee, J.S. (2012), "Preliminary evaluation of monopile foundation dimensions for an offshore wind turbine by analyzing hydrodynamic load in the frequency domain", Renewable Energy, (In Press). http://dx.doi.org/10.1016/j.renene.2012.08.007

Prowell, I., et al. (2010), "Estimation of Seismic Load Demand for a Wind Turbine in the Time Domain", *Conference Paper*, NREL/CP-500-47536, March 2010.

Ragan, P., and Manuel, L., (2007), "Statistical Extrapolation Methods for Estimating Wind Turbine Extreme Loads", 45th AIAA Aerospace Sciences Meeting and Exhibit 8 - 11 January 2007, Reno, Nevada.

Schepers, J.G., Brand, A.J., Bruining, A., Graham, J.M.R., Hand, M.M., Infield, D.G., Madsen, H.A., Paynter, R.J.H., Simms, D.A., (1997). *Final Report of IEA Annex XIV: Field Rotor Aerodynamics*. ECN-C-97-027. Petten, the Netherlands: Netherlands Energy Research Foundation ECN.

Seidel, M. (2007). "Jacket substructures for the REPower 5M wind turbine", Proc. Eur. Offshore Wind 2007, Berlin.

Skaare, B., Hanson, T. D., Nielsen, F. G., Yttervik, R., Hansen, A. M., Thomsen, K. and Larsen, T. J. (2007), "Integrated dynamic analysis of floating offshore wind turbines", In proceedings of 2007 European Wind Energy Conference and Exhibition, Milan, Italy, May 7-10.

Stone, K.J.L., Newson, T.A., El Marassi, M., El Naggar, H., Taylor, R.N., and Goodey, R.J., (2011), "An investigation of the use of a bearing plate to enhance the lateral capacity of monopile foundations", Frontiers in offshore Geotechnics II- Gourvenec & White (eds), 623-628.

Vermeer, L., Sorensen J., and Crespo, A., (2003), "Wind turbine wake aerodynamics." *Progress in aerospace sciences* 39.6 (2003): 467-510.

CHAPTER FOUR

PERFORMANCE OF HYBRID FOUNDATION SYSTEM FOR OFFSHORE WIND TURBINES

In this chapter, a novel offshore hybrid foundation system is proposed for large offshore wind turbines. This new system consists of circular precast concrete plate connected on site (i.e. offshore) to a steel monopole that is smaller than the usual pile size used. The displacements at different locations of the foundation and the rotation at the pile head were analyzed and evaluated using a 3D nonlinear finite element model under field-like loading conditions considering different foundation configurations. This chapter paves the way for the development of design guidelines for this novel foundation system in offshore wind turbine applications.

4.1. INTRODUCTION

Normally, strong winds have been associated with two types of wind in typhoon prone region. The first one is the nature wind and the other one is the typhoon, or say severe tropical cyclone. Many investigations about the vibration and buckling (static stability) characteristics of frames of various types have been carried out. Cheng (2011) have studied the elastic critical loads for plane frames by using the transfer matrix method. A general digital computer method has been described by Cheng and Xu (2012).

The offshore wind turbines industry is growing rapidly (Lozano-Minguez *et al.*, 2011, Hameed *et al.*, 2011). Offshore wind turbines foundations have to withstand significant lateral

wind loads, in addition to other environmental loads arising from waves and current. Initial sites proposed for offshore wind farms are usually located in shallow waters, but with ever growing wind turbine sizes sites with larger water depth are being considered. These sites present foundation design engineers with major challenges to provide efficient, reliable and constructible foundation systems in deep water. The cost of offshore foundations for these developments represents a significant percentage, about 35%, of the overall installed costs (Byrne and Houlsby, 2003), which fuels innovation to introduce cost-effective foundation options.

The engineering expertise in the design and construction of foundations of marine structures came mainly from platforms serving in the oil industry. However, there is a major difference between the platforms and wind turbines in terms of vertical to horizontal load ratios, as in oil industry this ratio is high. On the other hand, this ratio could be quite low in wind turbines foundations, which imposes different demands on their design.

The most common foundation type for shallow water is gravity base foundation, which depends on its high own weight to overcome the lateral loads from wind, wave and current actions. In order to minimize construction costs, these foundations are usually fabricated onshore as precast concrete sections that would then be transported for installation at the intended offshore positions. A novel system for gravity base was presented in Nysted and Thornton bank offshore wind farm (Thomes *et al.*, 2007) where a large hollow gravity base was cast onshore then moved offshore to be erected and then filled with backfill material from the sea floor.

Monopile foundations are also widely used. For example, they were used in Horns Rev, Denmark for 2.3 MW turbines (Gerdes *et al.*, 2008). The piles are typically 4 m or more in diameter and 20 m to 40 m long. The piles are usually hollow steel driven piles connected to the tower (shaft) by a transitional part. Suction caissons are another foundation type, which is lowered to seabed level, and then the trapped water is sucked by pumps to help install the foundation to its final position within the foundation soil (Houlsby *et al.*, 2001). Ibsen et al. (2004) presented a new bucket system and installation technique for 3 MW turbines, which includes rips to increase the system capacity. A hybrid monopile-footing (caped pile) system was proposed by (El-Marassi *et al.*, 2008) in order to enhance the lateral and axial load capacities and increased lateral stiffness, compared to monopole foundation. This system is further explored here considering precast concrete plates for the construction of the footing to reduce installation cost.

4.2. OBJECTIVE AND SCOPE OF WORK

The main objective of the current study is to examine the performance of a hybrid foundation system composed of precast reinforced concrete plates to form the footing, along with a central driven steel pile. It is envisioned that this system can reduce the installation cost considerably while providing reliable axial, lateral and rocking resistances to meet the requirements of wind turbine foundations. The construction sequence involves driving the pile first then lowering the precast concrete plates with a central whole with appropriate diameter to allow the monopile at the centre. The two parts are then grouted together to form an integral hybrid foundation system. It is envisioned that this system can reduce the size of the required monopile from 6 m to 4 m owing to the additional capacity of the precast plate. The system performance under wind and wave loads is examined using a 3-dimensioanl finite element model. The concept of the new system may also

be adapted to upgrade existing turbines to larger wind turbines using the existing monopole and adding a precast concrete plate foundation.

4.3. DESCRIPTION OF THE HYBIRD FOUNDATION SYSTEM

The new system involves a hollow steel pile connected to a precast concrete cap. This system is intended for installations in offshore water with depth of 20 m to 30m. The dimensions proposed herein are sized to meet the demands of the environmental loads and the example site conditions. However, these dimensions can be optimized for other environmental loads and site conditions. The intent of the analyses provided herein is to show the effectiveness of the proposed hybrid foundation system in reducing the size of the monopole while providing acceptable design.

The example hybrid system considered herein is composed of three parts: **Part 1** is a 4 m diameter steel driven pile with a wall thickness of 0.08 m, considering variable length (16, 24 or 36 m); **Part 2** includes a combination of a 6 m-diameter steel pipe with 0.08 wall thickness and 20 m long (wind turbine shaft), and a concrete precast concrete cap (with diameter of 12 or 16 m). Different configurations of the precast concrete cap are considered: a circular plate of a minimum thickness of 1 m, a circular precast concrete plate with eight rips of 1 m width, and a circular plate with 8 ribs of 2 m depth. **Part 3** is a cylindrical grout infilled offshore to connect part 1 and 2. The tower of the wind turbine will be connected to the top of the upper steel pipe.

The upper steel pipe (20 m long) weighs about 2376 kN and the concrete plate weighs approximately 2905 kN. The steel pipe will be connected at its base to the precast concrete cap during construction onshore. The connection between the precast concrete plate and the 6 m pipe will be achieved through steel shear connectors that will transfer the loads between the two parts.

The upper part of the foundation system (steel pipe and precast concrete plate) will be connected to the driven steel pile using a cylindrical grout (Part 3) infilled offshore reinforced with steel bars. **Figure 4.1** shows the hybrid system components and its proposed construction phases.

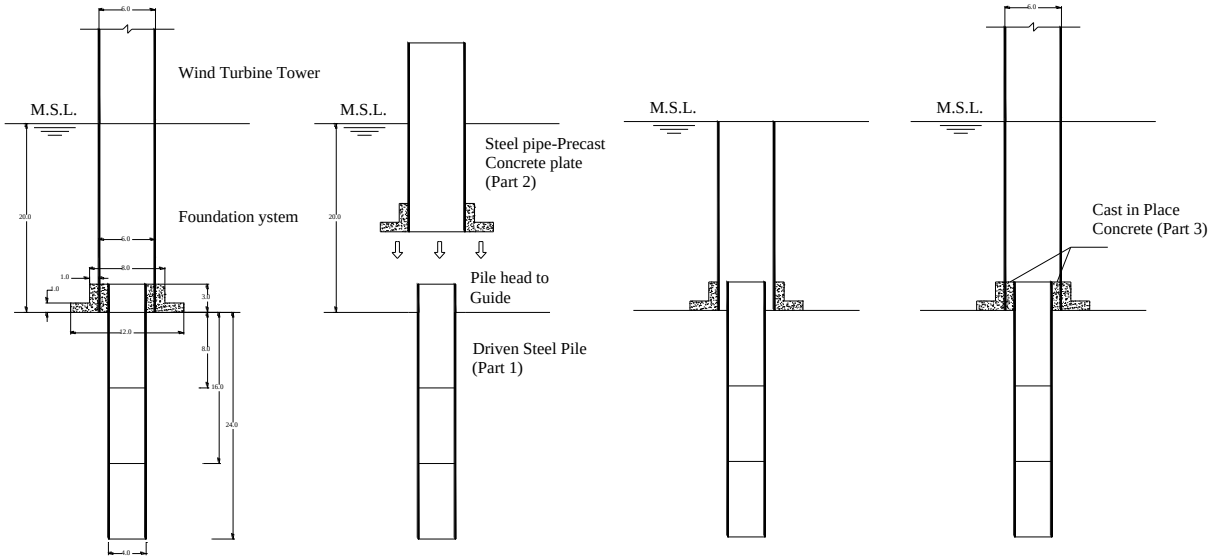

Fig. 4.1: The hybrid system installation process.

4.4. LOADS

DNV (2011) and IEC (2009) codes present guidelines for calculating wind climate parameters, loads, load effects and load factors for offshore wind turbines. The information in National Renewable Energy Laboratory (NREL) reports are used to characterize the force and moment exerted by the turbine at the top of the foundation at the mean sea level. Loads combinations can be seen in **Fig. 4.2** where 6 C represent six components as three translational loads (one vertical and two perpendicular horizontal) and three moments, 3C represent three components as two translational loads (one vertical and one horizontal) and one bending moment and 2C represent two components as one horizontal load and one bending moment. All forces are applied at mean sea level (MSL).

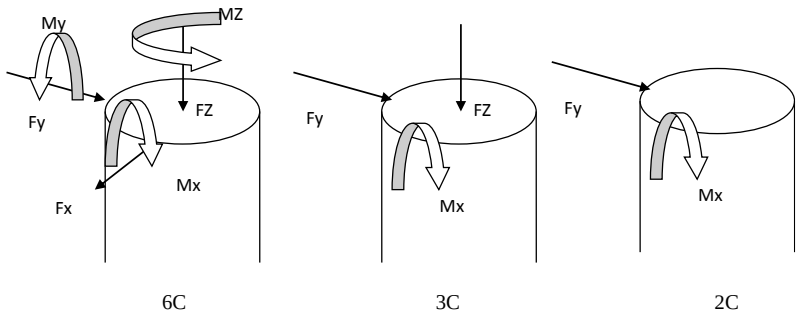

Fig. 4.2: Foundation systems under different load combinations: 6C, 3C and 2C.

4.4.1. Wind loads

4.4.1.1. Working Loads

Steady state loads as a function of wind speed were obtained from NREL studies conducted by using the programme FAST, which does not include aerodynamic loads on the tower. The aerodynamic loads were deemed negligible relative to rotor thrust while the NREL 5-MW turbine is operating at stage 3 (Jonkman, 2013) as shown in **Fig. 4.3**.

4.4.1.2. Ultimate loads

In order to establish representative wind loads from large wind turbines, a scaled model based on the 5MW National Renewable Energy Laboratory (NREL) wind turbine was constructed considering the data of NREL report (Jonkman *et al.*, 2009). The 5MW NREL wind turbine properties are summarized in **Table 4.1**, including the tower, nacelle, hub and blades. The scaled model (1:150) was tested in the Boundary Layer Wind Tunnel Laboratory (BLWTL) at Western University, London, Canada. The force balance technique was employed to measure the shear and moment loads at the base of the light-weight and stiff tower model. The static peak values for the moments and horizontal shear forces acting on the tower base are applied on the foundation system in the numerical analysis presented herein (Abdelkader *et al.*, 2013). These values are listed in **Table 4.2**.

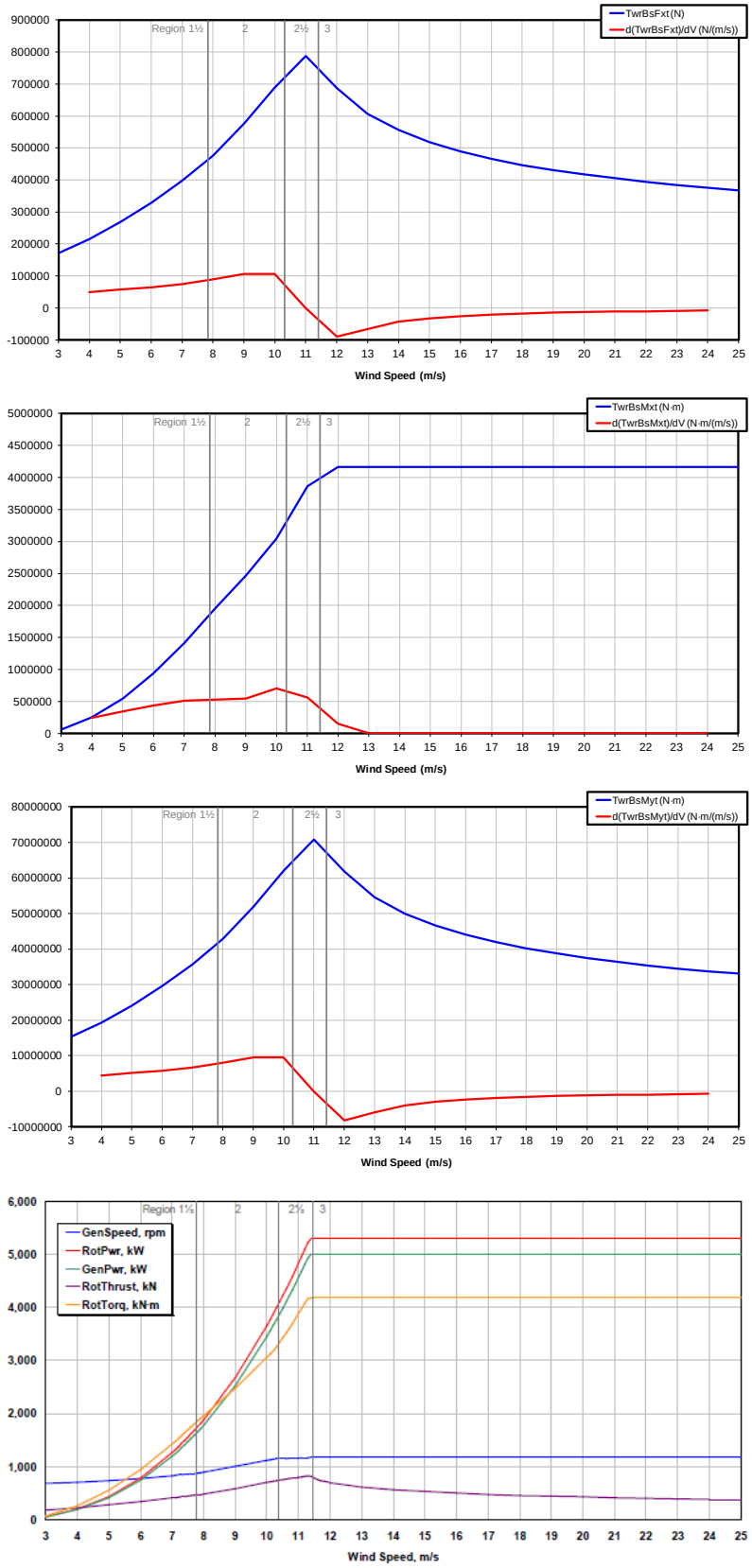

Fig. 4.3: Steady state responses as a function of wind speed (Jonkman *et al.*, 2009)

Table 4.1: 5MW NREL reference wind turbine properties (Jonkman *et al.*, 2009)

Parameter	Value
Rating	5 MW
Rotor Orientation, Configuration	Upwind, 3 Blades
Control	Variable Speed, Collective Pitch
Drive train	High Speed, Multiple-Stage Gearbox
Rotor, Hub Diameter	126 m, 3 m
Hub Height	90 m
Cut-In, Rated, Cut-Out Wind Speed	3 m/s, 11.4 m/s, 25 m/s
Cut-In, Rated Rotor Speed	6.9 rpm, 12.1 rpm
Rated Tip Speed	80 m/s
Overhang, Shaft Tilt, Precone	5 m, 5º, 2.5º
Rotor Mass	110,000 kg
Nacelle Mass	240,000 kg
Tower Mass	347,460 kg

Table 4.2: Ultimate loads combinations measured from wind tunnel tests (Abdelkader *et al.*, 2013).

	F_x (kN)	F_y (kN)	F_z (kN)	M_x (kN.m)	M_y (kN.m)	M_z (kN.m)
Load	1750	1500	8000	15 E4	15 E4	15000

4.4.2. Wave loads

The wave loads considered in this study were established based on the information provided in the technical reports NREL/TP-5000-48191 and NREL/CP-500-41930 (Jonkman *et al.*, 2010; Passon *et al.*, 2007). Wave kinematics for the deterministic and the stochastic wave conditions have been derived using the standard wave generator model from GH Bladed. The wave characteristics considered in deriving the loads are as follows: wave height, H = 6 m, wave period, T = 10 s, and water depth, W_D = 20m. The waves are considered to be applied on a pile (i.e. wind turbine shaft)

with a diameter, D = 6 m (the upper part of the new hybrid system). Wave loads were taken as a concentrated load of a value of 1500 kN to be added to the F_y from the wind at the tower base.

4.5. NUMERICAL MODELING

The numerical analysis was conducted using the finite element method. A 3-dimensional nonlinear finite element model of the foundation system and soil was established employing the Abaqus program (2009). The soil and components of foundation system were modeled using 3D deformable solid elements with different material models. The sand soil was simulated with an elastic-perfectly plastic constitutive model and the Mohr-Coulomb failure criterion. The steel pipe and steel pile were simulated using elastic-perfectly plastic model and the Mohr-Coulomb failure criterion with the following properties: yield strength, f_y = 240 MPa, Young's Modulus, E_s = 200 GPa and Poisson's ratio, ν = 0.3. Interaction properties were applied between different materials to ensure the actual simulation including: tangential behaviour with friction coefficient equal to 0.5 with fraction of characteristic surface dimension equal to 0.005; and normal behavior using the constraint enforcement method and pressure-overclosure as hard contact with allowing separation after contact. In order to evaluate the performance of the hybrid system relative to the conventional monopile system, five different foundation systems were analyzed. The different systems considered are (as shown in **Fig. 4.4**):

1) **Monopile foundation system**:
    a. A pile with diameter (D_p) = 4 m and an upper steel pipe (D_t) = 6 m diameter (This system is currently used to support 3 MW wind turbines, Gerdes *et al.*, 2008) (**Fig. 4.4.a**).
    b. D_p = 6 m , D_t = 6 m (This system is used by NREL to support the 5 MW NREL wind turbine) (**Fig. 4.4.b**).
2) **Hybrid foundation system**:
    a. D_p = 4 m, D_t = 6 m and a precast concrete plate (D_{pl}) = 12 m (without rips) (**Fig. 4.4.c**).
    b. D_p = 4 m, D_t = 6 m and D_{pl} = 16 m (without rips) (**Fig. 4.4.c**).
    c. D_p = 4m, D_t = 6 m and D_{pl} = 16 m (with rips) (**Fig. 4.4.d**).

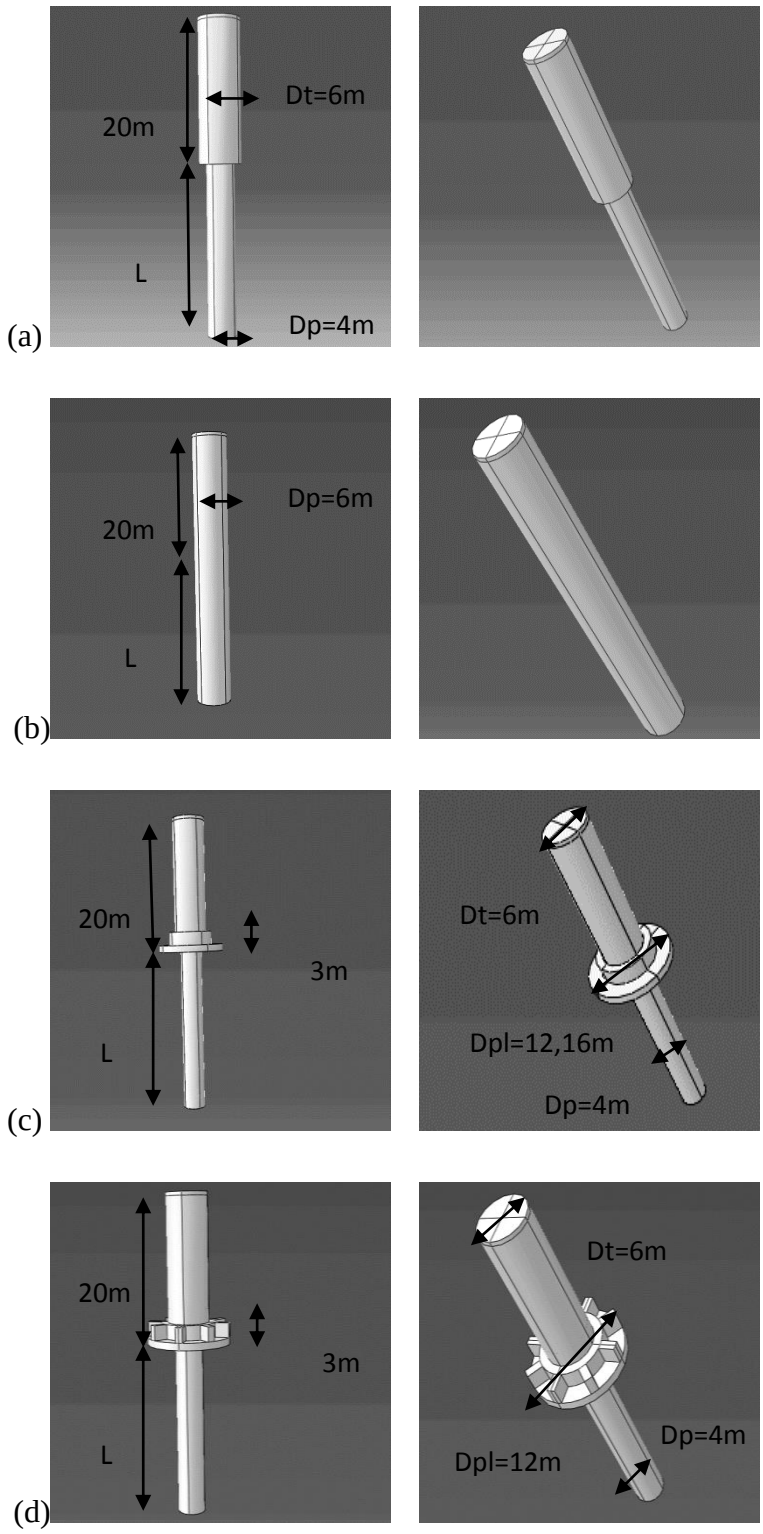

Fig. 4.4: Foundation systems considered in analysis (pile length L=8, 16, 24, 36 m for all systems): (a) pile system Dp=4 m, upper section Dt=6m; (b) pile system Dp=6 m, upper section, Dt = 6m; (c) Hybrid System with DPl=12, 16 m), (d) Hybrid system with ripped Plate.

4.5.1. Numerical model meshing

A sensitivity analysis was conducted to determine the suitable dimensions for the model and the size of elements. The horizontal boundary at the bottom of the model was placed at a distance at least three pile diameters below the pile toe. The vertical boundaries were located at a distance equal to 20 times the pile diameter from the centre of the model. The mesh was developed using the automatic sweep meshing technique and the medial axis algorithm, which is available in the Abaqus software (2009). The approximate global size of the element was in the range of 0.25-1.0 m depending on the size of soil model.

4.5.2. Boundary Conditions

Fixed translations in X, Y and Z directions were applied at the bottom boundary of the soil model. Fixed translations in both X, Y directions were applied at the vertical boundaries on the soil external surfaces. Interaction surfaces were applied at the interfaces between the elements representing the pile and adjacent soil that allow pile slippage and separation, which can properly simulate the tangential and normal behaviour. Both monopile sizes (D_p=4 and D_p=6m) and hybrid foundation systems (with rips and without) were analyzed considering different load cases. The geometrical dimensionless properties of the hybrid stems considered are given in **Table 4.3**.

Table 4.3: Dimensionless proportions of the hybrid systems considered in the analysis

D_{pl}/D_p=3,4	L=16 [m]	L=24 [m]	L=36 [m]
D_{plate} /L	0.75	0.5	0.33

D_{pl}: diameter of precast concrete plate, D_p:pile diameter,
L: embedded pile length.

4.5.3. Model Verification

A 36 m long steel pile with diameter, D_p = 6 m and wall thickness of 0.06 m was considered in the analysis similar to the monopile foundation system described in the NREL/TP-5000-48191 (Jonkman *et al.*, 2010), which was analysed using 15 different numerical models employing different computer programs. The monopile was installed in sand soil with an average friction angle, $\phi = 36°$ and submerged unit weight of γ_{sub} = 10 kN/m^3. A 3D numerical model was used to analyze the response of the monopile under horizontal force of 3000 kN at MSL (Jonkman *et al.*, 2010). The steel pipe and steel pile were assigned the following properties: yield strength, f_y = 240 MPa, Young's Modulus, E_s = 200 GPa and Poisson's ratio, $\nu = 0.3$. Lateral displacements at the mud level reported by (Jonkman *et al.*, 2010) was in the range of 15-20 mm. The calculated lateral displacement calculated in the current analysis under the same conditions was 16.6 cm, thus confirming the ability of the numerical model to properly simulate the behaviour of the foundation system.

4.6. RRESULTS AND ANALYSIS OF DIFFERENT FOUNDATION SYSTEMS

An extensive parametric study was performed to: i) evaluate the efficiency of the proposed hybrid system relative to the conventional monopile foundations; ii) evaluate the effect of considering different load components relative to the conventional approach of considering only the wind horizontal load and rocking moment. All foundation systems were considered to be installed in soil with the following properties: submerged unit weight, γ_{sub} = 9 kN/m^3, Young's modules, E = 30 MPa, Poisson's ratio, $\nu = 0.3$, friction angle, $\phi = 30°$, dilation angle, $\psi = 1°$ and maximum yield stress of 0.001 kPa. (El-Marassi et al., 2008). The steel pipe and steel pile were assigned the

following properties: yield strength, f_y = 240 MPa, Young's Modulus, E_s = 200 GPa and Poisson's ratio, ν = 0.3.

4.6.1. Response to working loads (Serviceability Steady State Loading Serviceability)

All foundation systems including monopole, D_p=4m, monopole, D_p=6m, hybrid system, D_{pl} = 12, 16 m and hybrid system with ripped plate are modeled under working loads considering different pile lengths and subjected to 5C (two perpendicular horizontal loads, one vertical loads and two rocking moments). The values of these forces were obtained from (Jonkman *et al.*, 2009) for the 5MW NREL wind turbine.

Figure 4.5 shows the variation of U_{MSL} and U_{ML} for the five systems as well as their pile head rotation for different pile lengths. **Figure 4.5 (a)** indicates that adding the precast concrete plate to the monopile with D_p=4 m decreased U_{MSL} owing to increased lateral resistance, but this beneficial improvement diminished as the pile length increased. The results also show that the difference in response between the hybrid system with and without rips was small. However, the monopile with D_p=6 m exhibited slightly better performance than the hybrid system. **Figure 4.5 (b)** shows U_{ML} of different systems at the mud level. It is clearly noted from the figure that adding the precast concrete plate to the pile with D_p=4m increased its lateral resistance, and hence U_{ML} decreased. It is also noted that the hybrid system with rips exhibited better performance than the monopile with D_p=6m with pile length up to 30 m, after which the monopile with D_p=6 has slightly less displacement. **Figure 4.5 (c)** shows that the pile head rotation displayed the same behaviour for the different foundation systems as the case for the lateral displacement.

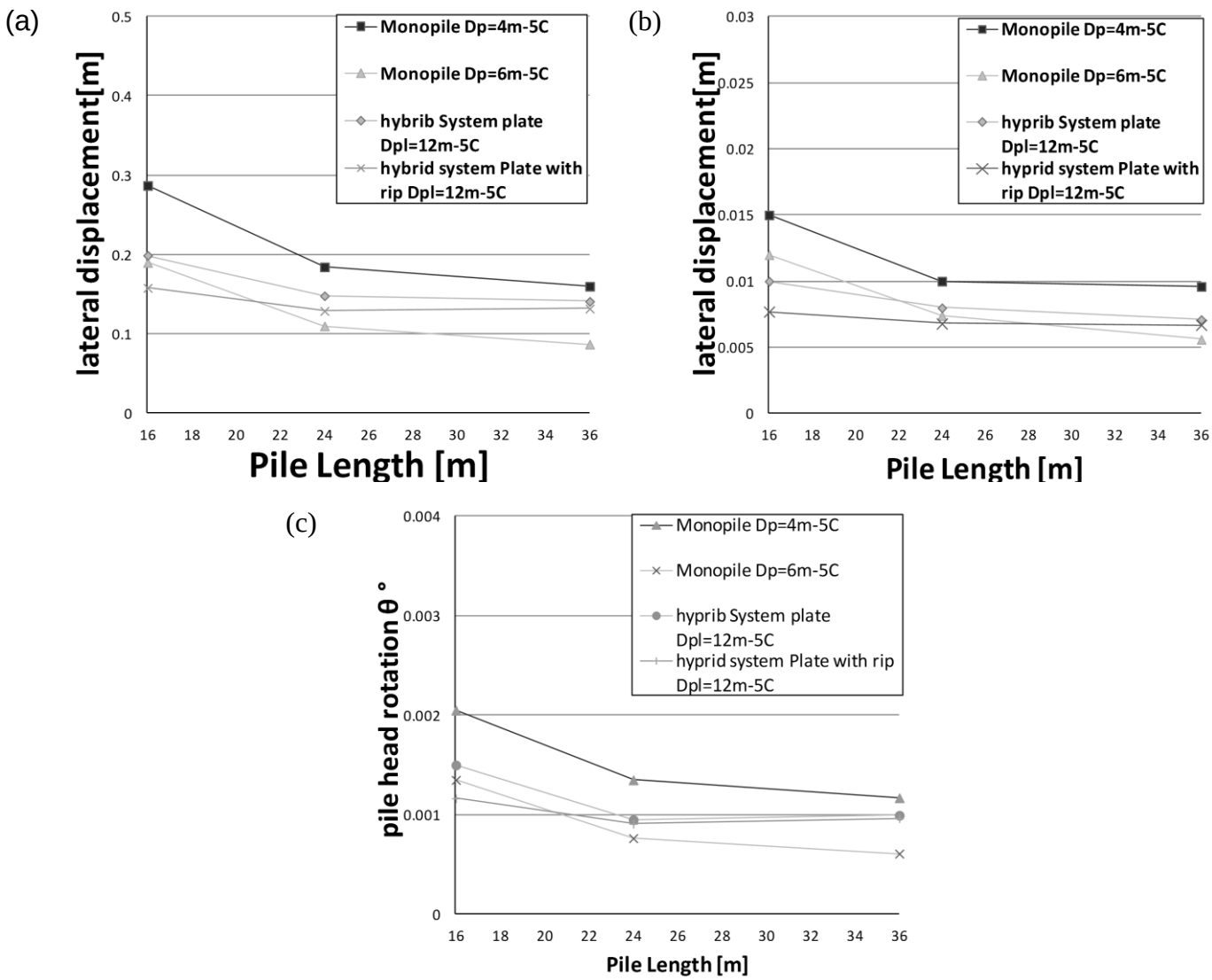

Fig. 4.5: Effect of different foundation systems under working load components 5C on: (a) lateral displacement at MSL; (b) lateral displacement at ML; and (c) pile head rotation θ_{ML}.

4.6.2. Response to ultimate loads

Five different foundation systems (as shown in **Fig. 4.4**) installed in water height of 20 m were investigated. More than 60 cases of loading were analyzed considering different load combinations, foundation systems and pile lengths**.** The lateral displacement was calculated at the mean see level for foundations with different pile lengths**.**

Figure 4.6 shows the lateral displacement of different foundation systems at MSL (U_{MSL}) for different ultimate load components combinations: (a) 2C, (b) 3C and (c) 6C. As shown in **Fig. 4.6**, the monopile (D_p=4 m), as expected, displays the largest displacements for all pile lengths considered due to its smaller diameter, and hence lowest lateral and rocking stiffness. Both hybrid systems (with and without rips and D_{pl} = 12, 16 m) displayed lateral displacement less than the monopile (D_p=4 m) system due to their increased lateral resistance attributed to the contributions of the plate, which is relatively large for the case of short piles. However, the results show that the effect of the pile diameter on the lateral resistance of the system is more significant as the pile length increases for the range of pile length considered in this study. This is demonstrated for the case of pile length of 36 m (i.e. B/L=0.33), where the monopile with D_p= 6m experienced lateral displacement lower than that experienced by the hybrid systems with D_p = 4m. It is also noted that the hybrid system with rips displayed lower displacement than the plate without rips due to the stiffening effect of the ribs on the upper part (wind turbine shaft) of the hybrid system.

Figure 4.7 shows the effect of different foundation systems on lateral displacement at mud level (U_{ML}) for different ultimate load components: (a) 2C; (b) 3C and (c) 6C. The results demonstrated the same trend as that observed for the lateral displacement at the mean sea level for different systems, but with much smaller displacement values. Figure 6 shows that the hybrid system had smaller displacement values for pile length of up to approximately 30 m. However, the hybrid system with rips exhibited lower U_{ML} than the case of monopole with D_p=6 for the most realistic (and demanding) loading case, 6C, for pile length, $L \leq 31$ m. At L=36 m, the difference was about 22% increase in U_{ML} for the hybrid system. This is because the response at ML is

dominated by lateral stiffness of the embedded pile, which is greatly affected by the pile diameter and less so by the footing plate.

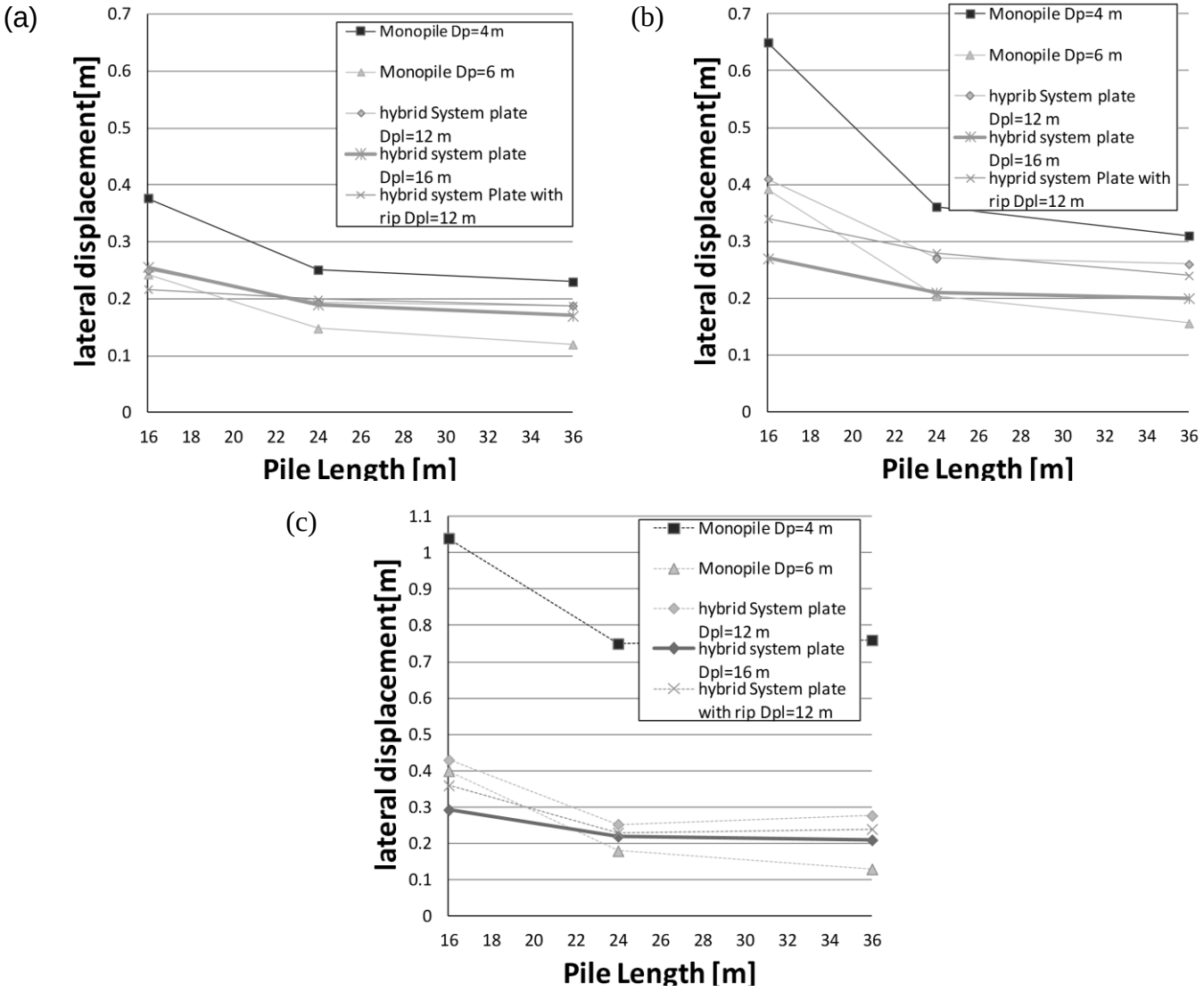

Fig. 4.6: Effect of different foundation systems on lateral displacement at MSL for different ultimate load components: (a) 2C, (b) 3C and (c) 6C.

On the other hand, the hybrid system with D_{pl} =16 m showed lower U_{ML} than the monopile with D_p=6 m for the cases 3C and 6C, which clearly demonstrated the advantage of the hybrid system with optimized D_{pl}/D_p ratio. However, for the case of 2C (i.e. neglecting vertical forces), the monopile system with D_p=6m displayed better performance. This is attributed to the fact that

neglecting the vertical force reduced the confining pressure acting on the soil beneath the plate and around the upper portion of the pile, hence reducing the stiffness of the system. It is, therefore, important to consider the realistic loading case in the design of wind turbine foundations.

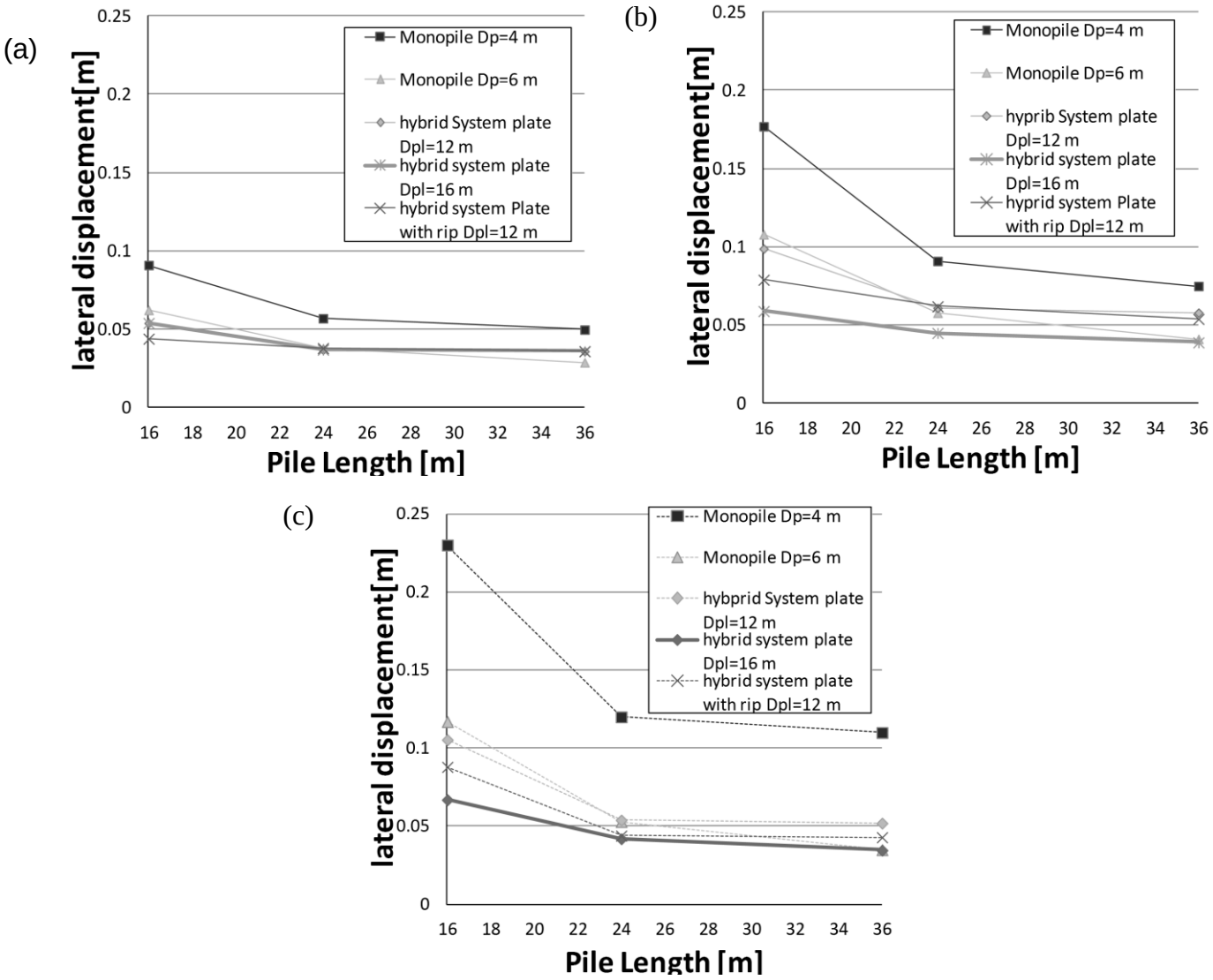

Fig. 4.7: Effect of different foundation systems on lateral displacement at ML for different ultimate load components: (a) 2C, (b) 3C and (c) 6C.

Figure 4.8 shows the pile head rotation, θ_{ml}, of different foundation systems considering different ultimate load components: (a) 2C, (b) 3C and (c) 6C. It is clear that the criteria specified by DNV-OS-J101 (2011) (i.e. pile head rotation < 0.5°) is satisfied. However, the monopile with

D_p=4 m displayed the largest rotation. Both the hybrid system with and without rips displayed nearly the same behaviour with increasing the pile length. Moreover, the hybrid system with D_{pl} =16 demonstrated the lowest rotation at ML, thus confirming its superior performance.

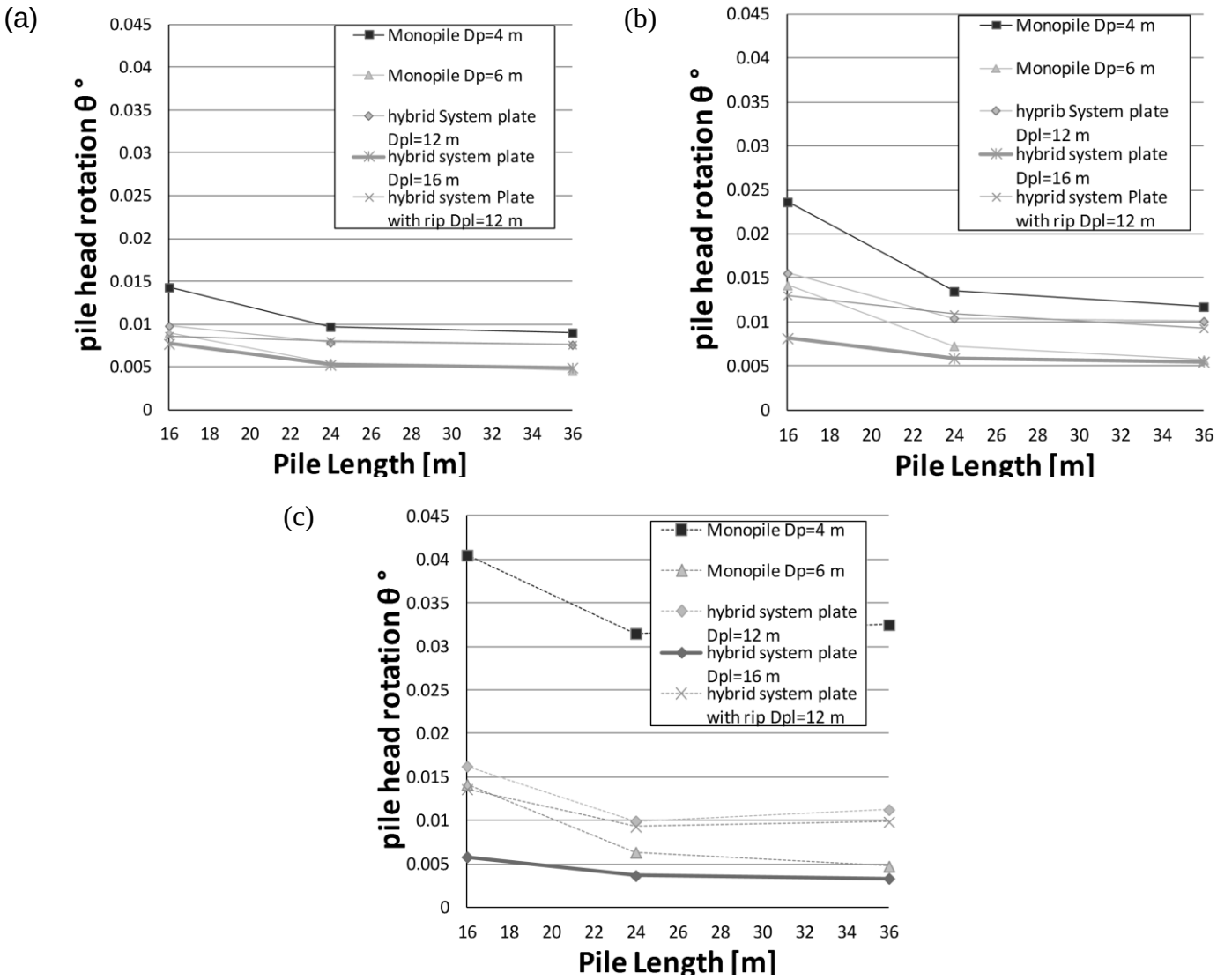

Fig. 4.8: Effect of different foundation systems on pile head rotation θ_{ML} for different ultimate load components: (a) 2C, (b) 3C and (c) 6C.

Figure 4.9 shows the pile head settlement, V_{ml}, of different foundation systems considering different ultimate load components: (a) 2C, (b) 3C and (c) 6C. The hybrid system with plate Dpl=16 m gives the lowest vertical settlement under 2C, 3C and 6C due to the participation of the

plate into the resistance of the vertical loads. On the other hand, the monopile D_p= 4m experienced the highest vertical settlement due to its small pile diameter. The favourable effect of the plate was further illuminated for higher load values.

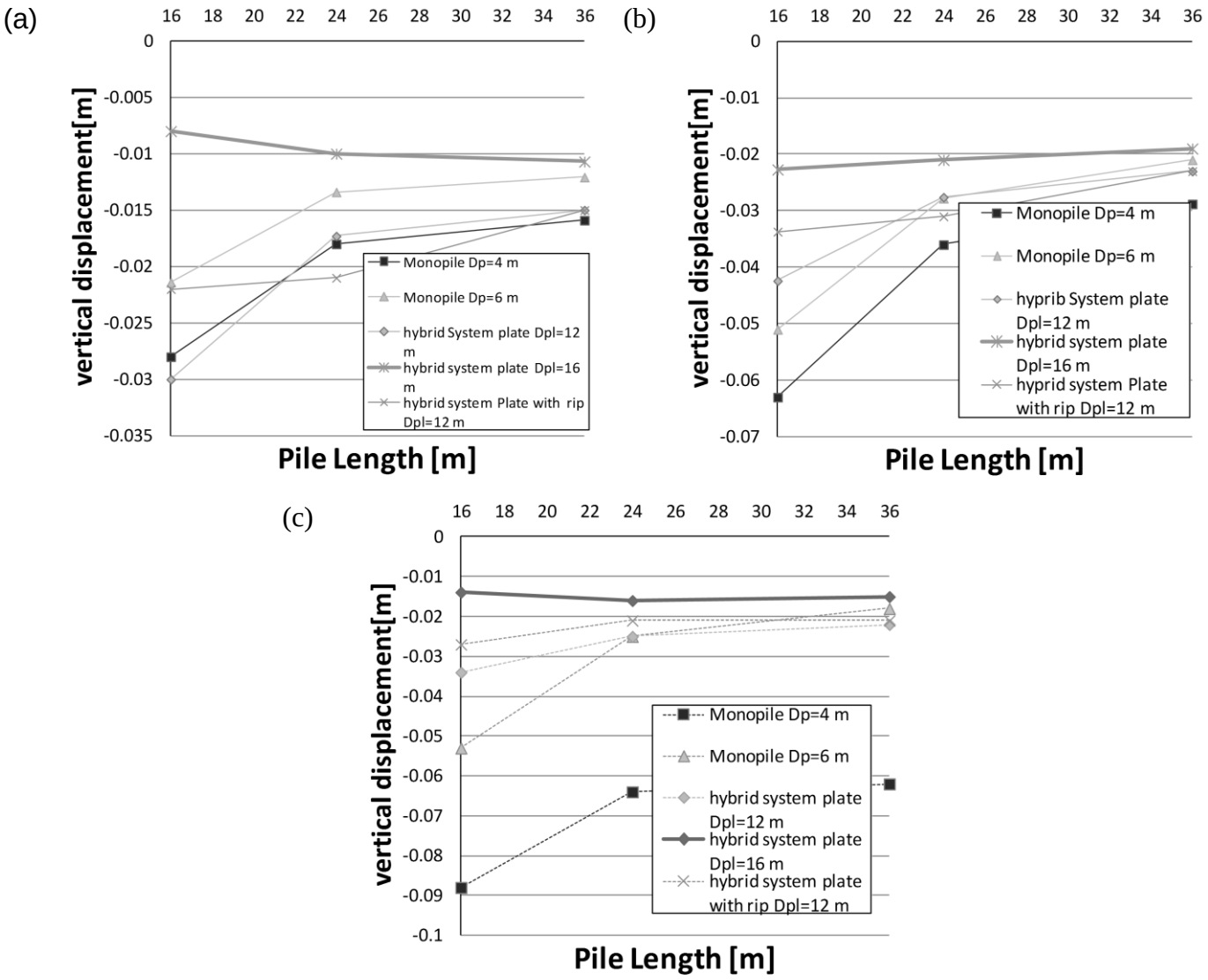

Fig. 4.9: Effect of different foundation systems on pile head vertical settlement V_{ML} for different ultimate load components: (a) 2C, (b) 3C and (c) 6C.

The standard practice in wind turbine foundation analysis under wind loading conditions is to consider only two load components, i.e., horizontal load and rocking moment. However, the actual loading condition, as verified by the wind tunnel testing (Abdelkader *et al.*, 2013), involves 6 load components. It is important to evaluate the effect of all loading components on the response of the wind turbine. The calculated responses considering different load combinations are shown in **Figs. 4.10 to 4.12**, including lateral displacements at MSL and ML as well as pile head rotation for different Foundation systems. It is clearly noted from the figures that considering 2C components only can grossly underestimate the lateral displacement of the wind turbine, both at MSL and ML. While we can see that in increasing the system stiffness both 3C and 6C can be close.`

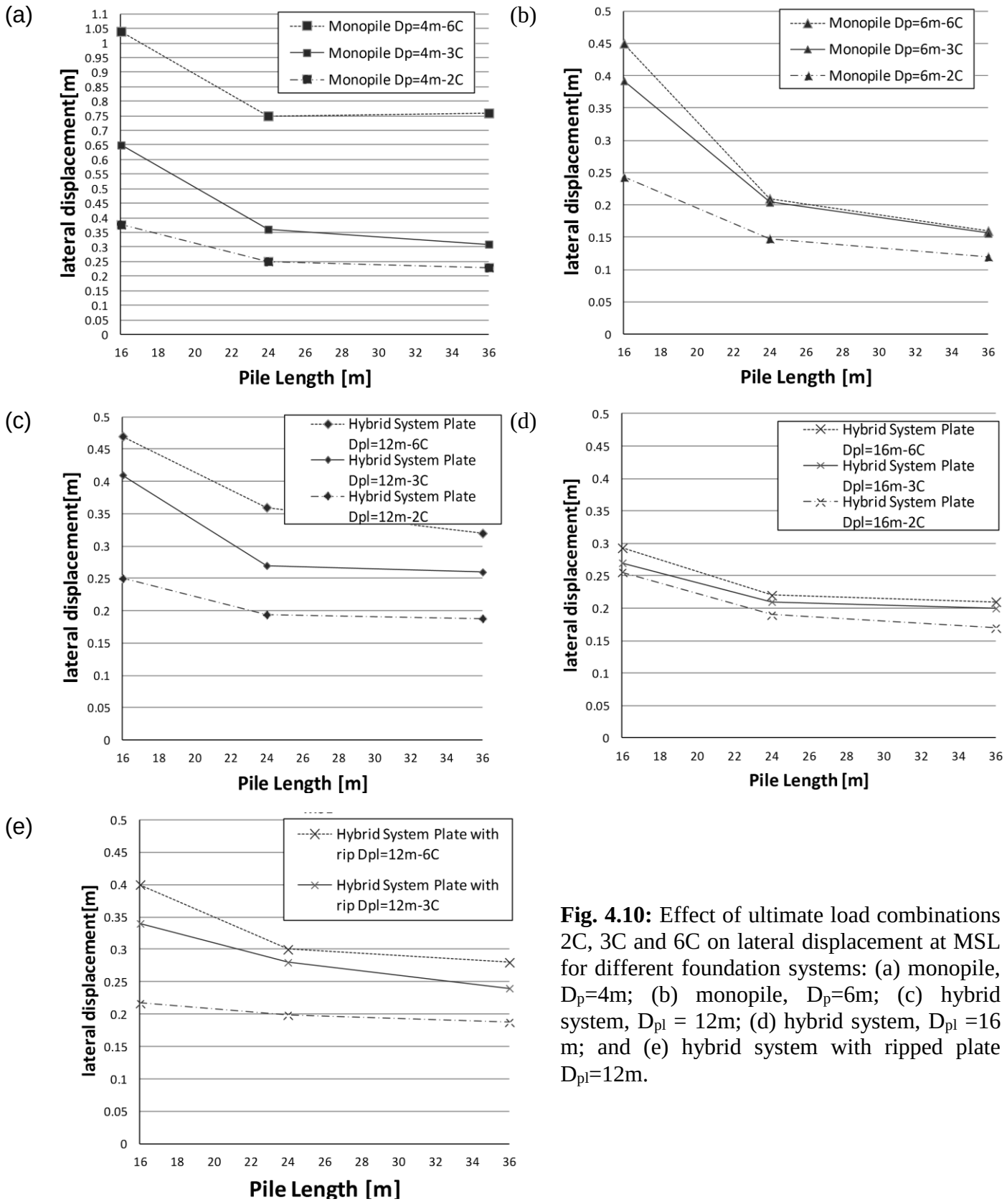

Fig. 4.10: Effect of ultimate load combinations 2C, 3C and 6C on lateral displacement at MSL for different foundation systems: (a) monopile, D_p=4m; (b) monopile, D_p=6m; (c) hybrid system, D_{pl} = 12m; (d) hybrid system, D_{pl} =16 m; and (e) hybrid system with ripped plate D_{pl}=12m.

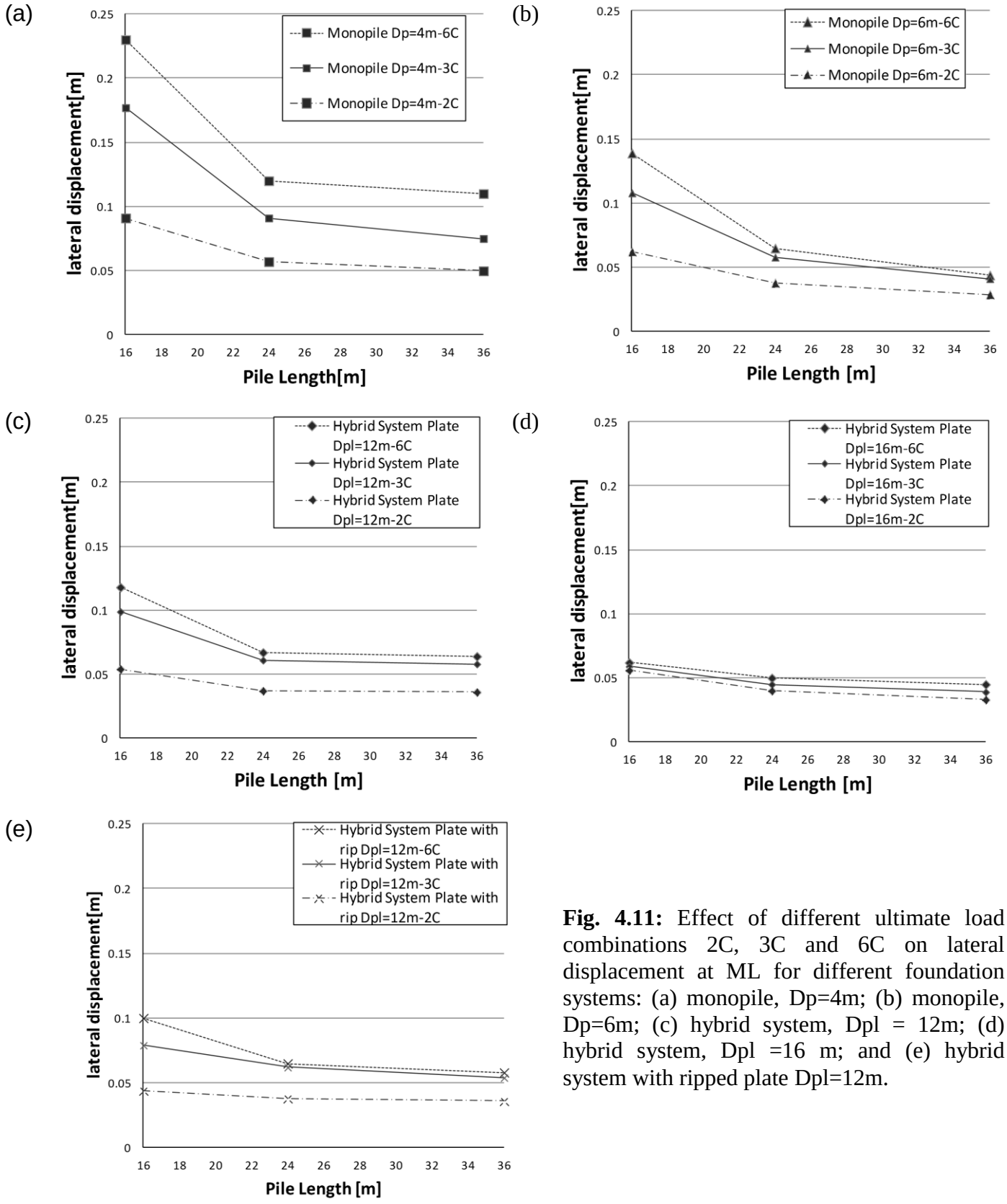

Fig. 4.11: Effect of different ultimate load combinations 2C, 3C and 6C on lateral displacement at ML for different foundation systems: (a) monopile, Dp=4m; (b) monopile, Dp=6m; (c) hybrid system, Dpl = 12m; (d) hybrid system, Dpl =16 m; and (e) hybrid system with ripped plate Dpl=12m.

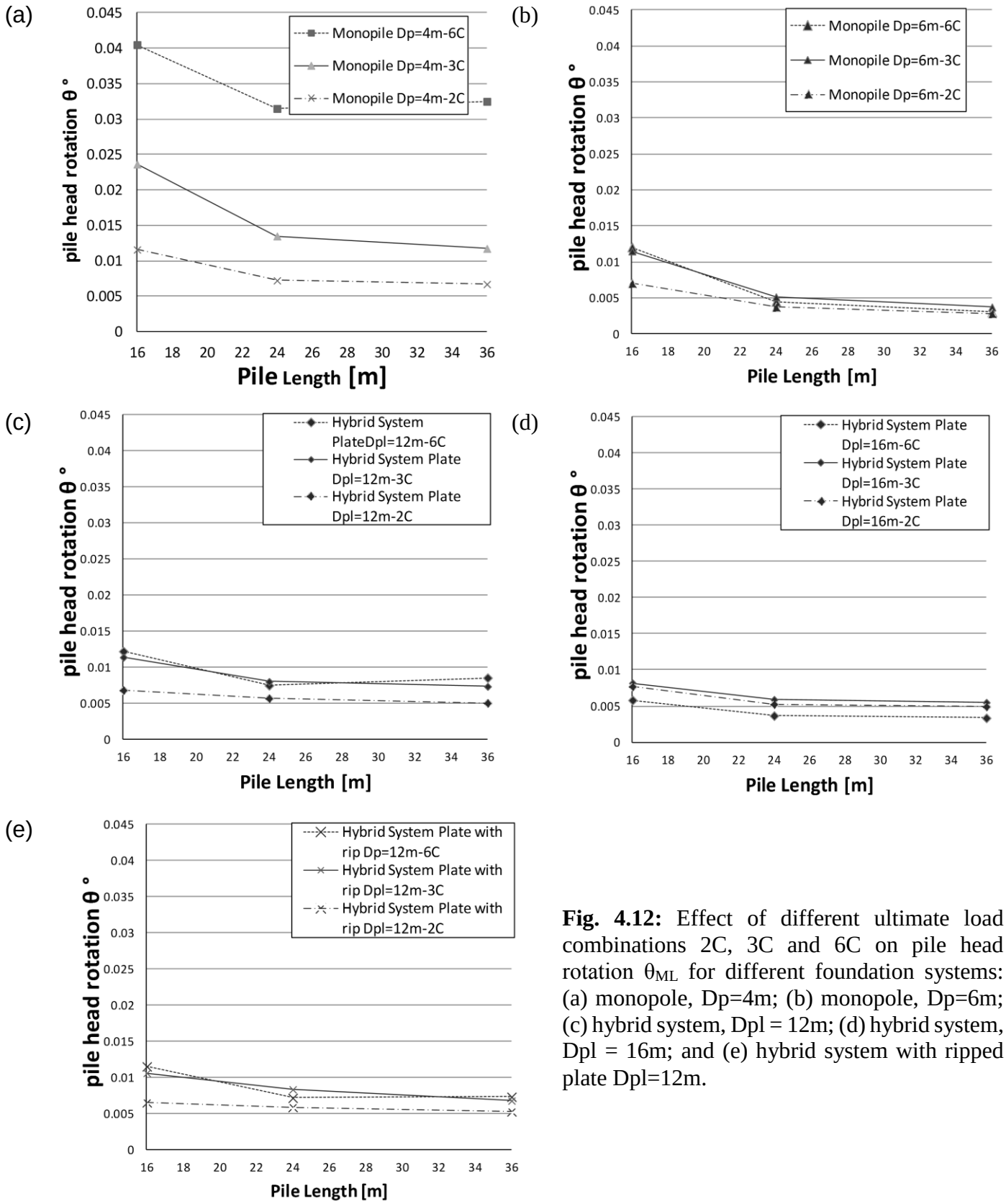

Fig. 4.12: Effect of different ultimate load combinations 2C, 3C and 6C on pile head rotation θ_{ML} for different foundation systems: (a) monopole, Dp=4m; (b) monopole, Dp=6m; (c) hybrid system, Dpl = 12m; (d) hybrid system, Dpl = 16m; and (e) hybrid system with ripped plate Dpl=12m.

4.7. CONCLUSIONS

The performance of the proposed hybrid system, which consists of a precast concrete plate and a central steel monopile, was evaluated considering different loading conditions. The hybrid system has the potential to reduce construction cost by employing a smaller pile. It can also be used to increase the capacity of an existing monopile foundation system by adding the precast concrete plate. A comprehensive numerical investigation was conducted involving 3D nonlinear finite element analysis using the computer program Abaqus (Hibbitt, 2009). The response of the hybrid system was calculated considering wind and wave loads pertaining to the 5MW wind turbine installed in 20 m water depth. The responses of the hybrid system were compared with the response of the monopiles with D_p = 4m and 6m and considering different pile lengths and static load conditions. The results of the analysis demonstrated that by adding the precast concrete plate, the lateral resistance of the monopile with D_p=4m increased sufficiently to provide comparable performance of monopole with D_p = 6m. The hybrid system was shown to meet the response requirements of the offshore wind turbine foundations according to DNV-OS-J101 (2011). Considering that the installation cost of 4m diameter pile could be significantly lower than the cost of installation of 6m diameter pile, these results demonstrate the potential of the hybrid system as an efficient foundation system for new wind turbines and an effective method for upgrading the lateral resistance of existing monopile foundations to facilitate upgrading the wind turbines from 3MW to 5MW. The analysis for different load combinations demonstrated that the conventional approach, which considers only two components (horizontal load and rocking moment) can grossly underestimate the response of the wind turbine system.

4.8. REFERENCES

ABAQUS (2009) documentation.

Abdelkader, A., Aly , A.M., Bitsuamlak, G., El Naggar, M.H. (2013), “Evaluation of Design Wind Loads for Wind Turbine Foundations”, Wind and Structures.

Byrne, B.W. and Houlsby, G.T. (2003), “Foundations for Offshore Wind Turbines”, Philosophical Transactions of the Royal Society of London, A(361), 2909-2930.

DNV-OS-J101, Offshore Standard, (2011), “Design of Offshore Wind Turbine Structures”, Electronic Version available at http://www.dnv.com/ (On Jan. 25, 2013)

El-Marassi, M., Newson, T., El Naggar, M.H. and Stone, K. (2008), “Numerical modelling of the performance of a hybrid monopiled-footing foundation”. Proceedings of 61st Canadian Geotechnical Conference, Edmonton, pp. 97-104.

Gerdes, G., Tiedemann, A., Zeelenberg, S, (2008). “Case Study: European Offshore Wind Farms - A Survey for the Analysis of the Experiences and Lessons Learnt by Developers of Offshore Wind Farms”, Pushing Offshore Wind Energy Regions.

Hameed, Z., Vatn, J. and Heggset, J. (2011), “Challenges in the reliability and maintainability data collection for offshore wind turbines“, Renewable Energy, 36(8), 2154-2165.

Houlsby, G.T. and Byrne, B.W. (2001), " Assessing Novel Foundation Options for Offshore Wind Turbines", Department of Engineering Science, Oxford University. No. of pages

Houlsby, G.T. (2003), “Modelling of Shallow Foundations for Offshore Structures”, Invited Theme Lecture, Proceeding. International Conference on Foundations, Dundee, Thomas Telford, pp 11-26.

International Standard, (2009), "Wind turbines – Part 3: Design requirements for offshore wind turbines", IEC 61400-3, Edition 1.0 2009-02.

Ibsen, L., Rune B. (2004), "**Design of a New Foundation for Offshore Wind Turbines**". Proceedings of IMAC-22: A Conference on Structural Dynamics, Dearborn, Michigan, USA. Society for Experimental Mechanics, p. 359-366

Jonkman, J., Butterfield, S., Musial, W., and Scott, G., (2009), "Definition of a 5-MW Reference Wind Turbine for Offshore System Development", National Renewable Energy Laboratory, Golden, CO, Technical Report, NREL/TP-500-38060.

Jonkman, J., Musial, W. (2010), "Offshore Code Comparison Collaboration (OC3) for IEA Task 23 Offshore Wind Technology and Deployment", Technical Report, NREL/TP-5000-48191.

Lozano-Minguez, E., Kolios, A.J., Brennan, F.P. (2011), "Multi-criteria assessment of offshore wind turbine support structures", Renewable Energy, 36(11), 2831-2837

Passon P., KÜhn, M. (2007), " OC3 – Benchmark Exercise of Aero-Elastic Offshore Wind Turbine Codes", Conference Paper , NREL/CP-500-41930.

Thomsen, J., Forsberg, T. (2007), "offshore wind turbine foundations - the cowi experience", proceedings of the 26th International Conference on Offshore Mechanics and Arctic Engineering, OMAE2007-29567.

CHAPTER FIVE

STRESSES AND CAPACITY OF HYBRID FOUNDATION SYSTEM OF WIND TURBINES

In this chapter, three-dimensional nonlinear finite element analyses were conducted to investigate the axial and lateral capacities of the hybrid foundation system proposed to support offshore wind turbines in comparison with the conventional monopile foundation. Four different foundation systems are analyzed, namely: monopiles with 4 and 6 m diameter; hybrid system with 4 m diameter pile and a 12 m plate; and hybrid system with 4 m diameter pile and a 12 m plate stiffened with ribs. The stresses in the soil around the pile and underneath the concrete plate are evaluated to aid in understanding the system behaviour. More than 40 3D nonlinear models were established and analyzed using the general purpose finite element program ABAQUS (Hibbitt et al., 2008) to simulate the different foundation systems considering displacement controlled loading conditions.

5.1. INTRODUCTION

Wind Industry is growing rapidly worldwide to deal with the rising demands for green energy (Lozano-Minguez *et al.*, 2011; Hameed et al., 2011). Offshore wind farms are considered a suitable option for wind farms, given the limitations on onshore ones or to take advantage of the high wind intensity at offshore locations. The cost of offshore foundations for these developments is a significant ratio of the overall installed costs, as it mounts for about 35% (Byrne and Houlsby,

2003). This may render the offshore wind turbine installations economically inefficient, which fuels innovation to introduce cost-effective foundation options.

Therefore, this study investigates a hybrid foundation system that has the potential to be economically advantageous, while performing similar to or even better than the conventional foundation options. The hybrid foundation system consists of a precast reinforced concrete plate attached to a steel pile. The addition of the precast concrete plate is envisioned to increase both the lateral and rotational stiffness of the foundation. Furthermore, the plate will further increase the lateral capacity of the hybrid foundation system over that of the monopile.

Offshore wind turbines foundations have to withstand significant lateral wind loads, in addition to other environmental loads arising from waves and current. Initial sites proposed for offshore wind farms are usually located in shallow waters, but with ever growing wind turbine sizes sites with larger water depth are being considered. These sites present foundation design engineers with major challenges to provide efficient, reliable and constructible foundation systems in deep water. In addition, the engineering expertise in the design and construction of foundations of marine structures came mainly from platforms serving in the oil industry. However, the platforms experience relatively high vertical loads compared to the environmental horizontal loading. In wind turbines, on the other hand, the foundations experience relatively small vertical loads compared to the horizontal environmental loads, which imposes different demands on their design.

5.2. OBJECTIVES AND SCOPE OF STUDY

The main objective of this chapter is to evaluate the stresses in the steel pile, concrete plate and adjacent soil to ensure suitability of the proposed hybrid foundation to meet the requirements of the ultimate limit state for foundations supporting a 5 MW wind turbine. The stresses in the soil below the concrete plate, along the pile shaft and below its toe are evaluated and employed to calculate the hybrid system axial and lateral capacities. The analysis is conducted using 3D nonlinear finite element model and the extreme wind loads considered in the analysis were evaluated from the wind tunnel tests reported in Chapter 3. Different wind and wave loads combinations were considered in the analysis to ensure realistic representation of the field conditions. The results are used to develop some design guidelines for the implementation of this novel foundation system in offshore wind turbine applications.

5.3. DESCRIPTION OF HYBRID FOUNDATION SYSTEM

As described in Chapter 4, the hybrid system involves a hollow steel pile connected to a precast concrete cap. This system is intended for installations in offshore water with depth of 20 m. The system is composed of three parts: ***Part 1*** is a 4 m diameter steel driven pile with a wall thickness of 0.08 m, and variable lengths (16, 24 and 36 m); ***Part 2*** includes a combination of a 6 m-diameter steel pipe 20 m long with 0.08 wall thickness, and a concrete precast concrete cap. Different configurations of the precast concrete cap are considered: a circular plate of a minimum thickness of 1 m, a circular precast concrete plate with eight rips of 1 m width, and a circular plate with 8 ribs of 2 m width. Part 3 is cylindrical grout infilled offshore to connect parts 1 and 2. The tower of the wind turbine will be connected to the top of the upper steel pipe.

The upper steel pipe (20 m long) weighs about 2376 kN and the concrete plate weighs approximately 2905 kN. The steel pipe will be connected at its base to the precast concrete cap employing steel shear connectors that will transfer the loads between the two parts. The upper part of the foundation system (steel pipe and precast concrete plate) will be connected to the driven steel pile using cylindrical grout (**Part 3**) infilled offshore reinforced with steel bars. The components fo the hybrid system are shown schematically in **Fig.5.1.**

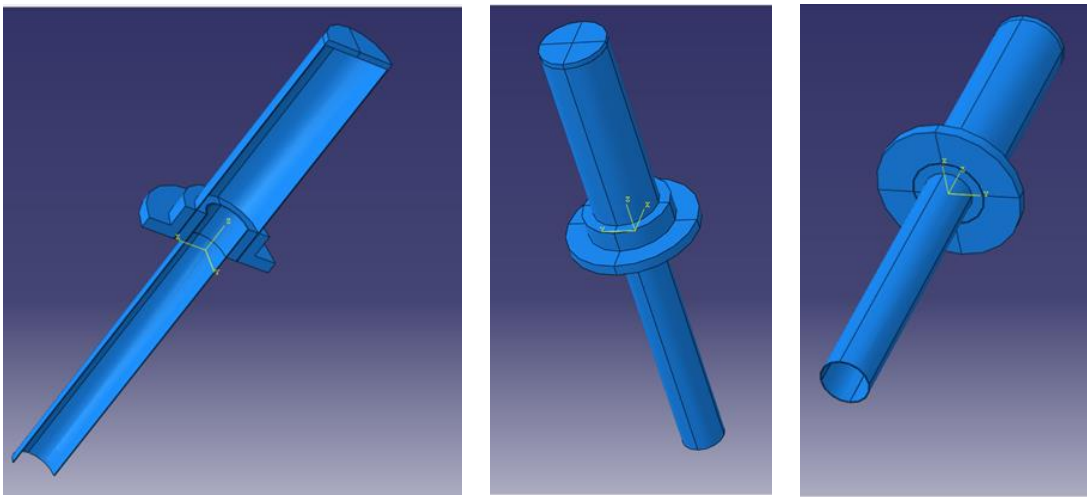

Fig. 5.1 Hybrid foundation with no rips system cross section and isometric view.

5.4. NUMERICAL MODELING

The numerical modeling was conducted using the finite element method. A 3-dimensional nonlinear finite element model of the foundation system and soil was established employing the ABAQUS program (Hibbitt et al., 2008). The soil and components of foundation system were modeled using 3D deformable solid elements with different material models. The sand soil was simulated as linear elastic perfectly plastic material considering the Mohr-Coulomb failure criterion, with the following properties: submerged unit weight, γ_{sub} = 9 kN/m^3, Young's modulus,

E = 30 MPa, Poisson's Ratio, $\nu = 0.3$, Friction angle, $\theta = 30°$, dilation angle, $\psi = 1°$. The steel pipe and steel pile were also simulated as linear elastic perfectly plastic material considering the Mohr-Coulomb failure criterion with the following properties: yield strength, $f_y = 240$ MPa, Young's Modulus, $E_s = 200$ GPa and Poisson's ratio, $\nu = 0.3$. For the concrete plate the properties was as unit weight $\gamma = 25$ kN/m^3, Young's Modulus, $E_s = 22$ GPa and Poisson's ratio, $\nu = 0.2$. The interaction properties were considered between different materials to ensure realistic simulation including tangential and normal behavior between pile and soil, concrete plate and steel pipe and concrete plate and steel pile.

In order to evaluate the performance of hybrid system, four different foundation systems were analyzed. The different systems considered are (shown in **Fig 5.2**):

1) Monopile foundation system 1 (Fig. 5.2a): a pile 4 m in diameter and an upper steel pipe 6 m in diameter. This system is currently used to support 3 MW wind turbines (Gerdes et al., 2008).

2) Monopile foundation system 2 (Fig. 5.2b): a pile 6 m in diameter and an upper steel pipe 6 m in diameter. This system is suggested by NREL to be suitable to support the 5 MW NREL wind turbine.

3) Hybrid foundation system 1 (Fig. 5.2c): a precast concrete plate 12 m in diameter attached to a pile 4 m in diameter along with an upper steel pipe 6 m in diameter.

4) Hybrid foundation system 2 (Fig. 5.2d): a precast concrete plate 12 m in diameter stiffened with ribs, attached to a pile 4 m in diameter along with an upper steel pipe 6 m in diameter.

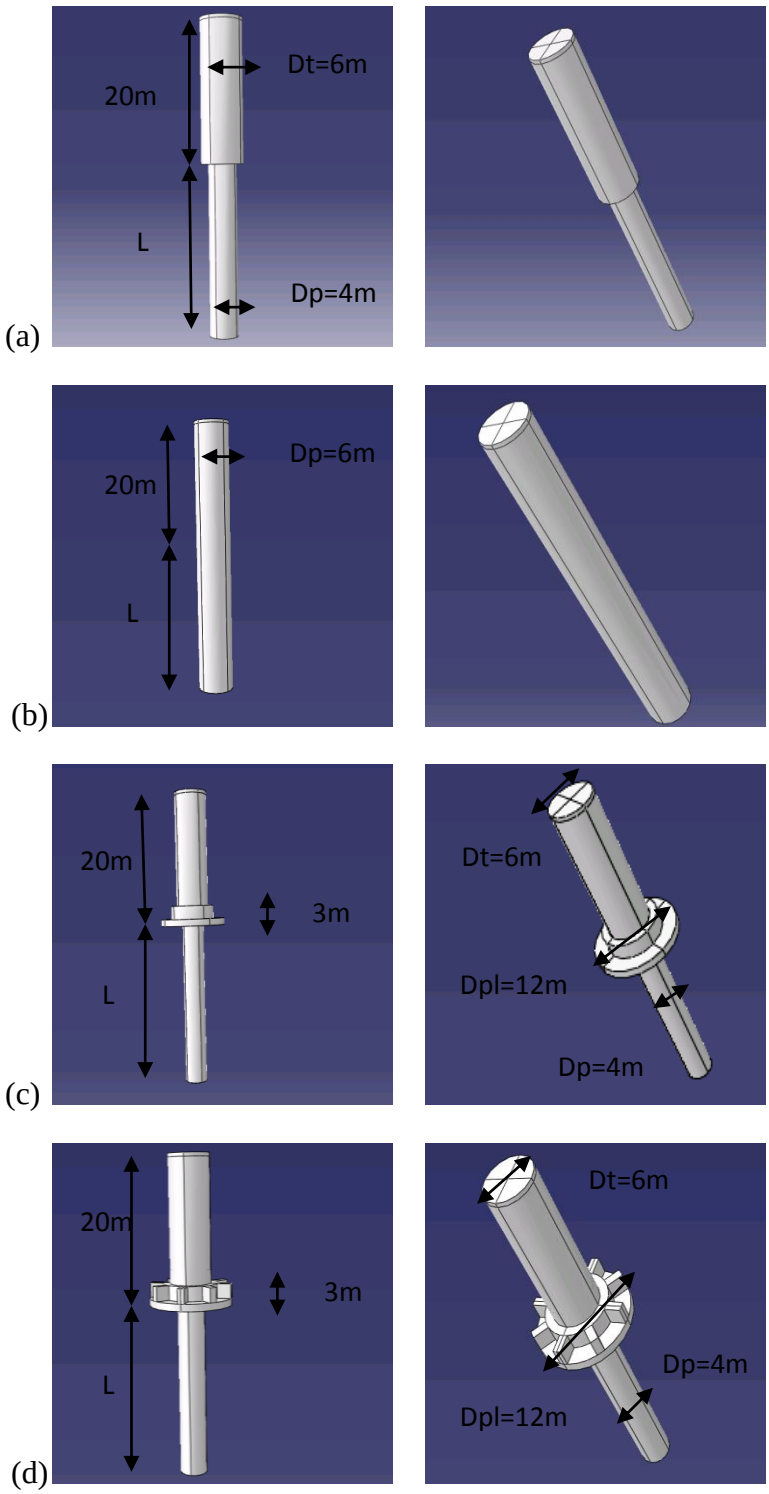

Fig. 5.2 Foundation systems considered in the analysis (pile length L=8, 16, 24, 36 m for all systems): (a) Monopile D_p=4 m, upper section D_{pl}=6m; (b) Monopil D_p=6 m, upper section, D_{pl} = 6m; (c) Hybrid System with plate, (d) Hybrid system with ribbed plate.

5.4.1. Numerical model meshing

A sensitivity analysis was conducted to determine the suitable dimensions for the model and the size of elements. The horizontal boundary at the bottom of the model, which prevents the movement in three directions, was placed at a distance equal to three pile diameters below the pile toe. The vertical boundaries, which allow only vertical movement, were located at a distance equal to 20 times the pile diameter from the centre of the model. The finite elements were primarily hex shaped and the mesh was developed using the automatic sweep meshing technique and the medial axis algorithm which is available in ABAQUS software. The approximate global size of the element was in range of 0.25-1.0 m depending on the size of soil model. The finite element mesh is presented schematically in Fig. 5.3.

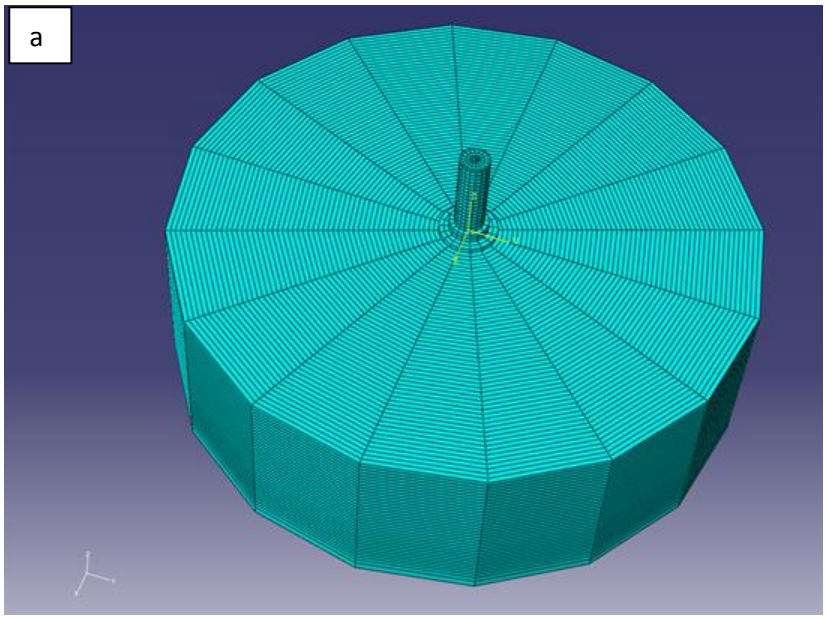

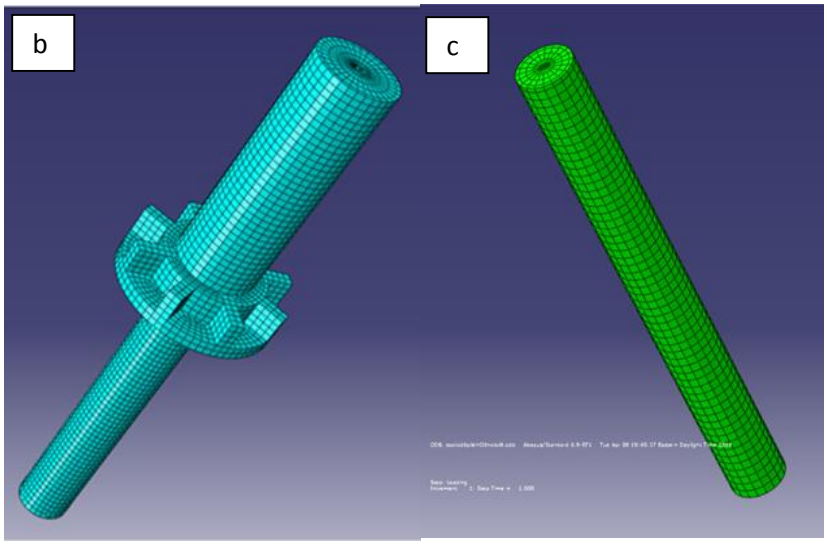

Fig. 5.3 finite element model: a) soil model; b) hybrid system element meshing; c) monopole element meshing.

5.4.2. Boundary Conditions

Fixed translations in X, Y and Z directions were applied at the bottom boundary of soil model. Fixed translations in both X, Y directions were applied at the vertical boundaries on the soil external surfaces. Interaction surfaces were applied at the interfaces between the elements representing the pile and adjacent soil that allow pile slippage and separation, which can properly simulate the tangential and normal behaviour. Both monopiles (D_p=4, D_p=6m) and hybrid foundation systems (with and without ribs) were analyzed considering different load cases. The geometrical dimensionless properties of the hybrid systems considered are given in **Table 5.1**.

Table 5.1 Dimensionless proportions of the hybrid systems considered in the analysis

D_{pl}/D_p=3	L=16 [m]	L=24 [m]	L=36 [m]
D_{pl}/L	0.75	0.5	0.33

Where: D_{pl} is precast concrete plate diameter, D_p pile diameter, L embedded pile length.

5.4.3. Model Verification

For the purpose of verification, a 36 m long steel pile with diameter of 6 m and wall thickness of 0.06 m was considered in the analysis, which is similar to the monopole foundation system described in the NREL/TP-5000-48191 (Jonkman, 2010). The monopile was installed in sandy soil with an average friction angle, $\phi = 36°$ and submerged unit weight of $\gamma_{sub} = 10$ kN/m^3, and was analysed using 15 different numerical models employing different computer programs. In the current study, a 3D numerical model was used to analyze the response of the monopile under horizontal force of 3000 kN at mean see level. Jonkman (2010) reported horizontal displacements at the mud level in the range of 15-20 mm. The calculated horizontal displacement calculated in the current analysis under the same conditions was 16.6 mm, thus confirming the ability of the numerical model to properly simulate the behaviour of the foundation system.

5.5. SYSTEM STRESSES AND CAPCITY.

After verification of the numerical model technique, the analysis was conducted for the different foundation systems with the geometrical and material properties and installed in the sand with properties as described previously. The different foundation systems were subjected to displacement controlled loading. The different systems were subjected to vertical displacement centrically at the top of the steel pipe, and increased incrementally to a maximum of 0.5 m In addition, lateral loading was applied at the top of the steel pile.

5.5.1 Axial load *capacity.*

Under vertical loads, the pile skin friction mobilizes as soon as the pile/hybrid system is loaded. With the increase of the vertical load, a failure zone initiates at the edges of the footing and extends downwards and outwards. Similar behaviour occurs at the pile toe.

For the single pile, the friction force along the pile shaft depends on the soil properties and the surface area of the pile, which can be calculated from:

$$\boldsymbol{Q_{ult} = \int K_s \tan \delta \sigma_v \, C d_z} \qquad \textbf{Eq. 5.1}$$

Where for most design purposes, $\delta = (2/3\ \phi)$; K_s is lateral earth pressure coefficient t after pile installation, which increases with the volume displaced of the soil. K_s =1-2 for driven displacement piles.

For a plate foundation, at failure rupture plane beneath the footing can be divided into three zones: triangle elastic zone right beneath it, radial shear zone and finally triangle passive zone.

Considering the shear resistance contributions from the three zones, the bearing capacity of circular plate can be calculated by *Terzaghi*, (1943):

$$\boldsymbol{Q_{ult} = 1.3 c' N_c + \sigma' N_q + 0.3 \gamma' D_{pl} N_\gamma} \qquad \textbf{Eq. 5.2}$$

Where: N_c cohesion factor, N_q surcharge factor, N_γ own weight factor, γ' soil effective unit weight, D_{pl} plate diameter, c' soil cohesion beneath the base and σ' effective vertical stress.

For long piles, most of the pile will be outside the elastic zone. Stone et al. (2007) proposed that the capacity of the hybrid foundation system should be approximately the sum of the capacity of

its two components in case of long piles. However, for hybrid systems with short piles the stress zones overlap, which prevents the development of full capacity of the hybrid system components, and consequently its capacity is less than the sum of two components capacity.

The finite element analysis involved 20 different cases for the considered foundation systems, including monopoles with different diameter, D_p = 4 and 6 m, and hybrid systems with different plate diameter, D_{pl} = 12 and 16 m. All models were subjected to displacement controlled loading until the displacement at the top of the pile reached 500 mm. in order to study the capacity of the systems. This allowed the evaluation of the gain in the vertical capacity of the hybrid system by adding the concrete plate, which can be attributed to the capacity of the plate as well as the increase in the frictional resistance of the pile shaft due to the increase in the confining pressure within the influence zone of the plate.

The vertical displacement is applied as a concentrated load at the pile head. **Figures 5.4, 5.5 and 5.6** display the obtained load-displacement curves for the different foundation systems analyzed. As can be noted from Figs. 5.4 to 5.6, the monopoles exhibited signs of failure (i.e. increased displacement with a small increase in applied load), while the hybrid foundation systems continued to resist much higher loads without exhibiting any sign of failure. This demonstrates that the hybrid foundation system does experience brittle failure, as it may be the case for monopoles. Also, comparing the results in Figures 5.4 to 5.6, it is noted that the maximum load resisted by the monopoles increased almost proportional to the increase in the pile length. However, for the hybrid foundations, the load increased as the pile length increased, but not at the same rate as the case for the monopoles. This is attributed to overlapping of the stress zones of the plate and the pile. It is

also noted that the increase in the plate diameter from 12 m to 16 m, resulted in stiffer response and larger vertical capacity.

The vertical capacity of foundations is typically evaluated from load-displacement curves using some specified criteria. For large diameter piles employed to support offshore structures, the pile capacity is usually determined using the method of intersection of two tangential lines (DNV), which is indicated in Figs. 5.4 to 5.6. It is clear from the figures that the capacity values for the hybrid foundation systems are much higher than those for the monopoles, which indicates the potential advantage of the hybrid foundation systems for supporting offshore wind turbines as well as other offshore structures.

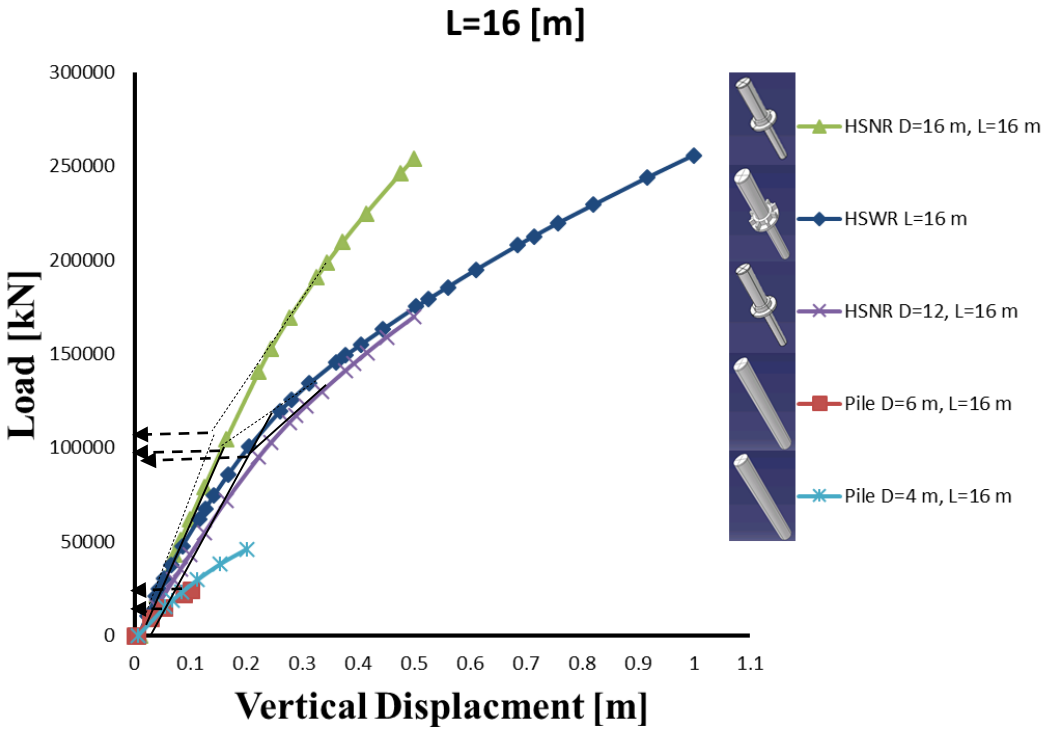

Fig. 5.4: Vertical bearing capacity of different systems with pile length *L*=16m.

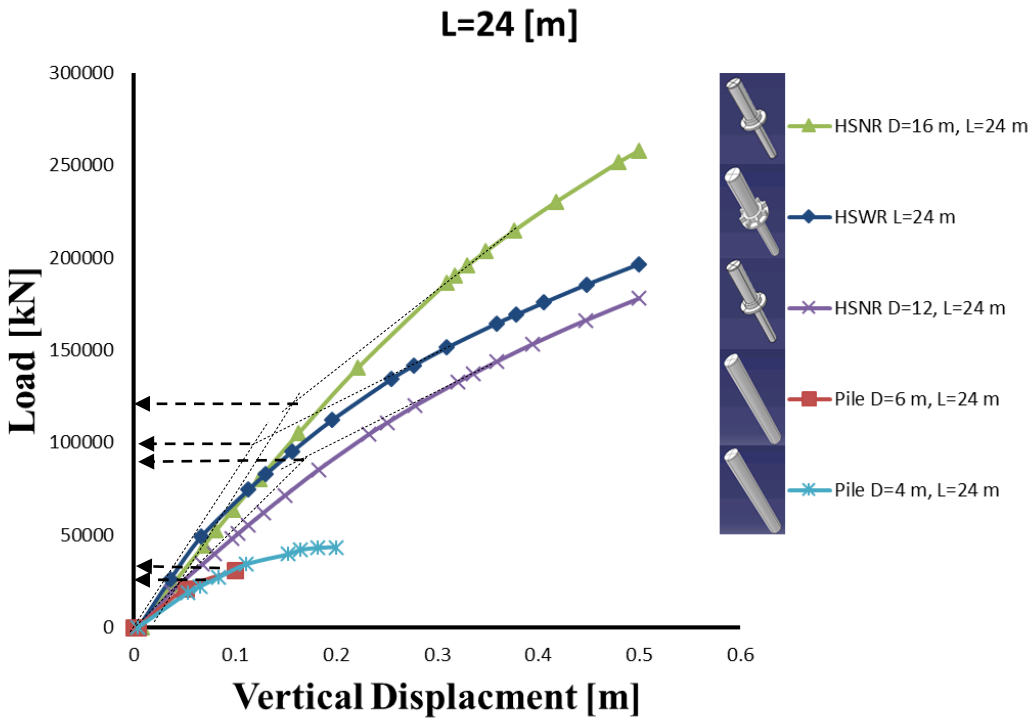

Fig. 5.5: Vertical bearing capacity of different systems with pile length *L*=24m.

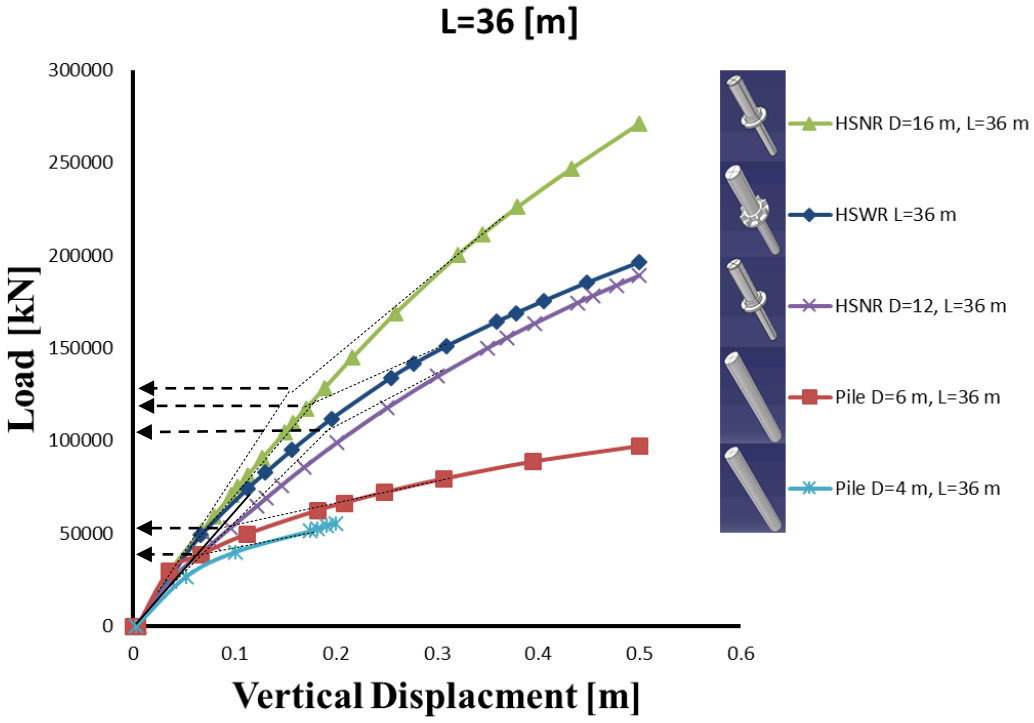

F ig. 5.6: Vertical bearing capacity of different systems with pile length *L*=36m.

Table 5.2 shows the increase in vertical capacity of different systems compared to the vertical capacity of monopile with D_p = 4 m. it can be noted from Table 5.2 that the hybrid system with no ribs (HSNR) with D_{pl} = 16 m has the greatest increase in vertical capacity due to the larger plate diameter followed by the hybrid system with ribs (HSWR) with D_{pl} = 12 m followed by HSNR with D_{pl} = 12 m. Also, the ratio of capacity increase for the 6 m monopile compared to the 4m monopile increased as pile length increased. This is attributed to increased resistance of cohesionless soil along the lower portion of the pile, as well as the contribution from the bearing resistance at the pile toe. The increase in hybrid systems capacity compared to the monopile is higher for short pile length, as in shorter pile the effect of the plate are maximum due to the increase of confining pressure along the pile shaft, and consequently the pile frictional resistance along the pile shaft. This effect decreases when the pile length increases beyond the plate influence zone.

Table 5.2: The increase in vertical capacity compared to the monopile D_p=4 m

	Monopile D_p=4m Capacity (kN)	**Monopile D_p=6m**	**HSNR D_{pl}=12m**	**HSWR D_{pl}=12m**	**HSNR D_{pl}=16m**
L=16 m	15000	20%	425%	450%	550%
L=24 m	25000	20%	320%	400%	480%
L=36 m	40000	42%	285%	348%	371%

To further explore the effect of the pile length on the response of the different foundation systems, **Figs. 5.7 to 5.11** compare the load-displacement curves for different systems with varying pile length. It can be noted from the figures that the effect of increase in pile length is minimal on the stiffness and response of hybrid foundations. This more so for the hybrid system with larger plate, i.e. D_{pl} = 16 m. On the other hand, the effect of the pile length is significant on stiffness and

response of monopiles. Only with largest pile length, L = 36 m, there was some noticeable increase in resistance of hybrid foundations.

A comparison between the finite element analysis and the capacity of the foundation systems predicted using **Equations 5.1 and 5.2** is provided in **Table 5.3.** It can be noted from **Table 5.3** that there is a good agreement in case of the monopile capacity. However, in case of hybrid system the empirical equations give higher capacity values. This is because the failure mechanism has developed fully for the plates, hence they contribute only partially to the capacity determined using the interpreted failure criterion specified by the interaction of the two tangents. At the time, the pile shaft resistance increases due to the additional confining pressure because of the stresses transferred from the plate to the underlying soil within its influence zone In order to account for these effects in realistic evaluation of the hybrid system capacity, an equation is presented herein that can be used for estimating the capacity of the hybrid foundation, i.e.

$$\mathbf{Q_{HSv} = 2.48\ Q_{monopile} + 0.4\ (D_{pl}/L)\ Q_{Plate}} \qquad \textbf{Equation 5.3}$$

Where Q_{HSv} is the vertical capacity of the hybrid system, $Q_{monopile}$ is monopole axial capacity determined from Eq. 5.1 and Q_{plate} is plate capacity determined from Eq. 5.2.

Equation 5.3 can provide reasonable estimate for the capacity of a hybrid system installed in sand. For hybrid system with geometrical properties within the range of parameters considered herein, the predictions of Eq. 5.3 are expected to be in good agreement with values obtained from finite element analysis. For hybrid systems with geometrical properties outside the range considered herein, Eq. 5.3 can be used in the preliminary design phase to predict the system capacity.

Table 5.3: Comparison of capacity of foundation systems obtained from finite element analysis and specified equations.

	Monopile D_p=4m Capacity (kN)		**Monopile D_p=6m Capacity (kN)**		**HSNR D_{pl}=16m Capacity (kN)**		**HSNR D_p=12m Capacity (kN)**	
	Equations	Finite element	Equations	Finite element	Equations	Finite element	Equations	Finite element
L=16 m	15700	15000	23600	25000	211100	110000	98196	80000
L=24 m	26600	25000	39900	35000	221950	125000	109000	85000
L=36 m	35900	40000	55900	50000	235300	130000	122350	10500

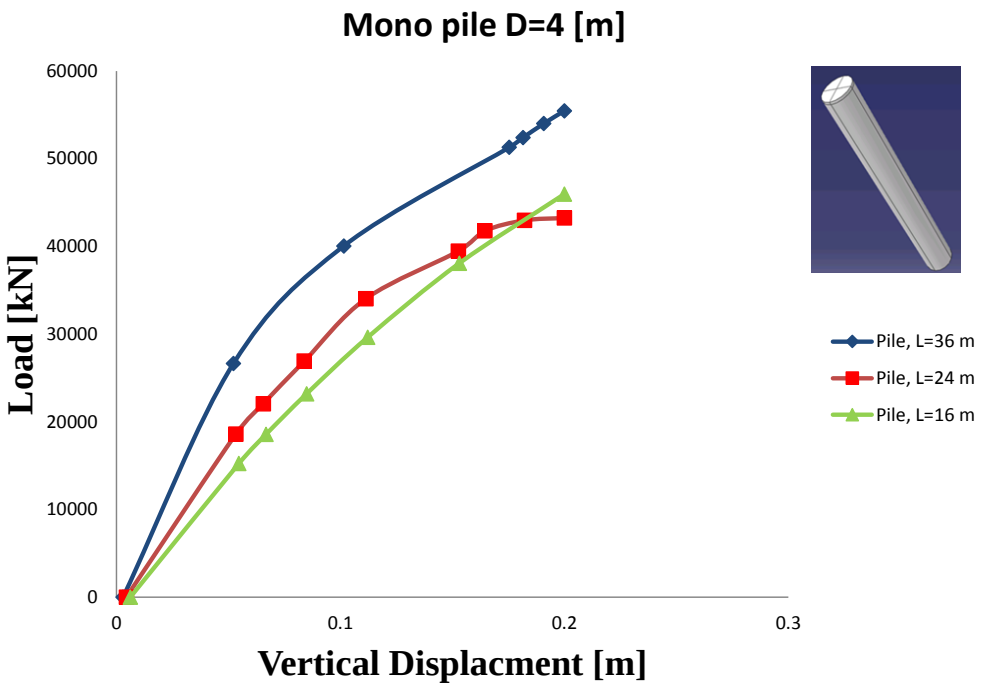

Fig. 5.7: Vertical bearing capacity of monopile with D_p=4m.

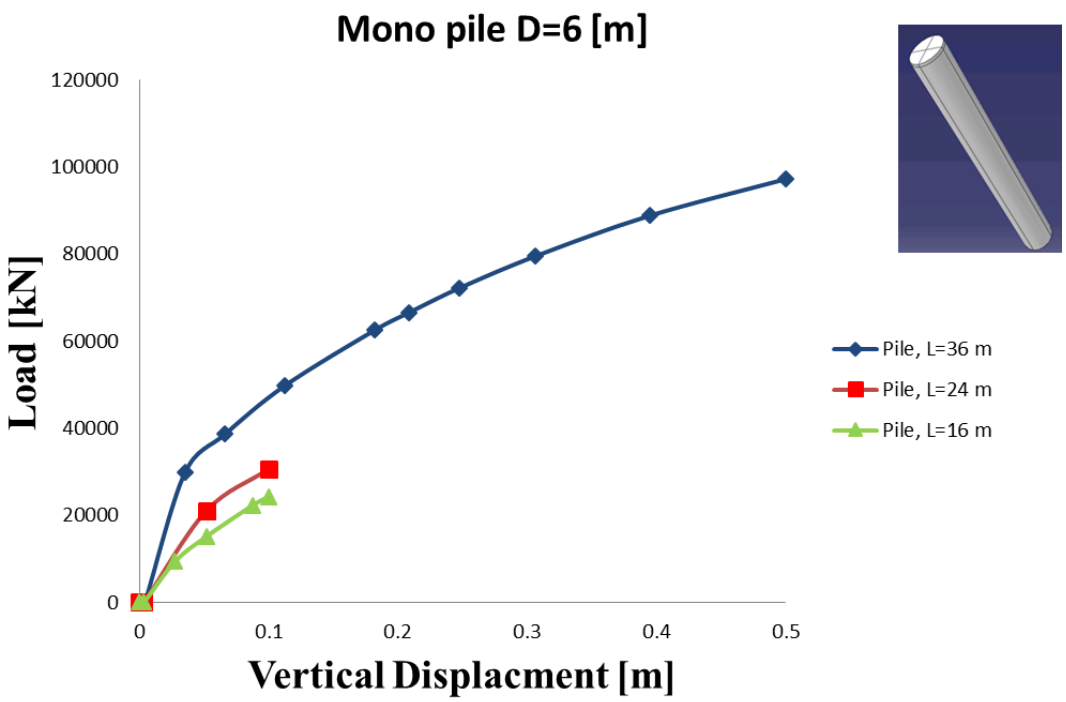

Fig. 5.8: Vertical bearing capacity of monopile with D_{pile}=6m.

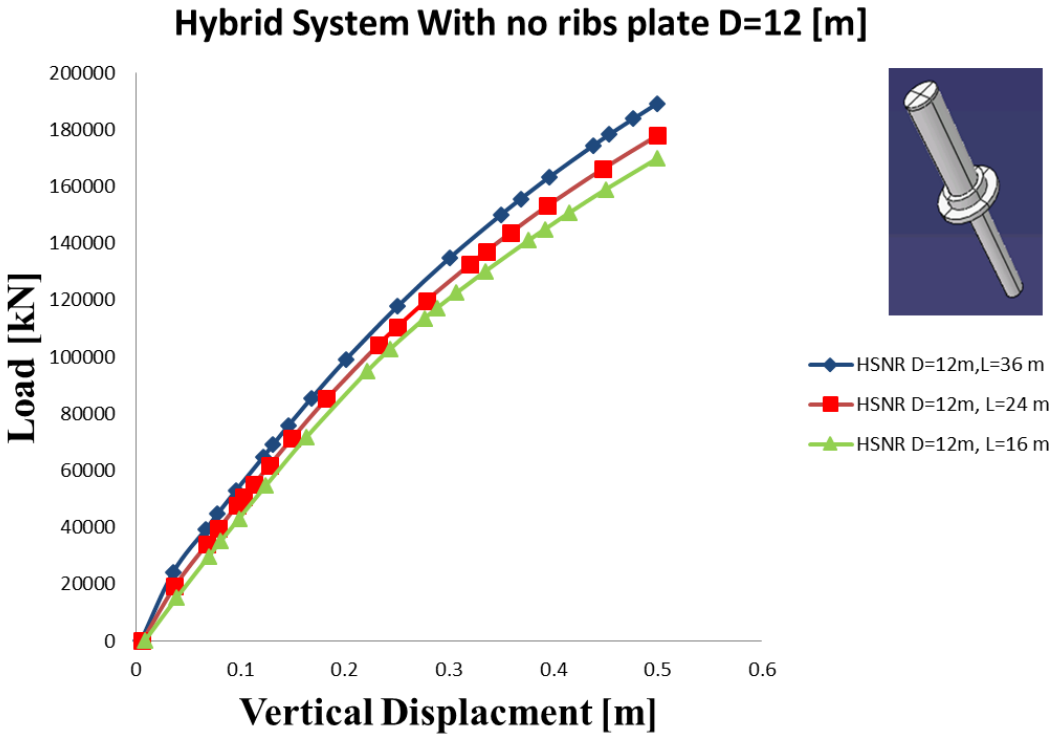

Fig. 5.9: Vertical bearing capacity of hybrid system with no rips D_{pl}=12m.

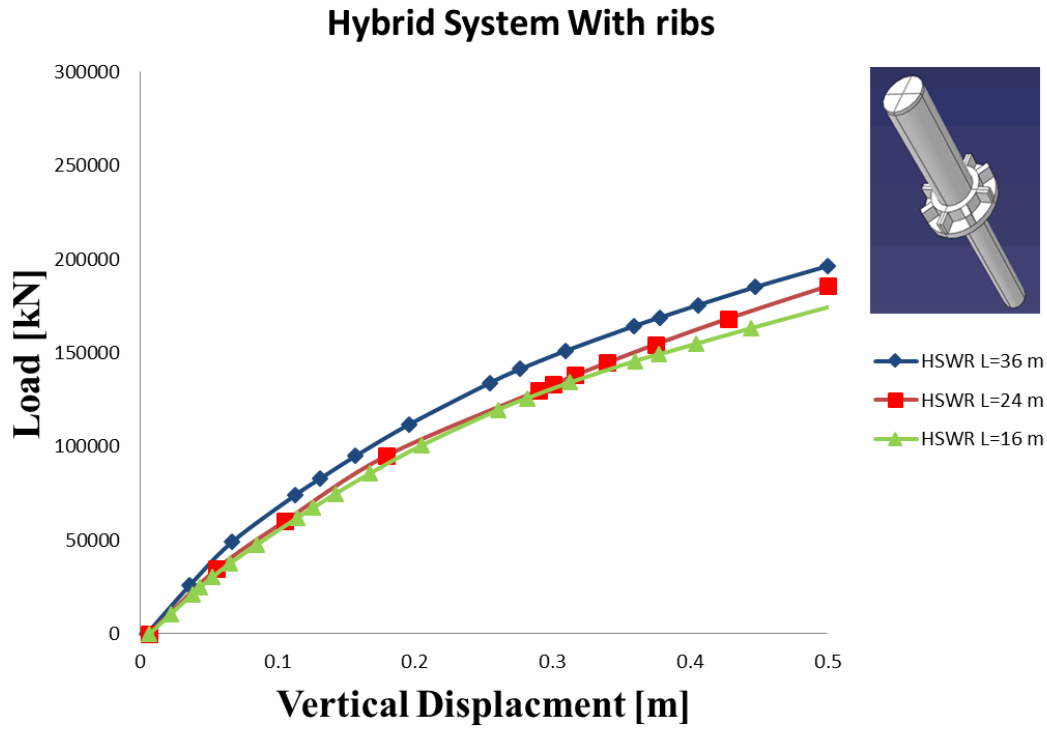

Fig. 5.10: Vertical bearing capacity of hybrid system with ribs D_{pl} = 12 m.

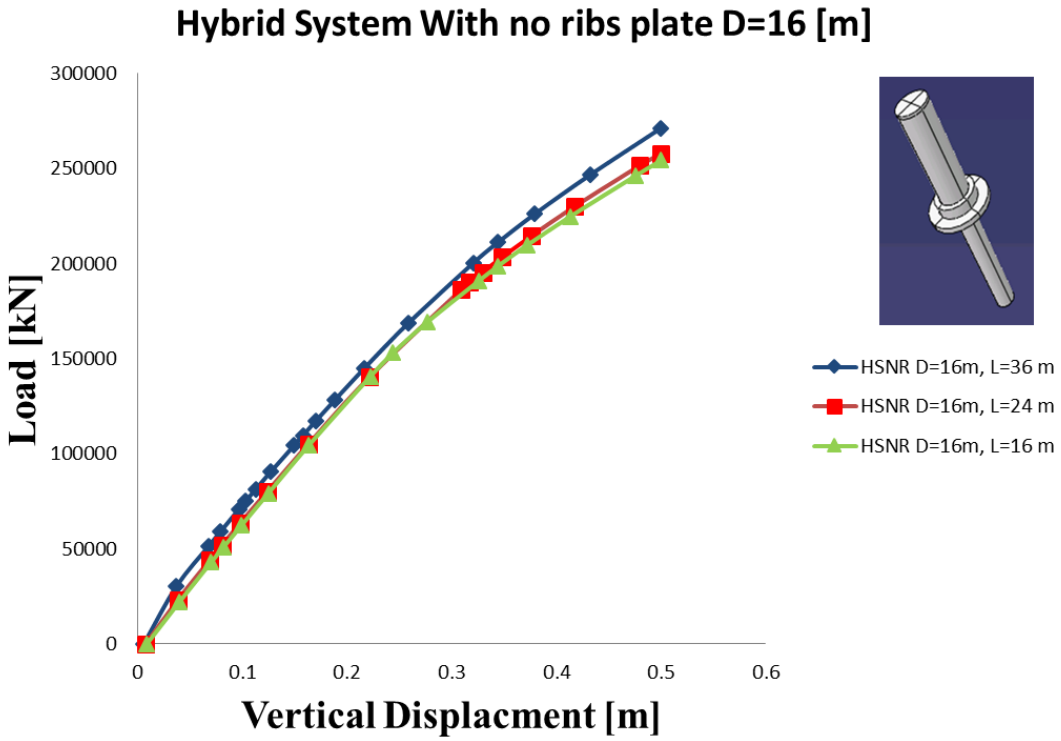

Fig. 5.11: Vertical bearing capacity of hybrid system with no rips D_{plate}=16m.

In order to further understand the behaviour of the different systems, the distributions of vertical soil displacement and stresses below the plates and along the pile shaft are inspected. **Figure 5.12** shows the vertical displacement of monopile system with D_p =4m and L =24 m. It is noted from Fig. 5.12 that the soil movement and additional stresses due to applied vertical loading are within $2D_p$ from the pile centre or below the pile toe, confirming that the boundaries are far enough to eliminate any effect on the results of the analysis.

It is also noted that the transition part between D_p =4m and the tower (6 m diameter) provides some bearing resistance near the ground surface. Finally, it is noted that the displacement of soil inside the pile is larger than the pile displacement, indicating soil plugging has occurred due to frictional resistance between the soil and the inner wall of the pile. This also led to increased bearing pressure (and resistance) at the pile toe. **Figure 5.13** shows the vertical stresses in the soil for monopile system with D_p =4m and L =24 m. As can be noted from Fig. 5.13, high compressive stresses occur below the pile toe and below the transition zone at the pile head due to the bearing pressures. It is also interesting to note the reduction in the soil stresses just outside the pile toe due to the failure mechanism of soil near the toe, which causes the soil in this zone to move upward. In addition, it is noted that the soil inside the pile at the toe (i.e. forming the soil plug) experiences significant stresses, which manifests the contribution of the bearing pressure to the vertical capacity of the system.

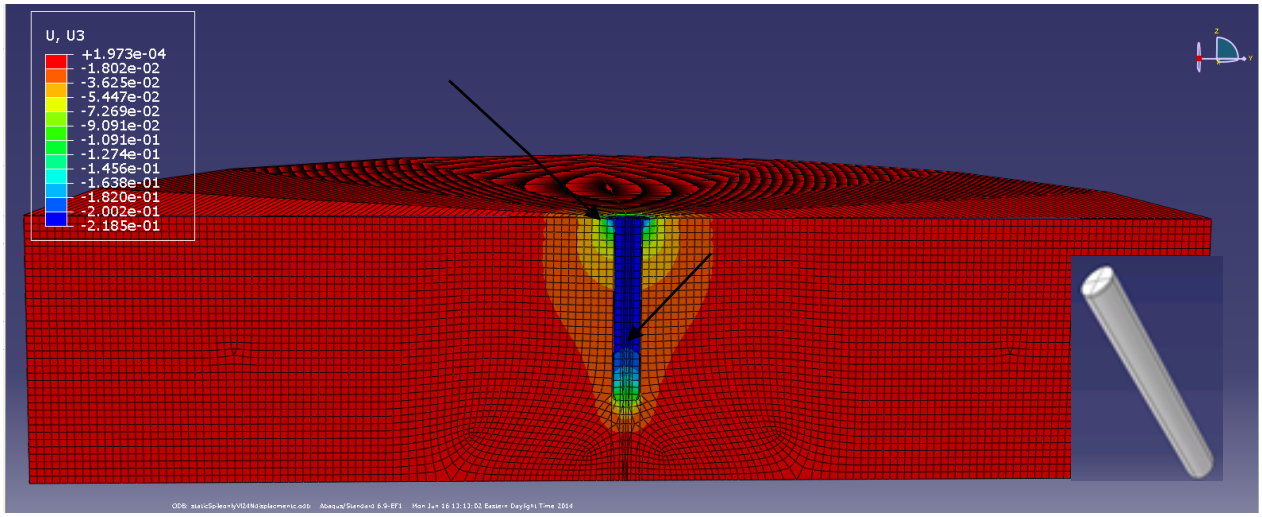

Fig. 5.12: Vertical displacement of monopile system with D_{pile} =4m and L_{pile} =24 m.

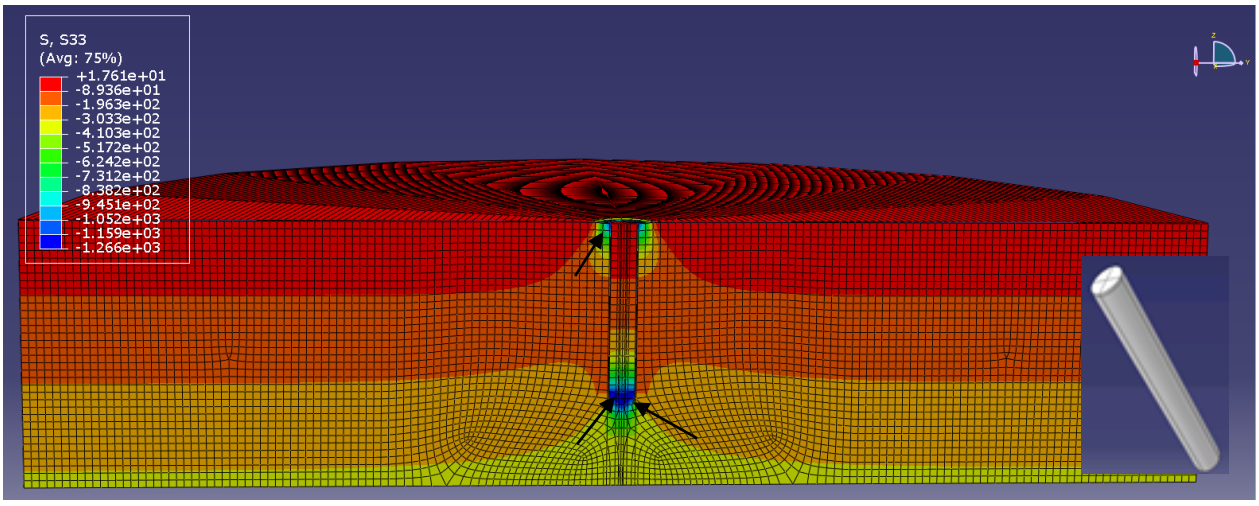

Fig. 5.13: Vertical stresses of monopile system with D_{pile} =4m and L_{pile}=24m.

Similar behaviour is observed for the monopole with D_p = 6 m as shown in **Figure 5.14** and **Figure 5.15.** In addition, similar behaviour was observed for different pile length for both monopole sizes (i.e. D_p = 4 m and 6 m).

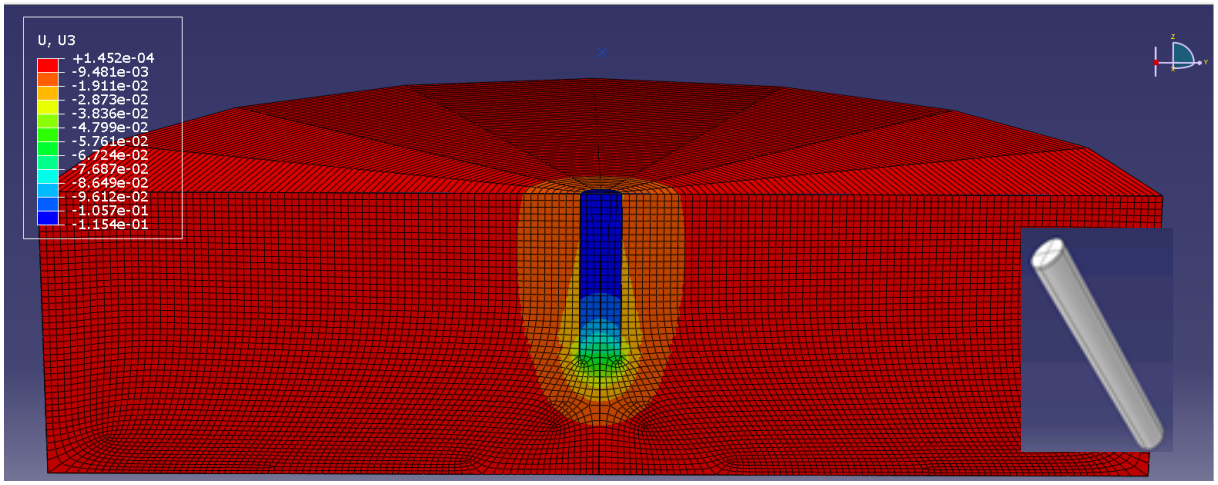

Fig. 5.14: Vertical stresses of monopile system with D_{pile} =6m and L_{pile}=24m.

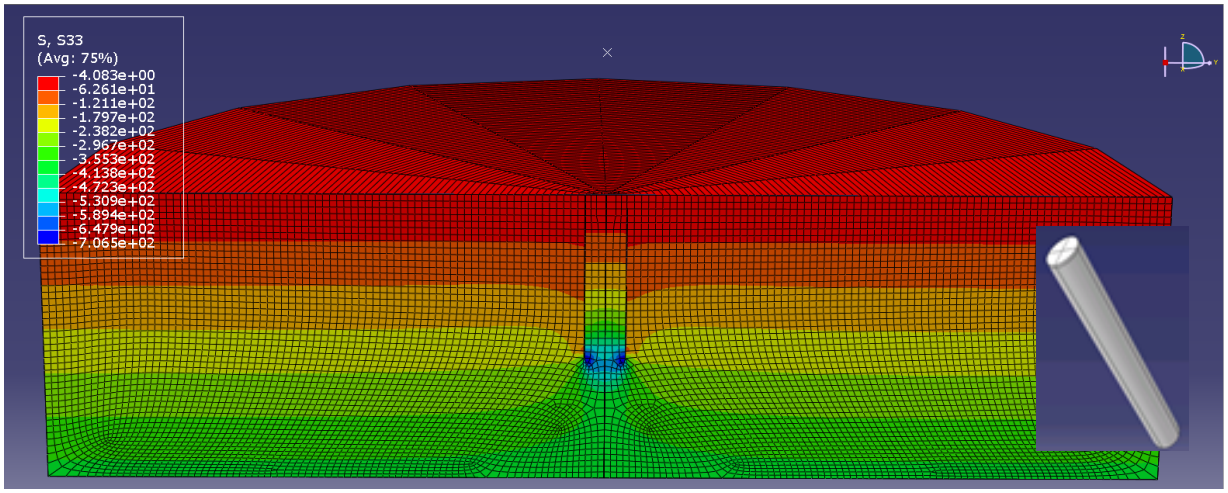

Fig. 5.15: Vertical stresses of monopile system with D_{pile} =6m and L_{pile}=24m.

In order to elucidate the interaction between the components of the hybrid system, **Figure 5.16.** shows settlement of (HSNR) for L=16, 24 and 36 m. Inspecting Fig. 5.16, it is noted that the pile shaft is outside the elastic zone of the plate, for all pile lengths considered, which causes the capacity of the system to be approximately the sum of capacity of both components (i.e. plate and

pile). Similar observation can be made from **Figure 5.17**, which shows the soil stress distribution for the same systems. In addition, Fig. 5.17 demonstrates the stress localization at the pile toe, which indicates the soil plug and consequently increased contribution of toe capacity.

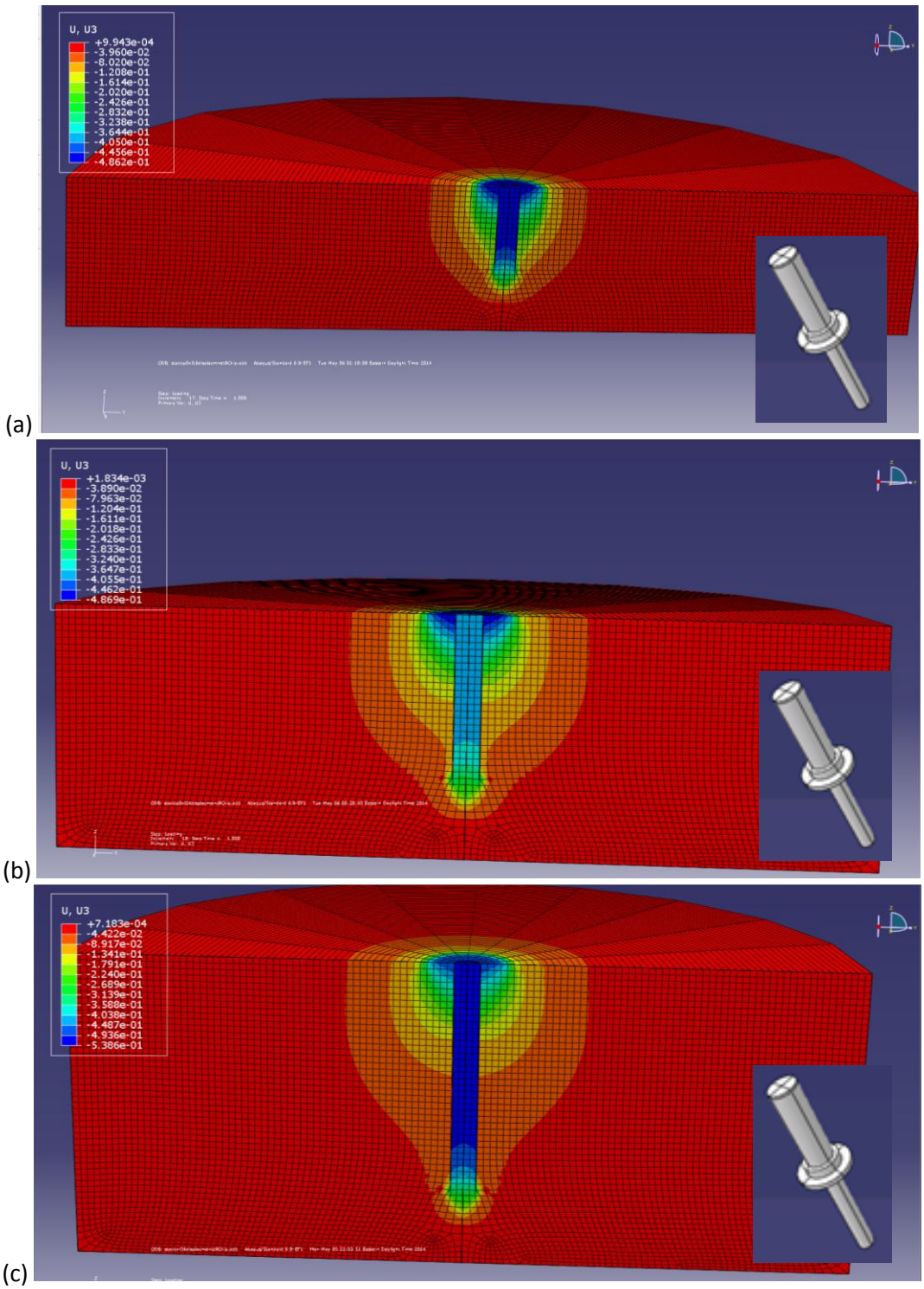

Fig. 5.16: Vertical stresses of HSNR with: a) *L*=16m, b) L=24m, and c) L =36m.

(a)

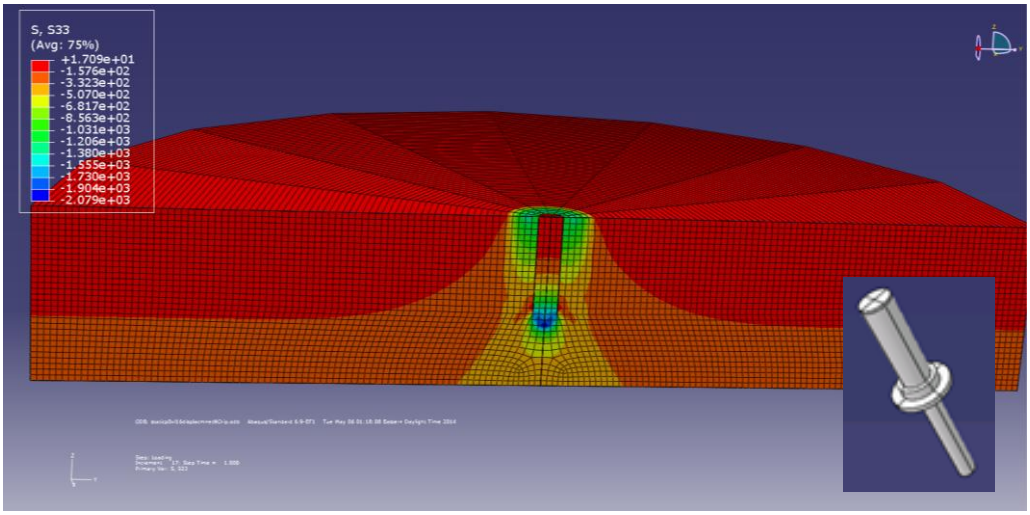

(b)

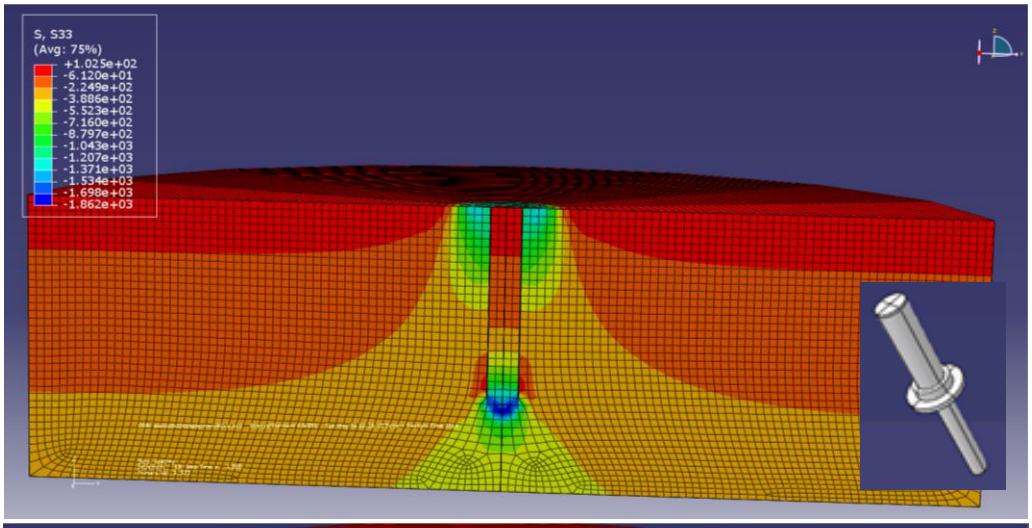

(c)

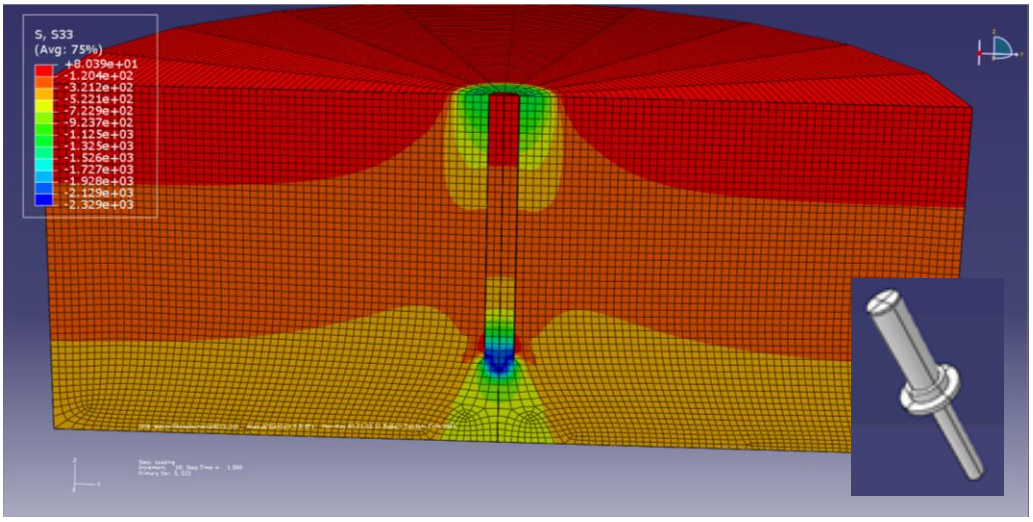

Fig. 5.17: Vertical stresses of HSNR with: a) *L*=16m; b) L= 24m, and c) L=36m.

Figure 5.18 presents the variation of vertical stresses of the soil adjacent to the pile shaft, both outside (out) and inside (in) the pile for monopile with D_p =4 m and L = 24 m. As can be noted from Fig. 5.18, the outside soil stresses near the pile head are high due to the bearing pressure on the base of the larger steel pipe (with 6 m diameter). This effect diminishes rapidly and is almost absent at a depth of less than 5 m, where the soil stresses are only equal to the frictional resistance along the pile shaft. The outside soil stresses remains constant afterwards at the limiting ultimate shaft friction for steel piles in dense sand, set at 120 kPa as per the Canadian Foundation Engineering Manual, CFEM (2006). On the other hand, the stresses of the soil inside the pile increases almost linearly approaching the pile toe, where it starts to increases more rapidly due to the bearing stresses at the soil plug near the pile toe.

The decrease of soil vertical stress at the pile for outer soil is due to the complex stress regime at the pile toe, which involves some soil dilation. Similar behaviour is noted for monopoles with D_p = 4 m and different lengths. Meanwhile, **Figure 5.19** displays the soil stresses for the monopole with D_p = 6m and L = 24 m. In this case, both outside and inside soil exhibit almost linear increase of stresses due to the increase in confining pressure until the limiting ultimate shaft friction along the pile shaft is achieved. After this point the vertical stresses in the outside soil remains almost constant, while the stresses of the inside soil increases due to the bearing on the soil plug near the pile toe. Similar behaviour is noted for monopoles with D_p = 6 m and different lengths.

The soil stresses for the case soil of HSNR is expected to be affected by the interaction between its components, i.e. the plate and the monopole. This is demonstrated in **Fig. 5.20**, where the effect

of the plate can be clearly seen as significant increase in the vertical stress of the outside soil up to a depth of approximately 15 m, where it reduces to the limiting ultimate shaft friction. The stresses of the outside soil near the pile toe are affected by the complex soil regime due to the movement of soil as the failure mechanism develops just below the pile toe. On the other hand, the stresses of the soil inside the pile follow the same trend as the monopoles.

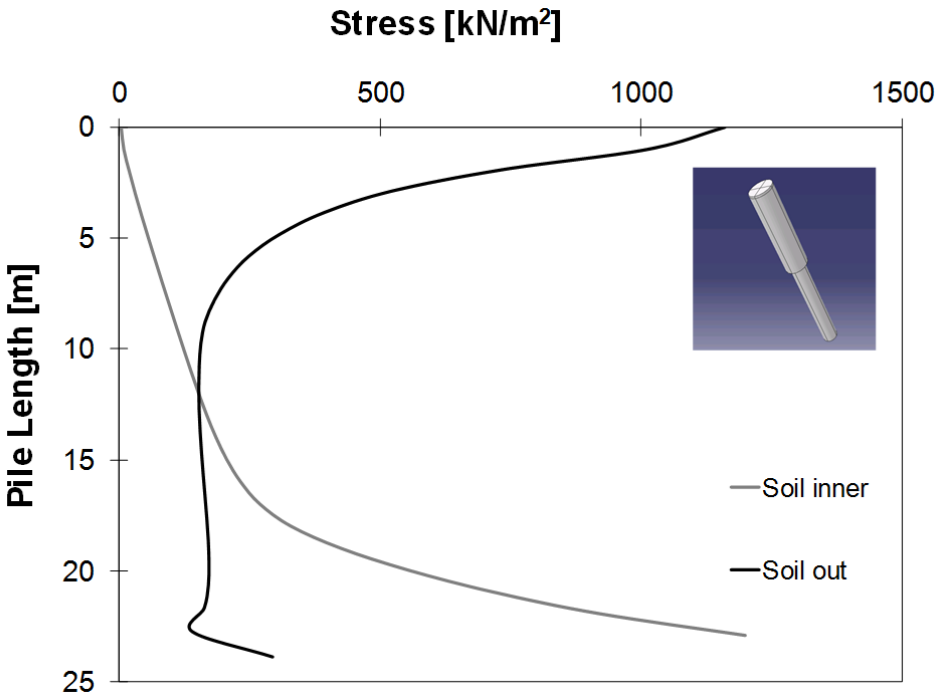

Fig. 5.18: Vertical stresses of monopile system with D_{pile} =4m and L_{pile}=24m.

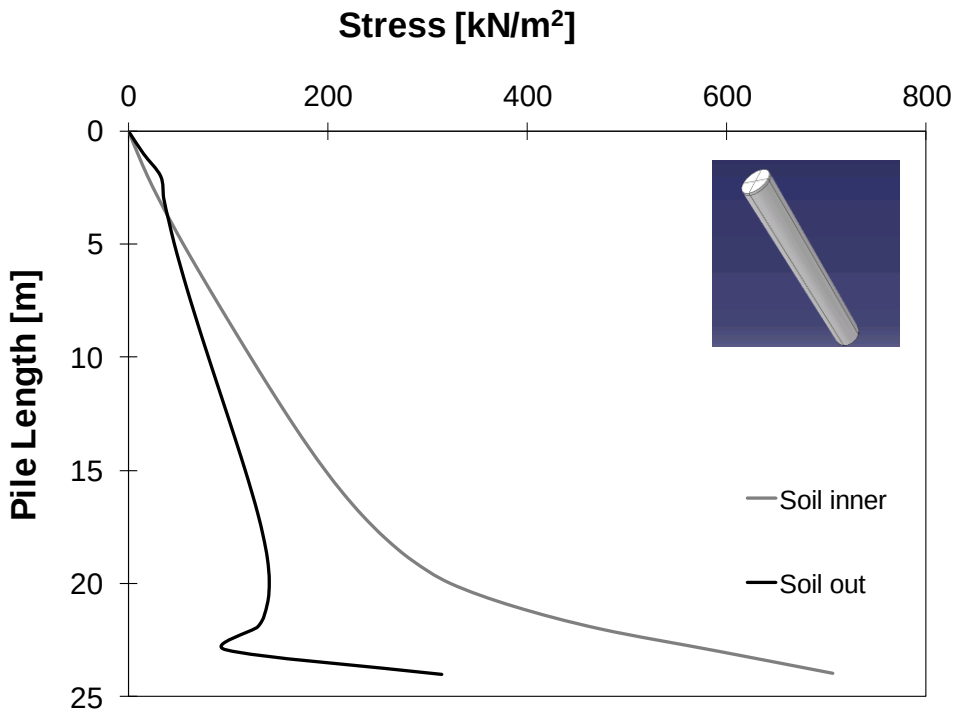

Fig. 5.19: Vertical stresses of monopile system with D_{pile} =6m and L_{pile}=24m.

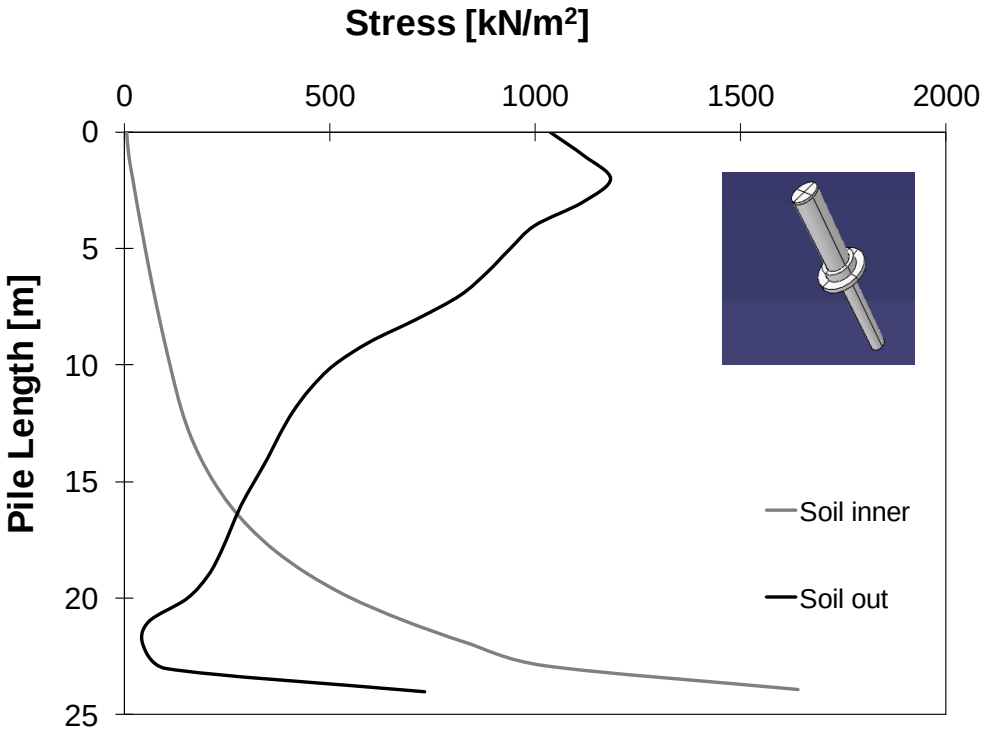

Fig. 5.20: Vertical stresses of (HSNR) system with L_{pile}=24m.

5.5.2 *Lateral load capacity.*

The response of the considered foundations to lateral loading is considered in this section. The finite element models of the foundation systems were subjected to displacement controlled applied at the top of the steel pipe at the sea level. The objective of this parametric study is to evaluate the gain in the lateral load capacity of the hybrid system due to the addition of the concrete plate. Also, the performance of the hybrid system under lateral loads is evaluated.

Lateral displacement was applied as a boundary condition at the top of the steel pipe (at sea level) and was increased incrementally until the maximum target displacement of 0.5 m was reached. At each displacement increment, the equilibrium of the system was satisfied and the corresponding load at both sea and mud level was tracked. The response of the different foundation systems under lateral loads is represented as lateral load-displacement curves. **Figures 5.21 to 5.23** compare the lateral load-displacement curves for the different systems considering various pile length, L=16 m, 24 m and 36 m, respectively.

It can be noted from Fig. 5.21 that for short piles (L = 16 m), the HSNR with D_{pl} = 16 m displayed the stiffest response and provided the highest lateral resistance. This is attributed to the stiffening effect of the large diameter plate and the fact that the response is dominated primarily by rotation. It is also noted that the response of the HSWR with D_{pl} = 12 m was stiffer than that of HSNR with D_{pl} = 12 m. This attributed to the stiffening effect of the ribs, which reduced the deflection of the plate and hence enhanced the rotational resistance of the system. Furthermore, the lateral resistance of HSNR with D_{pl} = 12 m is higher than that of monopole with Dp = 6 m, which demonstrates the superior performance of the hybrid system in supporting lateral loads. Figures 5.22 and 5.23 demonstrate that initially, the HSNR with D_{pl} = 16 m and HSWR displayed the stiffest response;

however, as the lateral displacement increased the pile provides higher contribution to lateral load resistance and hence rotation decreases, which in turn reduces the plate contribution to lateral resistance. This effect is more pronounced for L = 36 m, as monopole with D_p = 6 provided the highest resistance.

The capacity of each foundation system was evaluated as the load defined by the intersection of the two tangent lines of the initial and final loading phases as indicated in Figs. 5.21 to 5.23. The capacity of the different foundation systems are compared with that of the monopole with D_p = 4m in **Table 5.4.** The results presented in **Table 5. 4** demonstrate that the capacity of all systems increase with pile length, however, the most increase in capacity occur for the monopile with D_p = 6 m and HSNR with D_{pl} = 16 m.

It should be noted the capacity of the hybrid system HSNR with Dpl = 16 m fulfill the requirements of the DNV-OS-J101 (2011) for supporting 5MW NREL wind turbines.

Table 5.4: The increase in horizontal pile capacity compared to the monopile D_{pile}=4 m

	Monopile D_p=4m Capacity (kN)	**Monopile D_p=6m**	**HSNR D_{pl}=12m**	**HSWR D_{pl}=12m**	**HSNR D_{pl}=16m**
L=16 m	6500	138%	123%	130%	153%
L=24 m	10000	165%	120%	125%	150%
L=36 m	11000	213%	127%	136%	181%

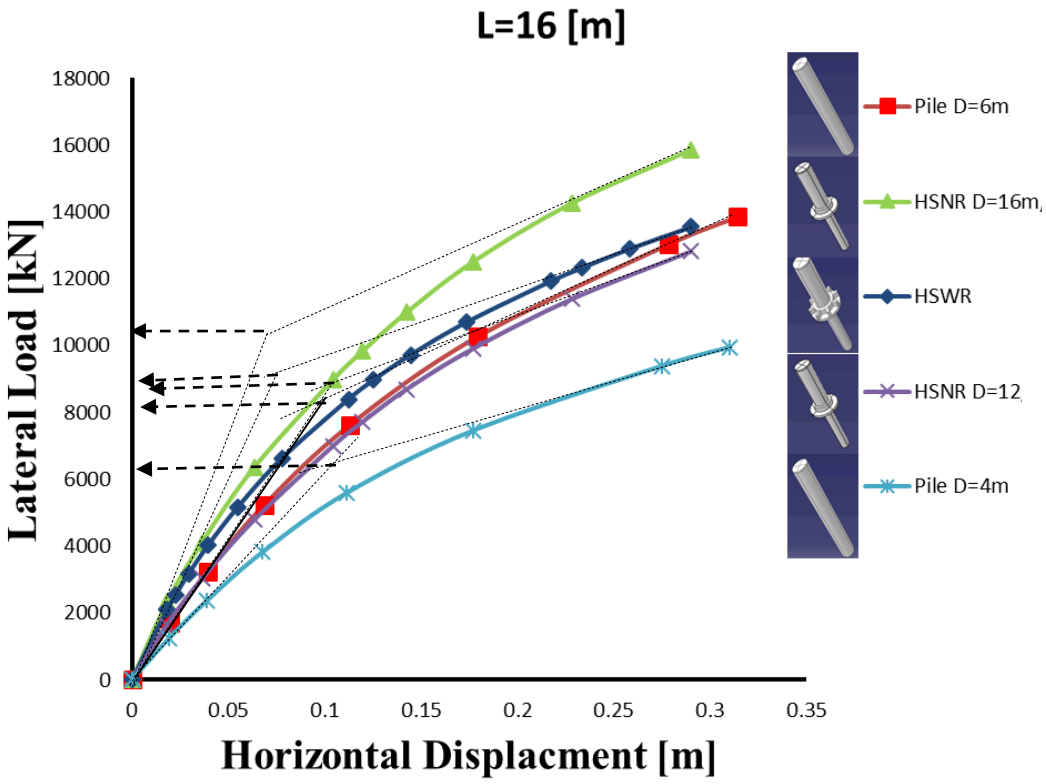

Fig. 5.21: Lateral capacity of different systems with L_{pile}=16 m.

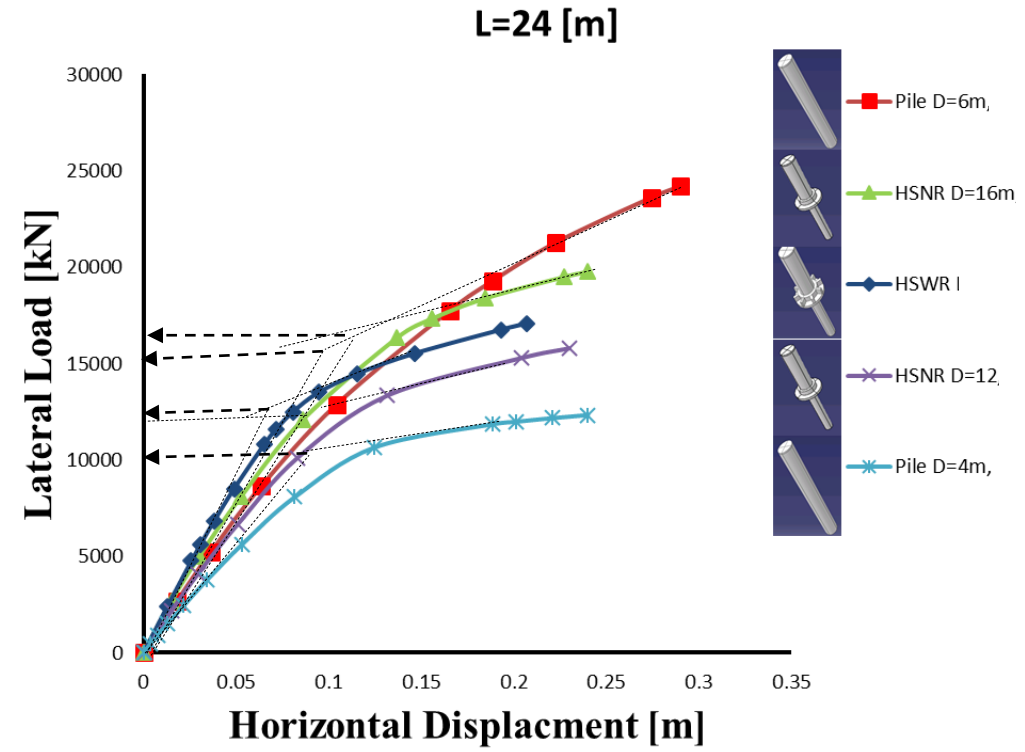

Fig. 5.22: Lateral capacity of different systems with L_{pile}=24 m.

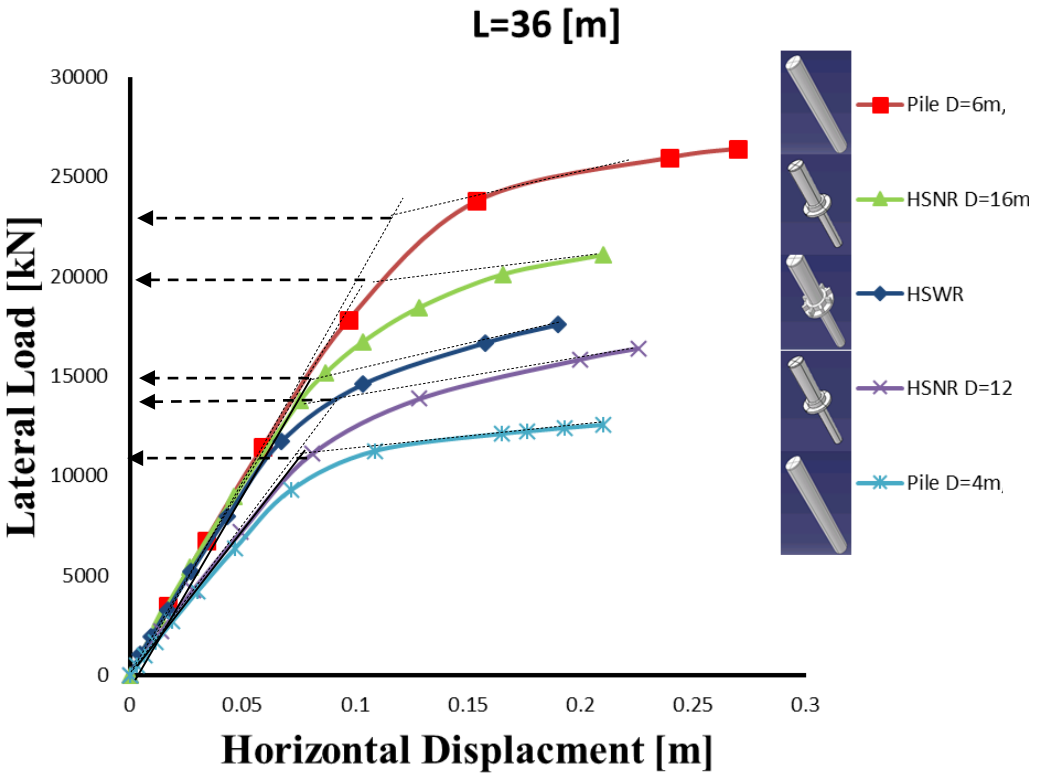

Fig. 5.23: Lateral capacity of different systems with L_{pile}=36 m.

Figure 5.24 compares the response of monopole of Dp = 6 m with different pile length. It is clear that its lateral resistance (stiffness and capacity) increases as the pile length increases because it behaves as a short pile. **Figure 5.25** demonstrates that the effect of pile length on the lateral performance of HSNR with D_{pl} = 16 m is similar, i.e. the lateral resistance increases as the pile length increases. However, the rate of increase in lateral resistance decreases as the pile length increases from 24 m to 36 m. On the other hand, the HSWR displayed somewhat different behaviour as demonstrated in **Figure 5.26**; the lateral resistance increased as the pile length increased from L = 16 m to L = 24 m due to the additional resistance from the pile as it displayed behaviour short pile (primarily rotational). As the pile length increased further to L = 36 m, the lateral resistance increased slightly because the pile started to transition to long pile behaviour, indicating that L = 24 m represents the optimum design for lateral resistance. HSNR with D_{pl} = 12 m displayed similar behaviour. The monopole with D_p = 4 m displayed similar behaviour as shown in **Fig. 5.27**.

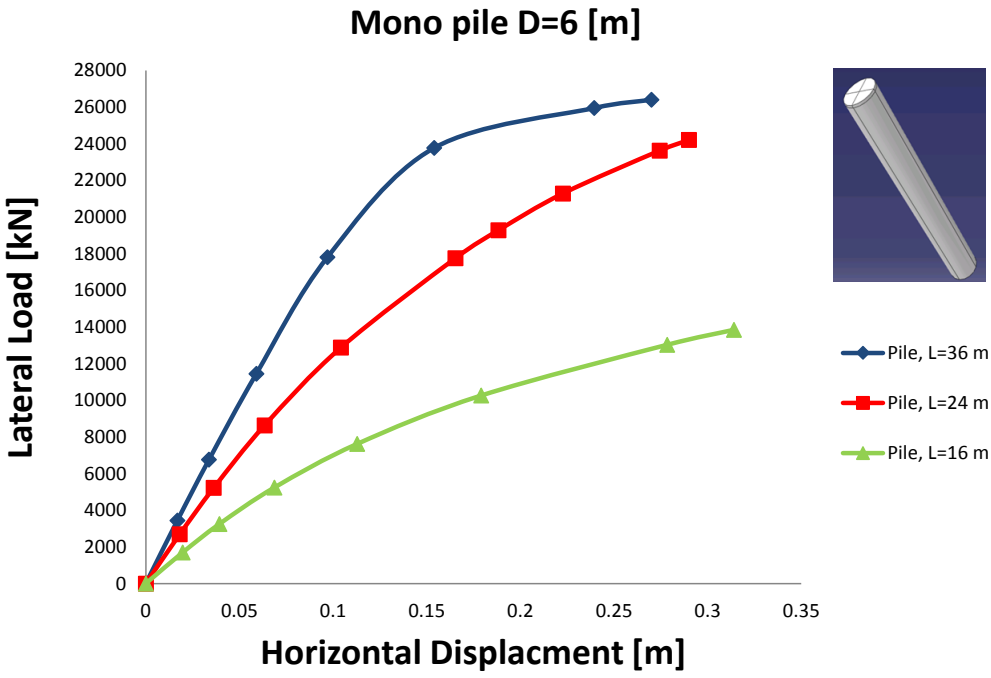

Fig. 5.24: Lateral capacity of monopile system with D_{pile} =6m

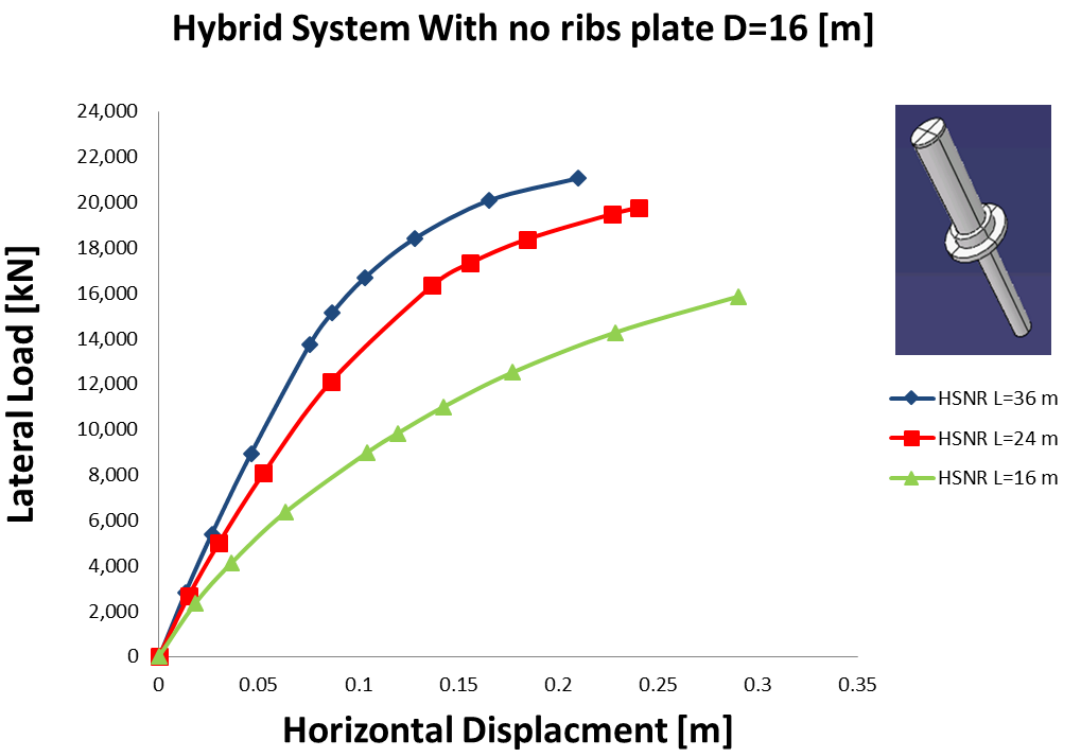

Fig. 5.25: Lateral capacity of (HSNR) system with D_{plate} =16m.

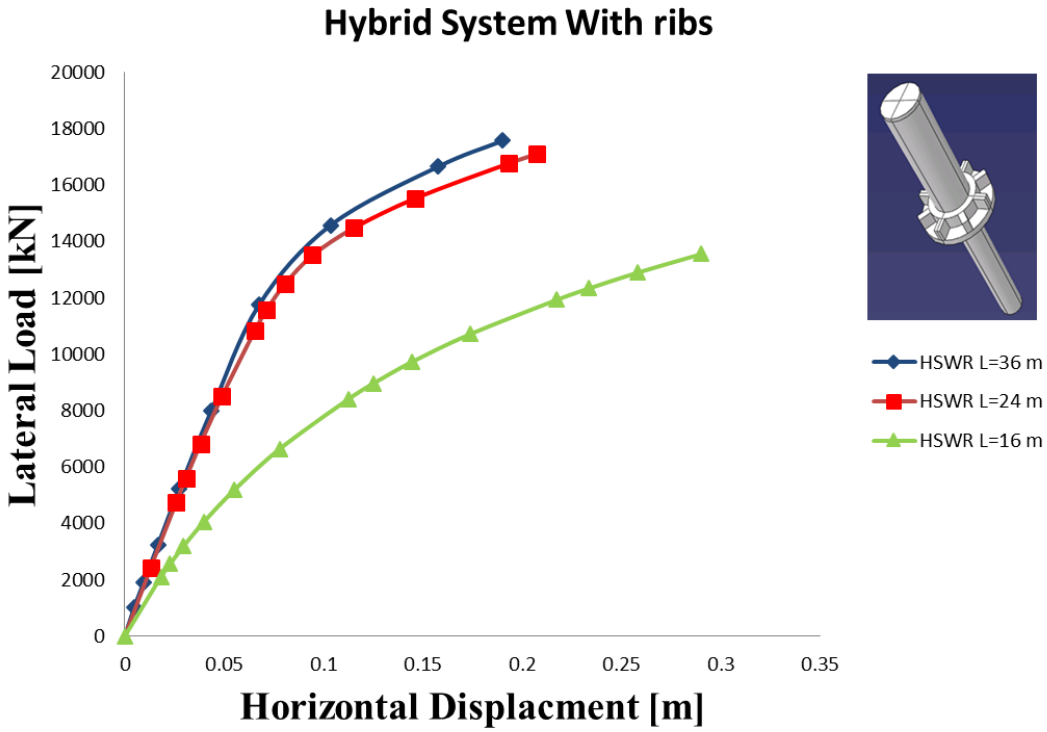

Fig. 5.26: Lateral capacity of (HSWR) system.

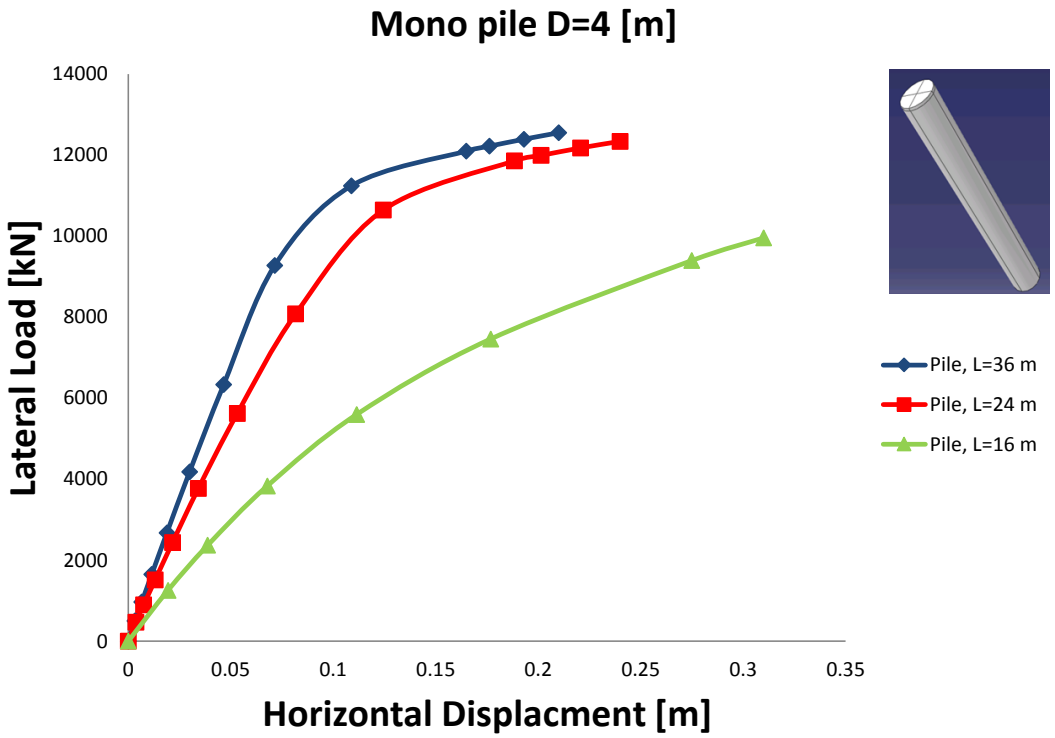

Fig. 5.27: Lateral capacity of monopile system with D_{pile} = 4m.

5.6. CONCLUSIONS

The responses of different foundation systems proposed to support wind turbines under vertical and lateral loads were investigated using 3 dimensional nonlinear finite element analyses. The results were used to evaluate the performance and capacity of the proposed hybrid foundation system in comparison to the conventional monopole system. The following conclusions may be drawn from the results of the analysis.

1. The vertical capacity of the hybrid system with D_p = 4 m is much higher than the capacity of monopile with D_p = 6 m due to the beneficial effect of the plate. However, the relative increase in capacity decreases as the pile length increases.

2. The axial capacity of the hybrid system can be given by Eq. 5.3, which includes an enhanced contribution of the monopole and partial contribution of the plate.
3. The lateral capacity of the hybrid system with D_{pl} = 16 m is 180% of the capacity of monopile that has the same diameter D_p = 4m, and is only 10% less than the capacity of monopole with Dp = 6 m. On the other hand, monopile with D_p = 6 m.
4. The vertical and horizontal capacity of the hybrid system with D_p = 4m fulfill the requirements of the DNV-OS-J101 (2011), and hence can be used to support 5 MW NREL wind turbines instead of the larger monopile with 6m diameter.

5.7. REFERENCES

Byrne, B.W. and Houlsby, G.T. (2003), “Foundations for Offshore Wind Turbines”, Philosophical Transactions of the Royal Society of London, **A**(361), 2909-2930.

DNV-OS-J101, Offshore Standard, (2011), “Design of Offshore Wind Turbine Structures”, Electronic Version available at http://www.dnv.com/ (On Jan. 25, 2013)

El Marassi et al numerical modeling of performance of a hybrid monopile footing foundation 2008.

Gerdes, G., Tiedemann, A., Zeelenberg, S, “Case Study: European Offshore Wind Farms - A Survey for the Analysis of the Experiences and Lessons Learnt by Developers of Offshore Wind Farms”, Pushing Offshore Wind Energy Regions, 2008.

Hameed, Z., Vatn, J. and Heggset, J. (2011), “Challenges in the reliability and maintainability data collection for offshore wind turbines“, Renewable Energy, **36**(8), 2154-2165.

Houlsby, G.T. and Byrne, B.W. (2001) "Assessing Novel Foundation Options for Offshore Wind Turbines", Department of Engineering Science, Oxford University. No. of pages

Houlsby, G.T. (2003) “Modelling of Shallow Foundations for Offshore Structures”, Invited Theme Lecture, Proceeding. International Conference on Foundations, Dundee, Thomas Telford, pp 11-26.

IEC 61400-3, International Standard, (2009), “Wind turbines – Part 3: Design requirements for offshore wind turbines”, Edition 1.0 2009-02.

Ibsen, L., Rune B. (2004) “Design of a New Foundation for Offshore Wind Turbines“**.** Proceedings of IMAC-22: A Conference on Structural Dynamics, Dearborn, Michigan, USA. Society for Experimental Mechanics, 2004. p. 359-366

Jonkman, J., Butterfield, S., Musial, W., and Scott, G., (2009), “Definition of a 5-MW Reference Wind Turbine for Offshore System Development”, National Renewable Energy Laboratory, Golden, CO, Technical Report, NREL/TP-500-38060,

Lozano-Minguez, E., Kolios, A.J., Brennan, F.P. (2011), “Multi-criteria assessment of offshore wind turbine support structures“, Renewable Energy, 36(11), 2831-2837

Passon P., KÜhn, M. (2007), “OC3 – Benchmark Exercise of Aero-Elastic Offshore Wind Turbine Codes“, *Conference Paper,* NREL/CP-500-41930

TERZAGHI, K. (1943) Theoretical Soil Mechanics. John Wiley & Sons, Inc., New York.

Thomsen, J., Forsberg, T. (2007), “offshore wind turbine foundations - the cowi experience“, proceedings of the 26th International Conference on Offshore Mechanics and Arctic Engineering, OMAE2007-29567

CHAPTER SIX

EFFET OF LONG TERM CYCLIC LOADING ON STIFFNESS AND CAPACITY OF HYBRID FOUNDATION

In this chapter, the long term performance of a hybrid foundation system intended to support large offshore wind turbines, which combines a monopile and concrete plate, is examined. The performance of the proposed foundation system, as well as the conventional monopoles, subjected to cyclic loading is evaluated. A scaled-down non-dimensional framework of stiff foundation models installed in sand was used to conduct a series of static and cyclic loading tests under 1-g. Four main model foundations were tested. Test results were then used to develop an equation to predict the stiffness of the proposed hybrid foundation system. In addition, three dimensional nonlinear analysis was conducted using the ABAQUS software to predict the response of the tested models.

6.1. INTRODUCTION

Green energy resources are essential to meet the growing energy demands in the near future while reducing the effects of global warming. Offshore wind energy is one of the main efficient renewable energy sources. Therefore, offshore wind farms are continually expanding, especially in North Sea and China. One of the main cost items in the construction of offshore wind turbines is the foundation. It represents about 30-40% of the total cost of the wind turbine (Byrne and Houlsby, 2003). There are several foundation systems that are used to support wind turbines depending on the soil conditions and water depth. The gravity base foundation, which depends on

its weight to resist the lateral load and overturning moment, is used in case of small water depth. It is usually cast onshore then moved to the offshore site to be erected in order to reduce its construction cost.

Monopile foundations can be used to support wind turbines in wide range of soil conditions and water depths due to its versatility and suitability of construction in different conditions. Large wind offshore wind turbines are typically supported by a steel pile with diameter, D = 4-6 m and length, L = 20-40 m (Houlsby, 2003). Suction caissons are also used to support wind turbines in a variety of soil conditions and water depth (Houlsby, 2003). Moreover, a combination of the shallow footing and monopile can provide efficient foundation system for large offshore wind turbines (Leblanc, 2010). The monopile and the combined (i.e. hybrid) offshore wind turbine foundations are presented schematically in **Fig. 6.1**

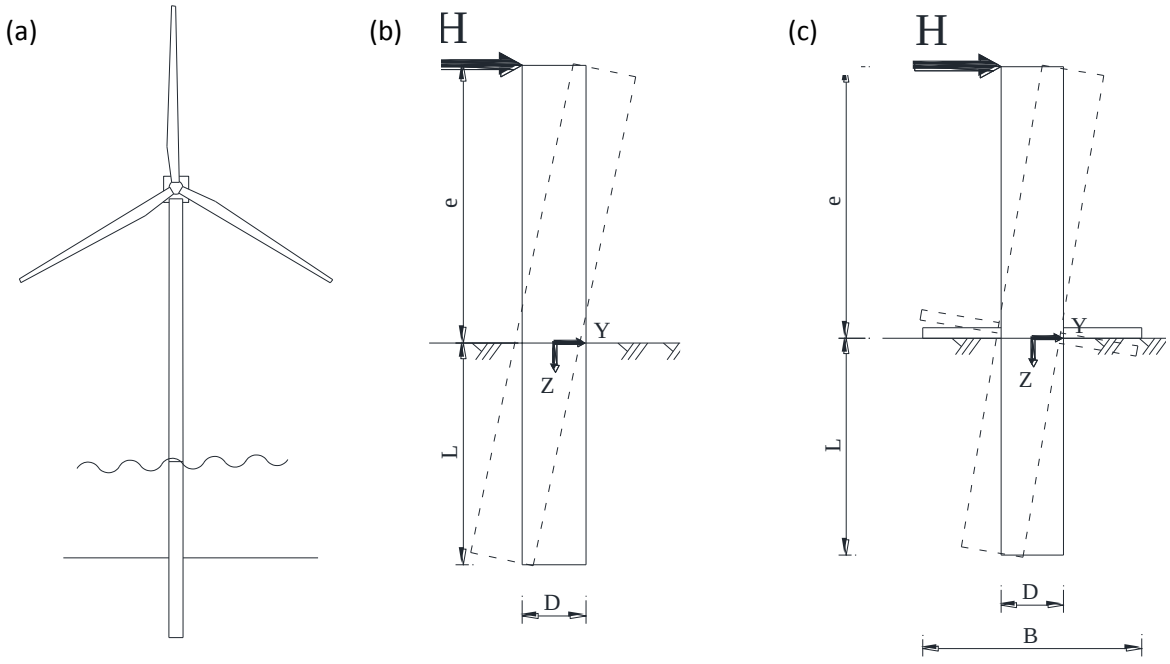

Fig. 6.1: Offshore wind turbine foundations considered: a) offshore wind turbine; b) monopile; and c) the hybrid foundation system

Most methods for analyzing and designing offshore wind turbines foundations are originated from the practices employed in the design of offshore oil and gas production rigs. However, there is a significant difference between the two foundation applications. Unlike the oil production rigs, the loading combination for wind turbines involves relatively small vertical loads but larger cyclic horizontal and moment loads. This relatively large lateral cyclic load can affect both the stiffness and the capacity of the foundation system. Additionally, while the monopole static capacity is important, the changes in its stiffness and accumulated rotation after long-term cyclic loading must be addressed as part of the stringent performance criterion that has to be satisfied (Leblanc *et al.*, 2010). Long term cyclic loading could change the soil stiffness and consequently the foundation stiffness can also be affected.

Cyclic response of laterally loaded pile is influenced by soil and pile yielding, soil-pile gapping and cyclic soil degradation. During cyclic loading, the response of piles installed in sand is also affected by soil cave-in and recompression. In addition, the soil may experience strength loss and modulus reduction. Hence, procedures that are used in evaluating pile response should be capable of accounting for these factors similar to previous work conducted by (Allotey and El Naggar, 2008[a,b]; and Heidari *et al.*, 2014).

The *p-y* curves approach is widely used to evaluate the response of piles subjected to lateral loads (Reese and Maltock, 1956; McCelleand and Focht, 1958). In this approach, the soil reaction, (*p*), is related to the pile deflection (*y*). The shape of the *p-y* curve can be estimated based on laboratory test results and back calculation of field performance data (e.g. Reese *et al.*, 1974) or based on in-situ test results (Robertson *et al.*, 1986) through solving the pile equilibrium equation:

$$E_p\, I_p \frac{d^4 y}{dz^4} - p(y) = 0, z \in [0; L] \qquad \textbf{Eq. 6.1}$$

Where E_p is the pile modulus, I_p is pile cross-sectional moment of inertia, and z is depth and L is pile length.

There are different methods available in the literature to establish the *p-y* curves for piles installed in saturated and unsaturated sand (Bhushan *et al.*, 1981; Bhushan and Askari, 1984) based on full-scale load test results. For long offshore piles installed in sand, DNV-OS-J101 Offshore Standard proposed an equation to generate *p-y* curves, i.e.

$$p = Ap_u tanh\left(\frac{Bz}{Ap_u y}\right) \qquad \textbf{Eq. 6.2}$$

Where *A*=0.9 for cyclic loading, *B* is initial modules of subgrade reaction and depends on the angle of friction and p_u is the soil ultimate lateral resistance.

The *p-y* curves are mainly employed for the analysis of long and flexible piles. However, piles supporting offshore wind turbine are usually short and rigid, hence the *p-y* curves approach is not suitable for their response analysis. The cyclic response of laterally loaded piles can also be evaluated utilizing the finite element method that treats soil as a continuous medium (e.g. Aristonous *et al.*, 1991, Bentley and El Naggar, 2000; Maheshwari *et al.*, 2004).

In chapters 4 and 5, three-dimensional finite element analyses were conducted to investigate the performance of different foundation systems subjected to working and ultimate loads representative of the 5 MW wind turbine. The considered foundation systems included hollow steel monopiles with diameters 4.0 and 6.0 m, and a hybrid foundation system, which combines a monopile and a concrete plate as shown in **Fig. 6.2**. The performance of these systems under long term cyclic loading will be examined herein.

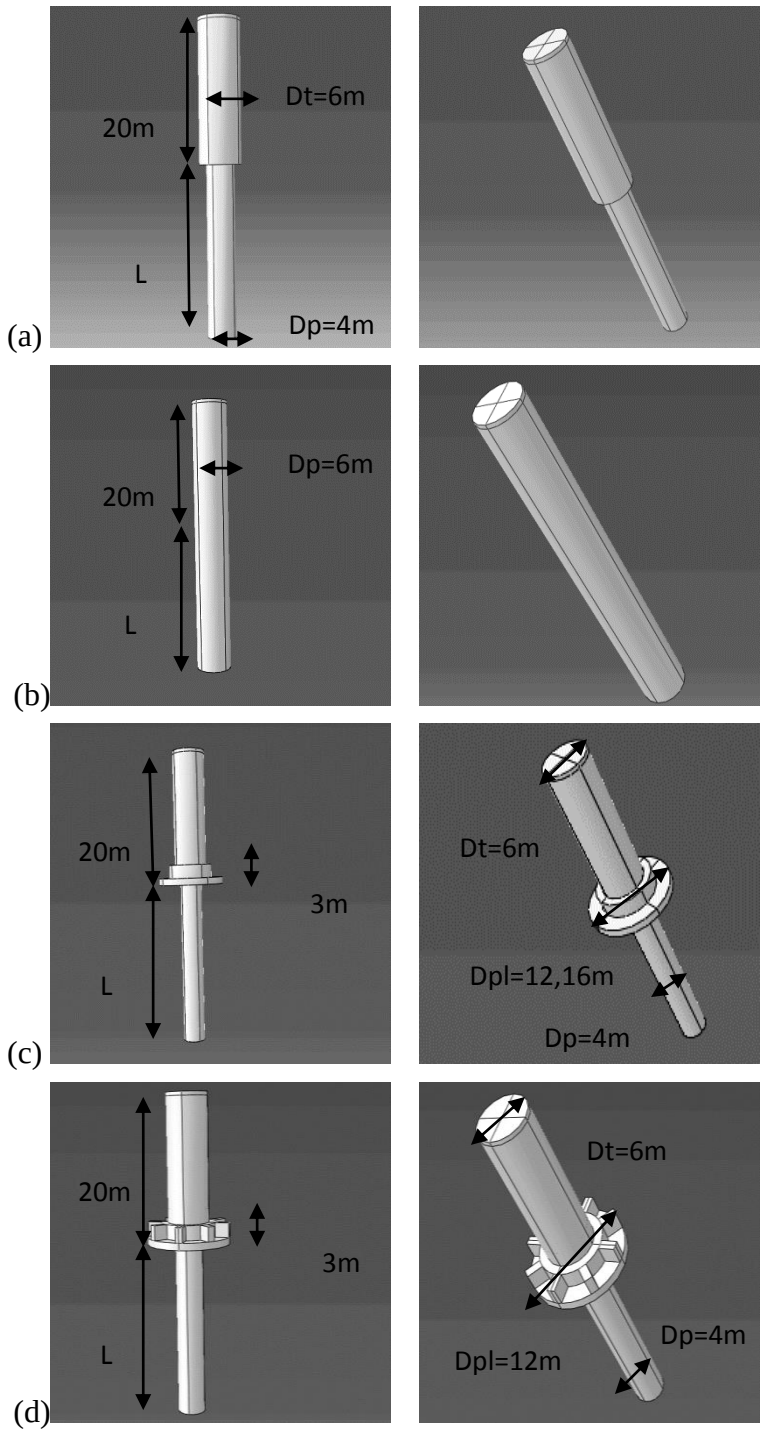

Fig. 6.2: Foundation systems considered in analysis (pile length L=8, 16, 24, 36 m for all systems): (a) pile system D_p=4 m, upper section D_t=6m; (b) pile system D_p=6 m, upper section, D_t = 6m; (c) Hybrid System with D_{Pl}=12, 16 m), (d) Hybrid system with ribbed Plate.

6.2. OBJECTIVES AND SCOPE OF WORK

The main objectives of this chapter are twofold: first, to evaluate the characteristics of the static and cyclic response of monopiles and hybrid foundation systems and compare their performance experimentally; second, to develop an equation to evaluate the lateral stiffness of the proposed hybrid foundation considering the contribution of the concrete plate. To achieve these objectives, 1-g small scale models of the monopiles and hybrid foundations were tested under both static and cyclic loads to investigate their effects on the stiffness and accumulated rotation. Cyclic loading involved up to 10,000 load cycles. In addition, numerical analyses of the experimental setup are conducted using the finite element program ABAQUS (Hibbitt et al., 2009). These analyses helped to further investigate the lateral behaviour of the tested foundation models.

6.3. METHODOLOGY

Current design of piles under lateral loads depends on *p-y* curves, which has been employed in design of flexible piles for several decades. However, it may not be applicable to offshore piles as it depends on empirical data from long, slender and flexible piles, which is not the case in offshore large diameter piles which act as rigid piles. In previous work carried by (Poulos and Hull, 1989), a pile flexibility factor (K_R) was defined as:

$$\boldsymbol{K_R} = \frac{E_s\, L^4}{E_p\, I_p} \qquad \textbf{Eq. 6.3}$$

Where E_s is the elastic modulus of the soil, L is embedded pile length, $\boldsymbol{E_p}$ is elastic modulus of pile and I_p *is* pile moment of inertia.

Poulos and Hull (1989) suggested a range for K_R, where a pile can be considered short, rigid and can rotate without flexing, is given by:

$$4.8 < \frac{E_s L^4}{E_p I_p} < 388.6 \qquad \textbf{Eq. 6.4}$$

Another limitation of *p-y* approach is the long term cyclic effects on the system stiffness, movements and behaviour. In offshore wind turbine foundations, it is expected to have a long-term cyclic loading that can densify or loosen the soil which will change the foundation system while it could not be taken into consideration in this equation.

Considering the geometrical properties of monopiles with 4.0 to 6.0 m diameter and length up to 36 m, these piles can be considered rigid according to **Eq. 6.4**. On the other hand, the plate of the hybrid foundation system can be considered rigid if its flexural rigidity falls within the range suggested by (IS 2950 - Part1- Clause C2, 1981) i.e.:

$$k_r = \frac{E_{pl}}{12E_s}\left(\frac{t}{2D_{pl}}\right)^3 \qquad \textbf{Eq. 6.5}$$

Where E_{pl} is the Elastic modulus of the plate, t is the plate thickness and D_{pl} is the plate diameter. Long and Vanneste (1994) introduced a method to take the effect of cyclic loading into p-y curves by reducing the soil static reaction modulus with the number of loading cycles, i.e.

$$\frac{R_N}{R_0} = N^{-\alpha} \qquad \textbf{Eq. 6.6}$$

Where R_N, R_0 are soil reaction modules on the N^{th} and the first cycle respectively and α is empirically determined degradation parameter depends on the installation method.

Lin and Liao (1999) studied the effects of cyclic loads on the accumulated displacement and proposed the following equation:

$$\frac{u_N - u_0}{u_0} = \beta \ln(N) \qquad \textbf{Eq. 6.7}$$

Where u_N and u_0 are pile head displacement in the nth and first cycle respectively, β empirical degradation parameter depends on the installation method, load characteristic and soil density.

A non-dimensional framework for scaling stiff piles in sand was developed by Leblanc *et al.* (2010). It was used to interpret the test results of 1-g monopile small models. This methodology simulates the monopile lateral and rocking response accounting for the frictional behaviour of the sand, which depends on the isotropic stress level and taking into consideration that the stress level is low in the test leads to a higher friction angle but lower shear stress than that of the full scale. In this method, soil conditions simulation will be carried out by lowing relative density with corresponding stress in the lab. The effect of stress level on the shear modules (*G)* can be represented by (Leblanc, 2010):

$$\frac{G}{P_a} = c_1 \left(\frac{\sigma_v^{'}}{p_a}\right) \qquad \textbf{Eq. 6.8}$$

Where P_a is atmospheric pressure, C_1 is dimensionless constant that varies from 0.435 to 0.765 for small strain to very large strain, respectively (Worth *et al.*, 1979), *n* is pressure exponent of value 0.5 (Kelly *et al*., 2006). The effective vertical stress ($\sigma^{'}_v$) can be calculated at depth of C_2L, where C_2=0.8, by:

$$\sigma_v^{'} = C_2 L \gamma^{'} \qquad \textbf{Eq. 6.9}$$

Where γ' is the soil effective unit weight.

For a case of pile subjected to horizontal load (*H*) and moment (*M*), causing pile head to have displacement (*u*) and rotate with an angle (θ) as shown in **Fig. 6.3**, the stiffness matrix can be written as follows:

$$\begin{bmatrix} M \\ \overline{L} \\ H \end{bmatrix} = DG \begin{bmatrix} K_1 & K_2 \\ K_2 & K_3 \end{bmatrix} \begin{bmatrix} L\theta \\ u \end{bmatrix} \qquad \textbf{Eq. 6.10}$$

Where L is the embedded pile length, D is the pile diameter and G is the shear modulus, while k_1, k_2 and k_3 are dimensionless constant parameters. Hence, by eliminating u , M can be given by:

Eq. 6.11

$$M = \left[\frac{GL^2D(K_1K_3 - K_2^2)}{K_3 - K_2(HL/M)}\right]\theta$$

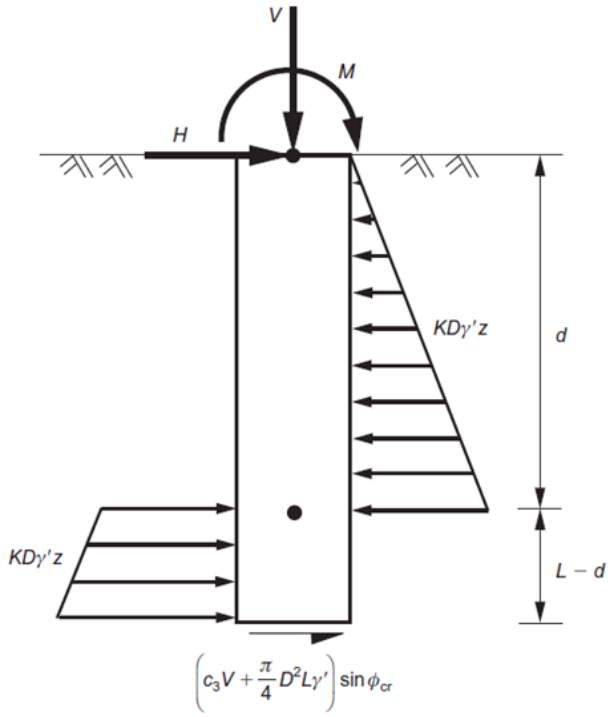

Fig. 6.3: Horizontal stress distribution in ultimate limit state for laterally loaded stiff pile in sand (after Le Blanc 2010).

The scaling rules were developed by incorporating **Eqs. 6.8** and **6.9** in **Eq. 6.11** to obtain the moment - rotation relationship, i.e.

$$\underbrace{\frac{M}{DL^3\gamma'}}_{M'} = \underbrace{\frac{c_1\sqrt{c_2}\left(K_1K_3-K_2^2\right)}{K_3-K_2(HL/M)}}_{k'}\underbrace{\sqrt{\frac{P_a}{L\gamma'}}}_{\theta'}\theta \qquad \textbf{Eq. 6.12}$$

$$M' = k' \theta'$$

From **Fig. 6.3**, it is assumed that the shear stress is at the critical state represented by frictional angle Φ_{cr}, hence, from horizontal and moment equilibrium at the pile head, the following equations can be derived:

$$\frac{3}{K}\underbrace{\frac{M}{DL^3\gamma'}}_{M'} = \alpha + 1 \pm 2\left(\frac{1}{2} + \alpha + \frac{1}{K}\underbrace{\frac{H}{L^2D\gamma'}}_{H'}\right)^{\frac{3}{2}} \qquad \textbf{Eq. 6.13}$$

$$\alpha = \left(c_3\underbrace{\frac{V}{DL^2\gamma'}}_{v'} + \frac{\pi}{4}\underbrace{\frac{D}{L}}_{1/\eta}\right)\frac{\sin\emptyset_{cr}}{K} \qquad \textbf{Eq. 6.14}$$

The non-dimensional parameters that are used to scale down the model monopiles are presented in **Table 6.1**. These parameters depend mainly on producing lower relative density to simulate the same stress level in the lab.

Table 6.1: Non dimensional parameters (Leblanc *et al.*, 2010)

Non Dimensional Parameters	
Moment Loading	$M' = \frac{M}{L^3 D\gamma'}$
Vertical Force	$V' = \frac{V}{L^2 D\gamma'}$
Horizontal Force	$H' = \frac{H}{L^2 D\gamma'}$
Rotation Degree	$\theta' = \theta \sqrt{\frac{p_a}{L\gamma'}}$
Load Eccentricity	$e' = \frac{M}{HL}$
Aspect Ratio	$\eta = \frac{L}{D}$

6.4. EXPERIMENTAL SETUP

An extensive model testing under 1-g conditions to evaluate the performance of a pile foundation system subjected to long term cyclic loading was presented by LeBlanc et al. (2010). In this model, an air-compressed (AC) motor was used in the dynamic loading and load wire technique in the static loading in a rectangular 0.55× 0.60× 0.60 m container. Another test was conducted by Hellmigk (2012) using the same techniques employed by LeBlanc et al. (2010) in a cylindrical container and the load was applied through an Instron 8872 loading device. Moreover, Joonyong *et al.* (2012) presented test setup that was used successfully to evaluate the lateral behaviour for offshore wind turbine foundations, which involved a steel container with 1.20×1.00×1.00 m internal dimensions. Another technique for 1-g modeling was presented by Altee *et al. (*1994), which involves calculating stress and strain within the soil by considering rigid pile behaviour.

The experimental test setup employed in the current study was based on the similitude relationships and test procedures established by LeBlanc et al. (2010). It comprised a steel cylinder container to enclose the test sand bed. It has a diameter of 1.35 m and depth of 1.55 m as shown in **Fig. 6.4**. A steel frame was installed on top of the container in order to guide the installation and leveling of the model piles. Moreover, the steel frame was used as a platform to support two linear variable displacement transducers (LVDTs), the static and dynamic load cells.

A pulley system was used to conduct the static lateral loading as shown in **Fig. 6.5**. Cyclic loading was conducted using an air pressure actuator (SMC Cylinder, CDBXWL25-100), as shown in **Fig. 6.6**. The air pressure in the laboratory air pressure line was used to provide the required pressure to the actuator to generate the load. A pressure gauge was provided to measure the pressure. The cyclic loads were applied at different load eccentricity (*e*) values (i.e. 0.50, 0.75 and 1.00 m) to produce horizontal load and rocking moment combinations representative of wind turbine loading conditions.

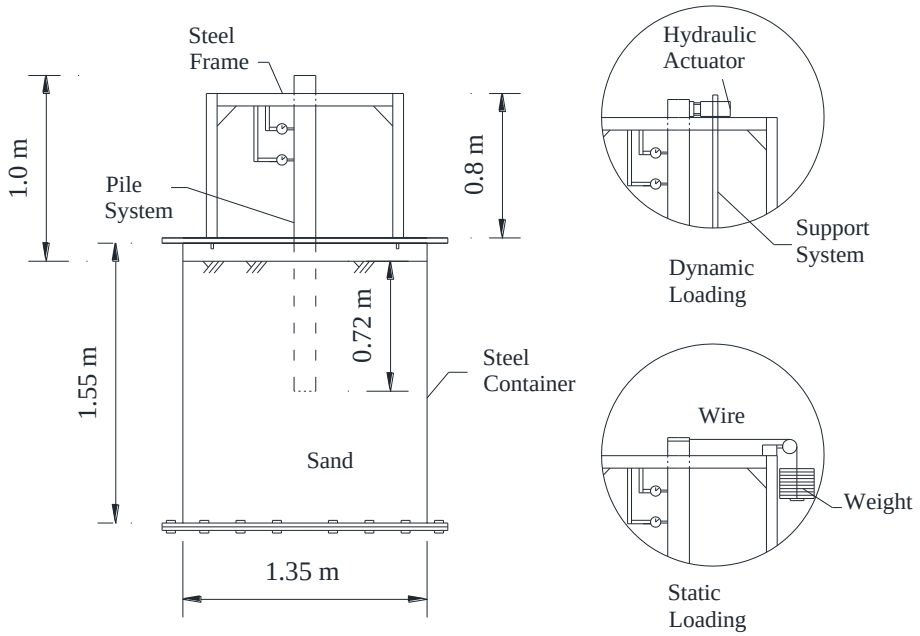

Fig. 6.4: Load test setup for both static and dynamic loading.

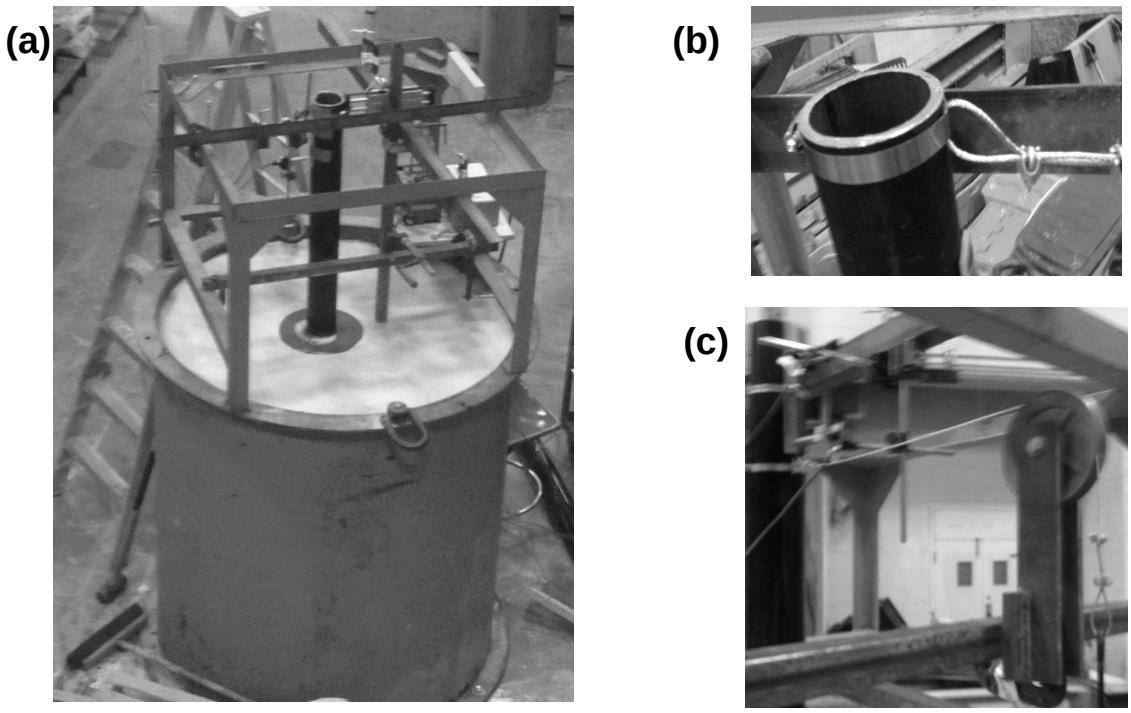

Fig. 6.5: Test setup: (a) isometric view showing the support system for dynamic load actuator; (b) connection between the steel wire and the pile; (c) pulley for static loading.

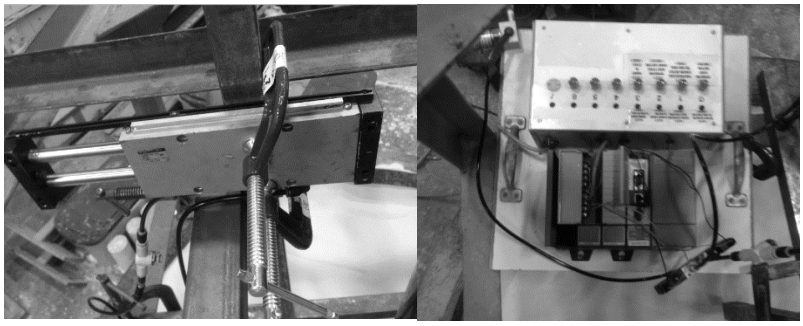

Fig. 6.6: SMC Cylinder (CDBXWL25-100) actuator

6.5. SOIL MODEL

The framework for small scale model tests of stiff piles installed in sand developed by Leblanc (2010) depends on scaling the soil stiffness. It considers soil angle of internal friction and relative density in order to scale down the vertical stress at 0.8 *L*. For yellow Leighton Buzzard sand, the

scaling relationship between the model and full scale sand properties are shown in **Fig. 6.7** (Leblanc, 2010). Relative density for the full scale pile at the actual effective vertical stress will be reduced to a smaller value equivalent to that at the effective vertical stress in the laboratory with the same friction angle.

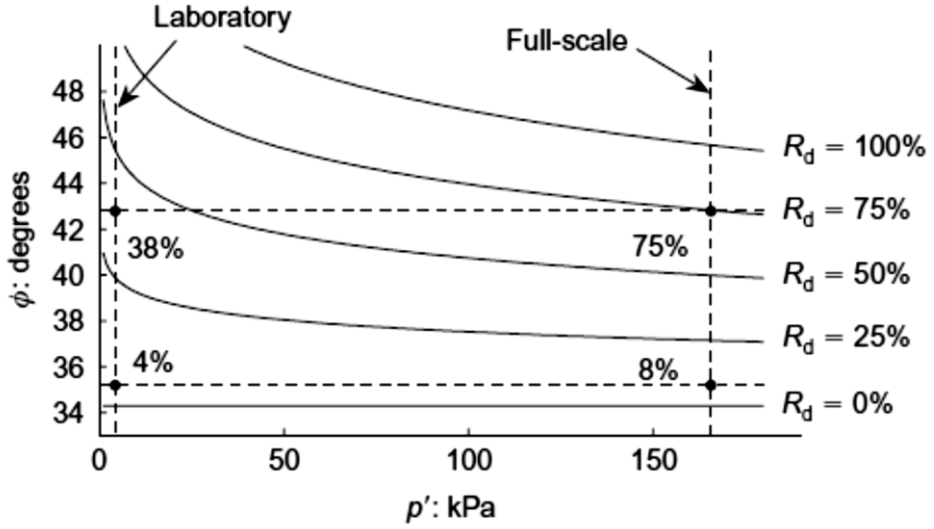

Fig. 6.7: scaling relationship between laboratory and full scale sand properties (Leblanc, 2010)

On the other hand, Ottawa sand F(50) was well characterized by Hellmigk *(*2012) through extensive laboratory testing, which involved sieve analysis and direct shear tests. The results of sieve analysis are given in **Fig. 6.8**. The variation of the sand angle of internal friction (ϕ) with confining pressure for different values of relative density (D_r) is presented in **Fig. 6.9**. The sand physical and engineering properties are provided in **Table 6.2**.

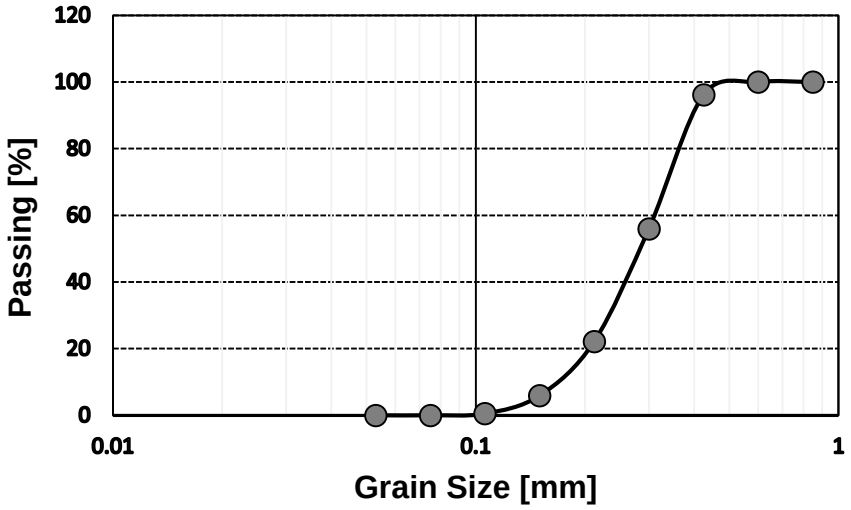

Fig. 6.8: Sieve analysis for Ottawa sand F(50).

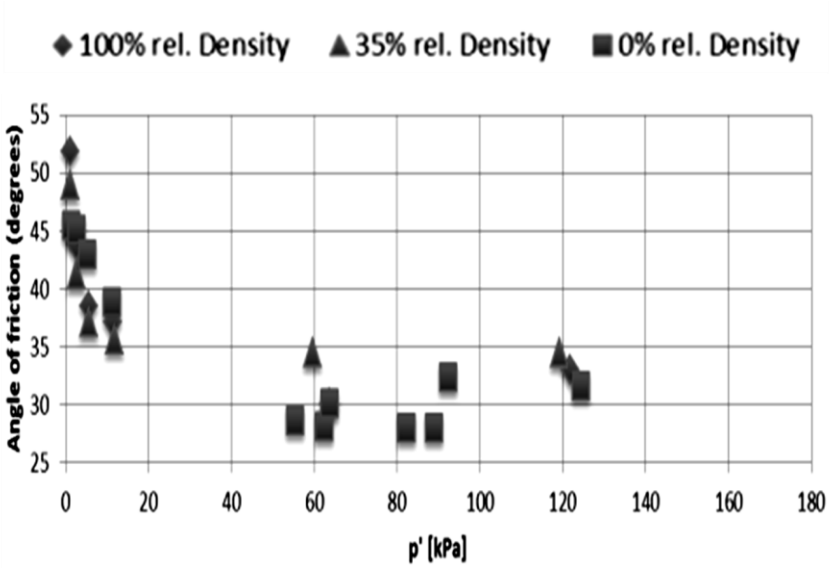

Fig. 6.9: Variation of friction angle of Ottawa sand F(50) with D_r and vertical effective stress (After Hellmigk, 2012)

Table 6.2: Characteristics of Ottawa Sand (F50) (After Helimigk., 2012)

Property		Value
Particle sizes, D_{10}, D_{30}, D_{50}, D_{60} mm		0.17, 0.24, 0.28, 0.32
Specific Gravity G_s		2.65
Void Ratio (%)	Maximum	0.79
	Minimum	0.59
Unit Weight KN/m^3		14.14
Critical Angle of Friction, ϕ_{cr}		32.00

Several tests were conducted on different dry densities for Ottawa sand F50 with range of 1378 kg/m^3 to 1682 kg/m^3. The range of stress at 0.8 L will be in the range of 9 kPa that require relative density less than 0% in the model which is not possible. Hence, (Helimigk, 2012) suggested using critical state approach to scale the soil employing the following equation (Altaee, 1994):

$$e_m = e_p + \lambda \ln(n) \qquad \textbf{Eq. 6.15}$$

Where e_m model void ratio, e_p prototype void ratio, λ is the slope of the critical state line (-1.46) and n is the geometric scale ratio as shown in **Fig. 6.10**. **Table 6.3** shows the scaling laws for soil void ratio.

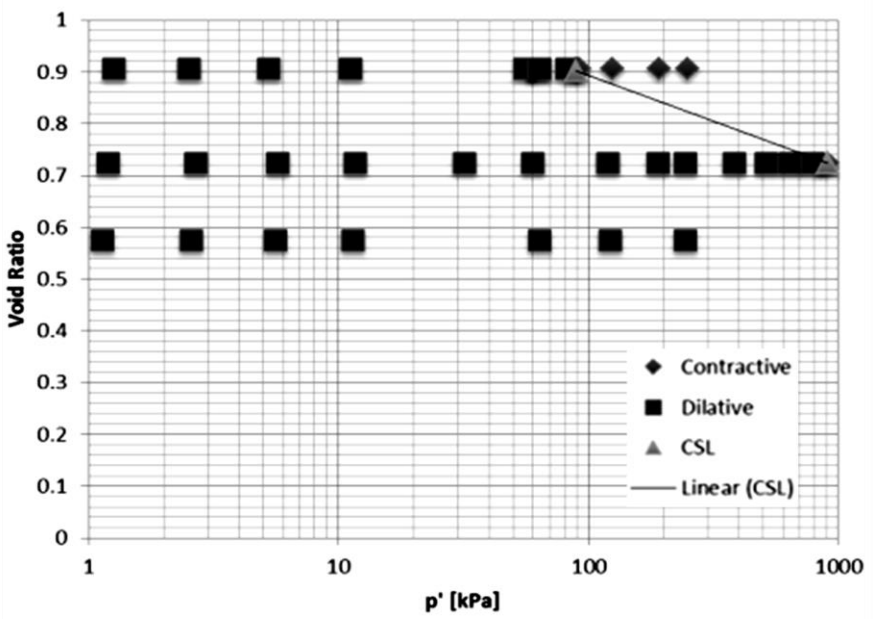

Fig. 6.10: Critical state line for Ottawa F-50 sand (After Hellmigk, 2012).

Table 6.3: Void ratio in the model depending on the void ratio in the prototype and the geometric scaling (Helimigk *et al*., 2012)

	n=0.1	**n=0.01**	**n=0.001**
e_p	**e_m**	**e_m**	**e_m**
0.55	0.71	0.87	1.03
0.60	0.76	0.92	1.08
0.65	0.81	0.97	1.13
0.70	0.86	1.02	1.18
0.75	0.91	1.07	1.23
0.80	0.96	1.12	1.28
0.85	1.01	1.17	1.33
0.90	1.06	1.22	1.38

6.6. FOUNDATION MODELS

Four different foundation models were tested: two monopiles with diameter 0.08 and 0.12 m; and two hybrid systems. Each hybrid system comprised a monopile and a surface plate. The model foundations were scaled with 1:50 scale taking into consideration that the geometry scaling is not related to soil scaling and qualifying **Eq. 6.4** requirement to have a rigid system. One hybrid foundation had a steel plate 0.32 m in diameter and the other had a very stiff concrete plate with a diameter of 0.45 m. **Figure 6.11** shows the four tested foundation models, while **Table 6.4** presents their geometrical details.

Table 6.4: Properties of steel pile used in the model.

Property	Model scale dimensions (mm)	Prototype scale dimensions (m)
Pile diameter (D)	120, 80	6.0, 4.0
Plate Diameter (B)	450, 320	22.5, 16.0
Wall thickness (t)	5	0.25
Penetration depth (L)	720	36.0
Load eccentricity (e)	500, 700, 1000	25.0, 35.0, 50. 0

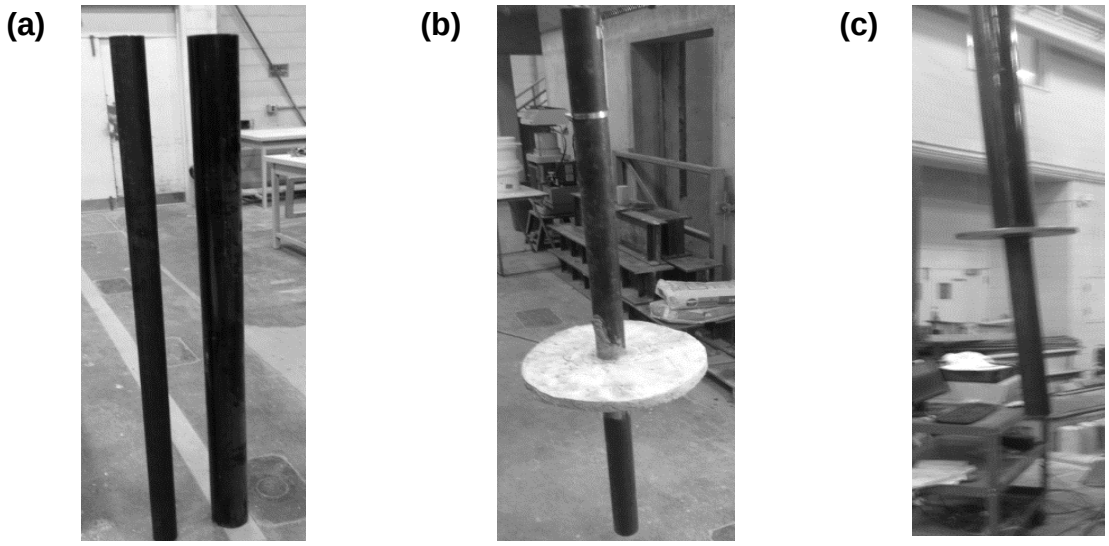

Fig. 6.11: Different foundation models: (a) monopiles; (b) hybrid system with concrete plate; (c) hybrid system with steel plate

The model piles were driven into the sand bed with the aid of a hammer falling from fixed dropping distance. It took approximately 350 and 500 hammer blows to reach the final penetration depth for piles with diameter of 0.08 m and 0.12 m (prototype diameter 4.0 and 6.0 m) with leveling at each stage as shown in **Fig. 6.12**, respectively.

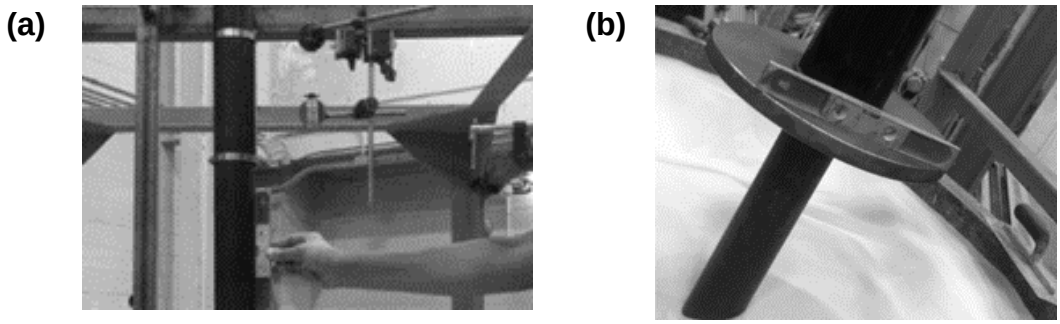

Fig. 6.12: Leveling foundation models: (a) monopile, D = 4 m; (b) hybrid system.

Two hybrid foundation models were tested. One hybrid foundation model comprised of very stiff concrete plate and a pile with a 0.08 m diameter to study the effect of varying the plate rigidity on the behaviour of the hybrid system. **Figure 6.13** shows the added steel stiffeners to

ensure adequate connection between the pile and concrete. The composition of the used concrete mixture is given in **Table 6.5**. As per **Eq. 6.4,** the rigidity of the plate will not affect the system behaviour as long as it falls within the range of rigid value.

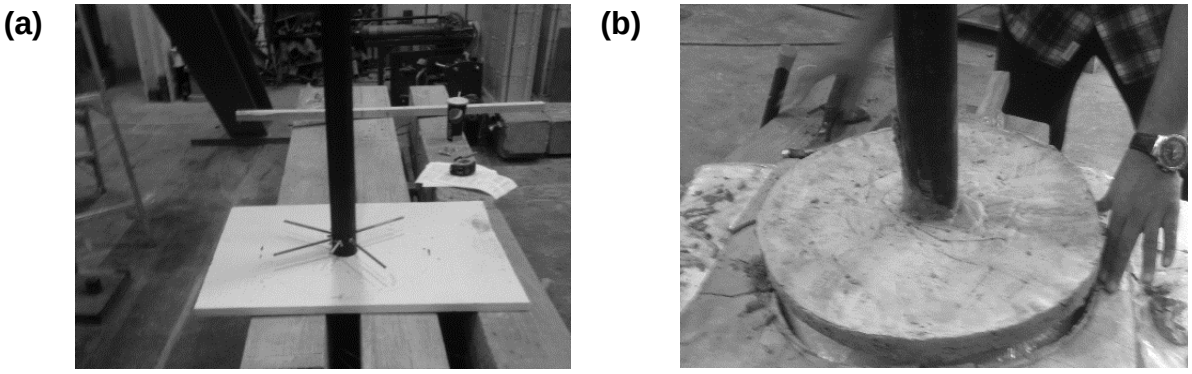

Fig. 6.13: Construction of the very stiff concrete plate to form the hybrid system: (a) attaching stiffeners to the pile to ensure full contact; (b) casting the plate.

Table 6.5: Composition of ultra-strength concrete mixture (Soilman and Nehdi, 2010)

Material	**(Mass/cement mass)**
Cement	1.00
Silica fume	0.3
Quartz sand (0.1-0.5 mm)	0.43
Quartz sand (0.3-0.8 mm)	1.53
Water	0.25
HAWRA	0.03

6.7. TESTING AND DISCUSSION

A series of 12 static load tests for the four systems with three different eccentricities (0.5, 0.75 and 1m) were conducted as shown in **Fig. 6.14**. Pulley and C clamps were used with steel bars to set the test for each eccentricity.

Figures 6.15 to **6.17** show the static moment- rotation curves determined from the static load tests for the different foundation models subjected to load with different load eccentricity (i.e. e = 0.5, 0.70 and 1.0 m). In these figures, the failure was defined to be attained when θ' = 4°=0.0698 rad and is represented by dotted lines at θ' = 0.0698 rad. Inspecting these figures, it is observed that the monopile with 0.08 m diameter (i.e. monopile with prototype diameter of 4.0 m) experienced the largest rotational displacement, which is in agreement with the results obtained from the finite element analyses reported in Chapters 4 and 5. In addition, the hybrid system with plate of 0.32 m in diameter (i.e. prototype diameter of 16 m) exhibited rotational displacement less than that of the monopile with 0.12 m diameter (i.e. prototype diameter of 6.0 m). Finally, the results demonstrate that the effect of increasing the plate diameter is to further enhance the performance of the hybrid system. This is manifested in the superior performance of the hybrid system of 0.45 m plate diameter (i.e. prototype diameter of 22.5 m diameter), which exhibited the best performance among all tested foundation models.

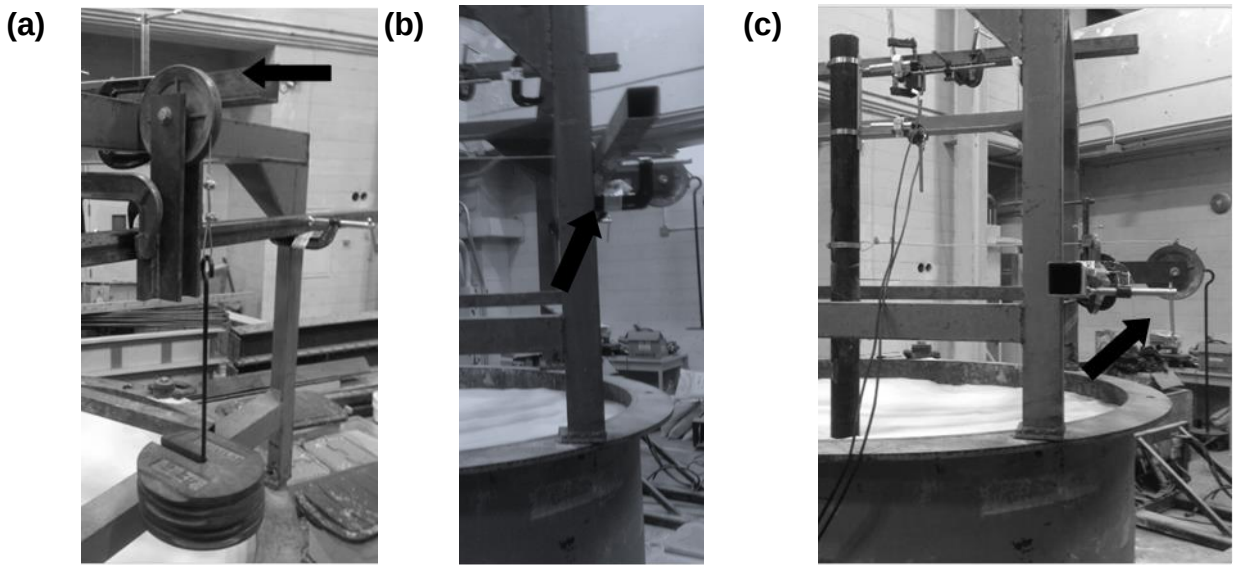

Fig. 6.14: Use of pulley and C clamps for different load eccentricities: (a) e=1m; b) e=0.75 m; c) e=0.5 m.

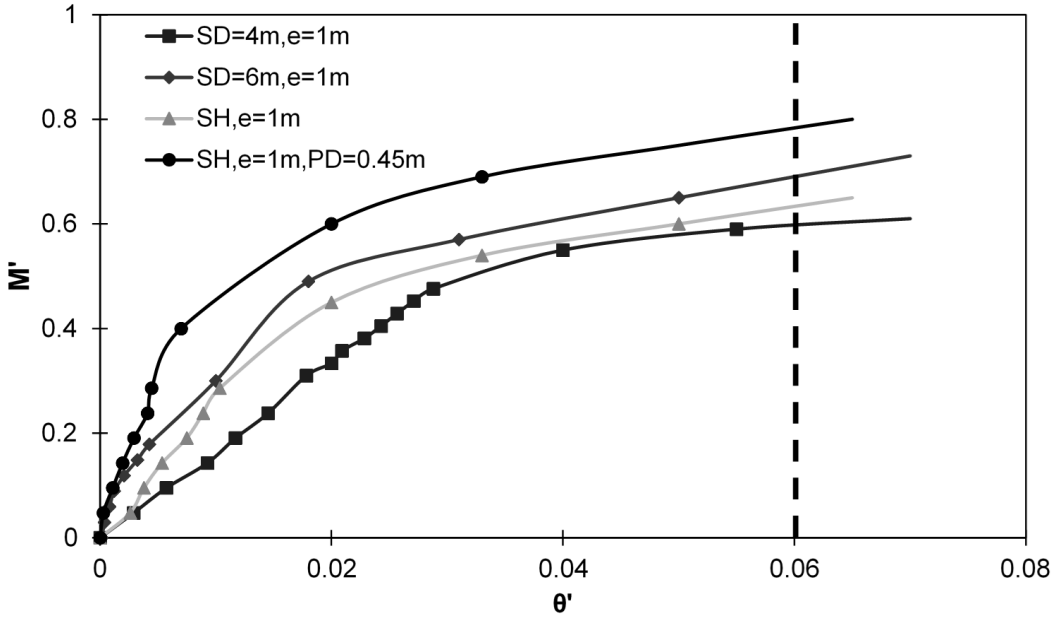

Fig. 6.15: Static moment-rotation curve of different systems with load eccentricity e = 1 m.

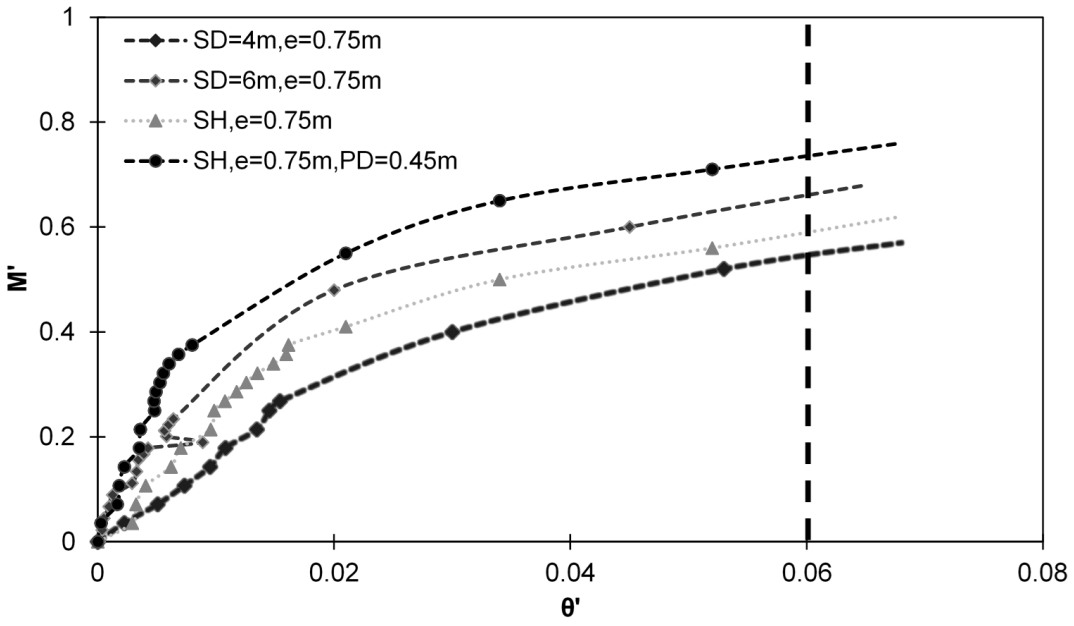

Fig. 6.16: Static moment-rotation curve of different systems with load eccentricity e = 0.75 m.

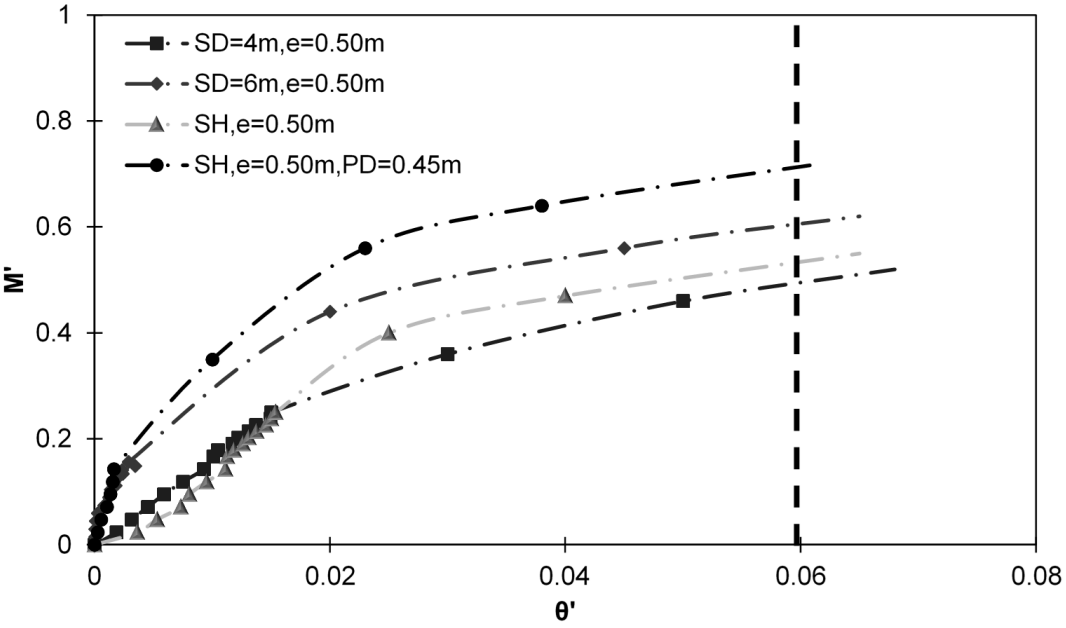

Fig. 6.17: Static moment-rotation curve of different systems with load eccentricity e = 0.5 m.

The static moment – lateral load capacity relationship (i.e. interaction diagram) of the different foundation models were evaluated using Eqs. 6.11 and 6.12. A comparison between the measured moment – lateral resistance capacity results at failure (i.e. $\theta = 4^{\circ}$) and the theoretical values calculated using **Eqs. 6.11** and **6.12** is presented in **Fig. 6.18**. Good agreement between the measured and calculated responses for the two monopile cases can be noted from Figure 6.18. As expected, Figure 6.18 shows that the two hybrid foundation cases exhibited increased lateral resistance over that of the monpopile cases.

In order to establish a moment – lateral resistance capacity relationship for the hybrid foundation system, the moment – lateral resistance contributions of its components (i.e. monopole and circular plate) are considered. The moment – lateral resistance interaction diagram for the monopile is established first. This is followed by plotting the moment – lateral resistance interaction diagram for the hybrid foundation system on the same graph. The additional resistance over that of the monopile (after discarding any points that fall within the interaction diagram) can be attributed to the plate. Curve fitting these data points, new equations can be proposed to describe the plate effect on improving the foundation system lateral capacity, i.e.

$$\frac{M}{DL^3\gamma'} = -\frac{a}{B} + 0.33K(\alpha + 1 \pm 2\left(\frac{1}{2} + \alpha + \frac{1}{K}\frac{cBH}{L^2D\gamma'}\right)^{\frac{3}{2}}) \qquad \textbf{Eq. 16}$$

$$\frac{M}{DL^3\gamma'} = -\frac{a}{B} + 0.33K(\alpha + 1 \pm 2\left(\frac{1}{2} + \alpha + \frac{1}{K}\frac{cBH}{L^2D\gamma'}\right)^{\frac{3}{2}}) \qquad \textbf{Eq. 17}$$

The values of the curve fitting parameters, *a* and *c*, are provided in Table 6.6. Employing Eqs. 6.16 and 6.17, it is possible to predict a safe combination of bending moment and lateral forces acting on a hybrid foundation system as function of the plate width (B=D_{pl}). The proposed

equations (i.e. **Eqs. 6.16** and **6.17**) with the curve fitting parameters listed in Table 6.6 are valid for 16.0 m < (D_{pl}) < 22.5 m, but can be used approximately for other values of D_{pl}.

Table 6.6: Plate factors

B	***a***	***c***
***D_{pl}*=16 [m]**	5	0.0136
***D_{pl}*=22.5 [m]**	4	0.00476

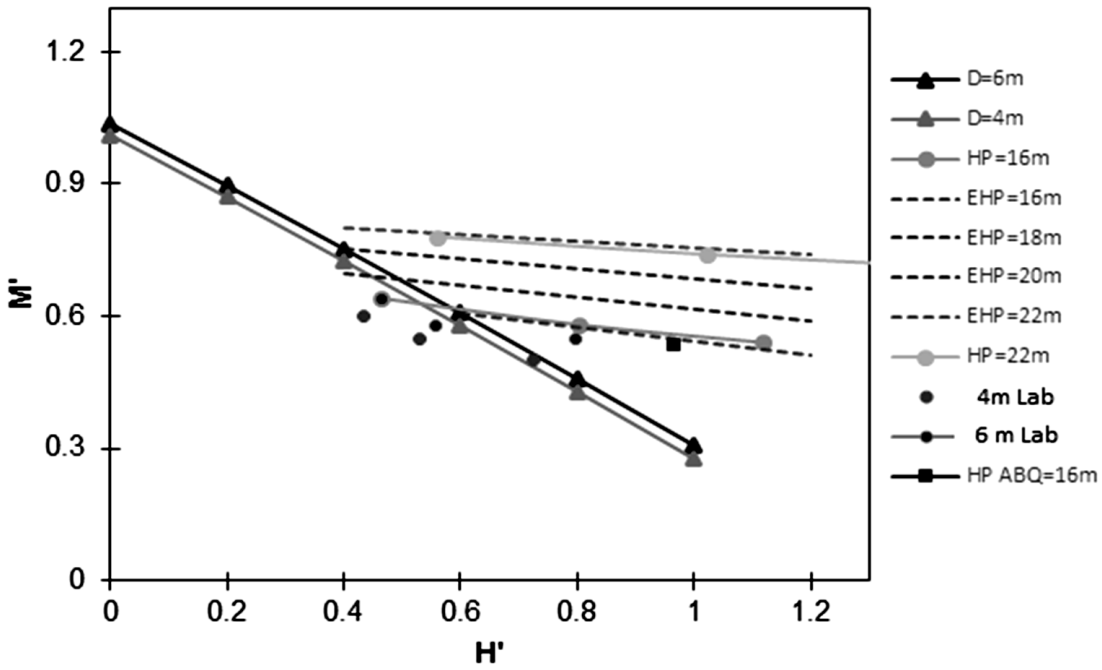

Fig. 6.18: Moment – lateral capacity interaction diagrams for considered foundation systems

6.8. CYCLIC LOADING

The main purpose of cyclic loading is to investigate the performance of the hybrid foundation system under the effect of long term cyclic loading. The cyclic loading system involved employing a low cost SMC Cylinder (CDBXWL25-100) actuator (as shown in **Fig 6.6**) to apply a one way cyclic loading on the different foundation systems. **Figure 6.19** presents the set up for the cyclic loading for different foundation systems with load eccentricity, e = 1m.

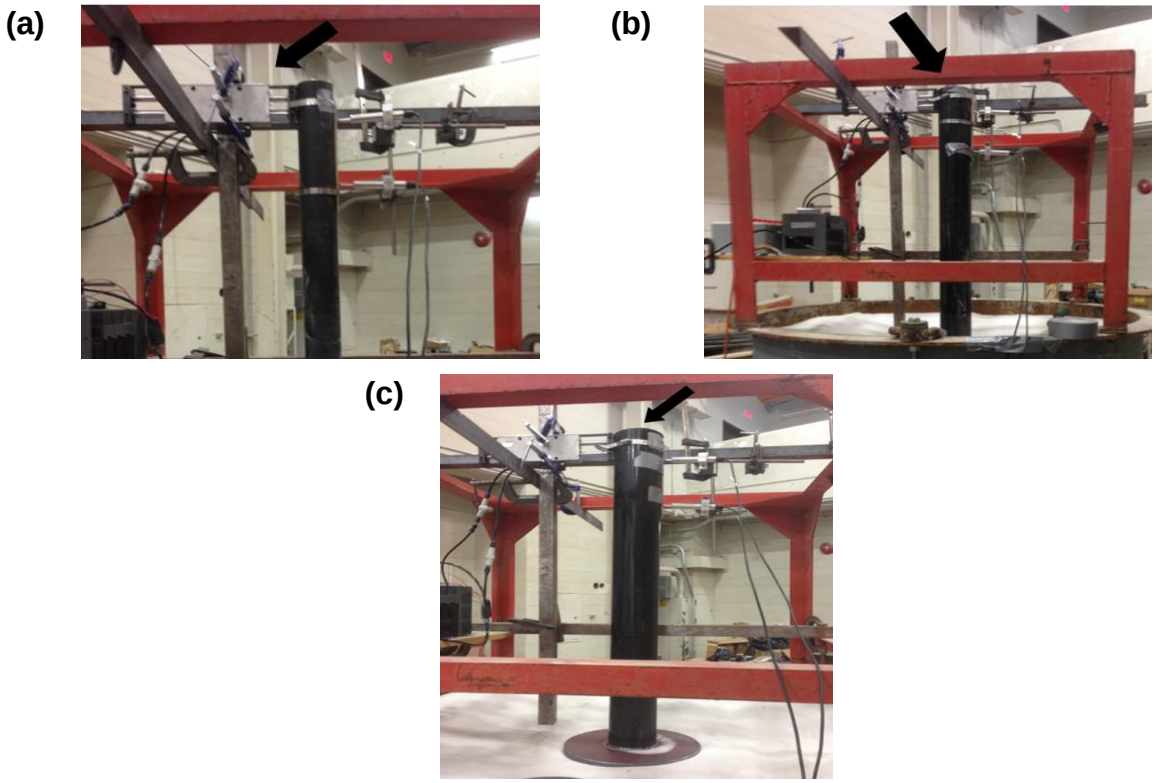

Fig. 6.19: Dynamic setting for the different systems;(a)pile with 4 m diameter; (b) pile with diameter 6 m ; (c) hybrid system.

A scaled down horizontal load of 21 N and 24 N for pile with D_{pile}= 0.08 cm and 0.12 m respectively, representing the prototype load of 3000 KN that was obtained from the wind tunnel

test on the 5 MW wind turbine, was applied to the foundation models. To achieve this load, the air pressure applied to the actuator was adjusted considering its cross-sectional area to produce the target load. The lateral displacement and rotation of the tested foundation were measured at the end of each load cycle. The accumulated rotation and corresponding foundation stiffness at each load cycle is calculated as defined in **Fig. 6.20**.

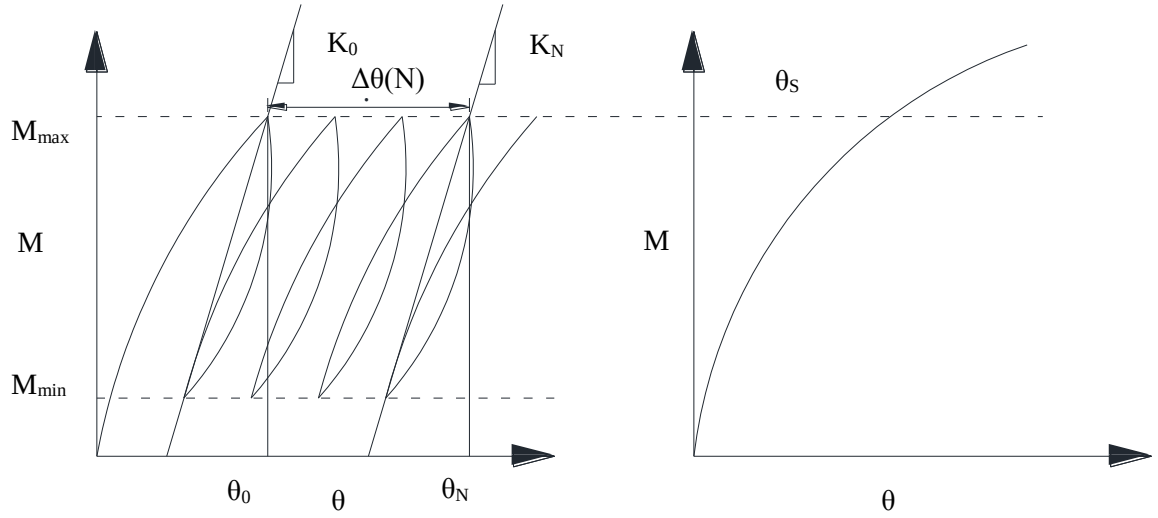

Fig. 6.20: Method for determination of stiffness and accumulated rotation (a) cyclic test; (b) static test (after LeBlanc *et al.*, 2010)

Both accumulated rotation and stiffness are a function of the number of cycles. To account for the effect of cyclic loading on the accumulated rotation and stiffness of the piles subjected to cyclic loading, Leblanc *et al.* (2010) proposed the following two equations to indicate the change in the dimensionless rotation, $\Delta\theta/\theta_s$, and stiffness, :

$$\frac{\Delta\theta(N)}{\theta_s} = \frac{\theta_N - \theta_0}{\theta_s} \qquad \textbf{Eq. 6.18}$$

$$\tilde{k} = \frac{k}{L^{5/2} D \sqrt{p_a \gamma'}}$$ **Eq. 6.19**

Although (Leblanc *et al.*, 2010) demonstrated that the loading range and the soil relative density can change both stiffness and rotation, only one value of soil relative density was considered in this study with the main focus on evaluating the relative performance of the different foundation systems.

Figures 6.21 and **6.22** display the readings of the upper and lower LVDTs representing the displacement at two different points along the top of the monopiles, while Fig. 6.23 shows the readings of the upper and lower LVDTs along the top of the hybrid system. Comparing the results in Fig. 6.23 with those in Figs. 6.21 and 6.22, it is clear that the lateral displacement of the hybrid foundation system is much lower than that of both tested monopoles. In addition, the difference between the readings of the two LVDTs, which indicate the rotation of the foundation system, is much lower for the hybrid foundation case compared to the monopiles.

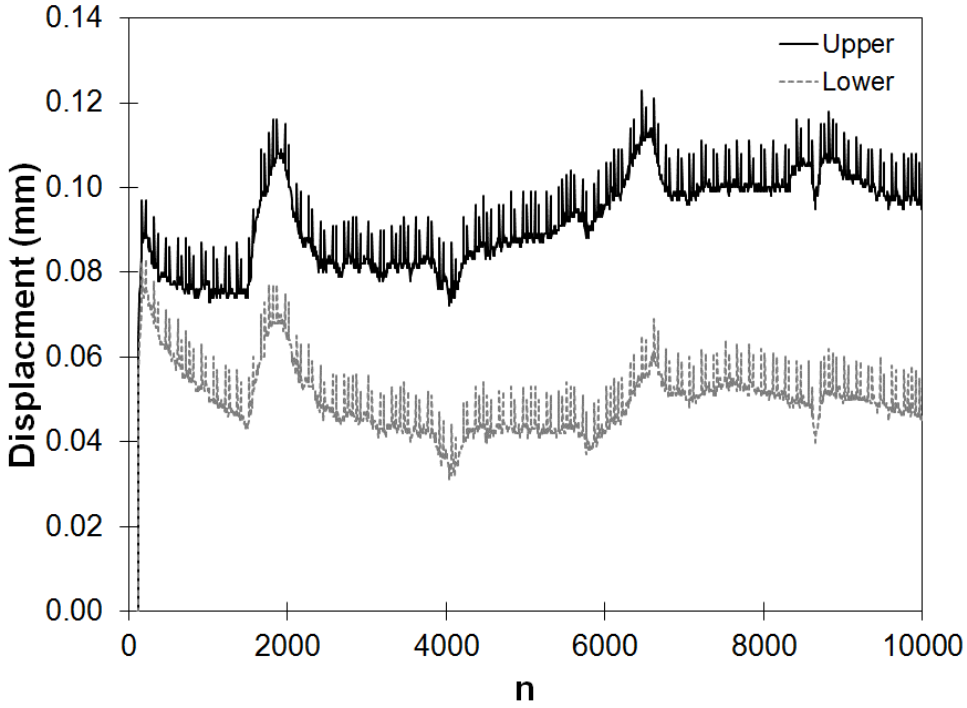

Fig. 6.21: LVDT readings for pile with D_p = 4 m under cyclic loads.

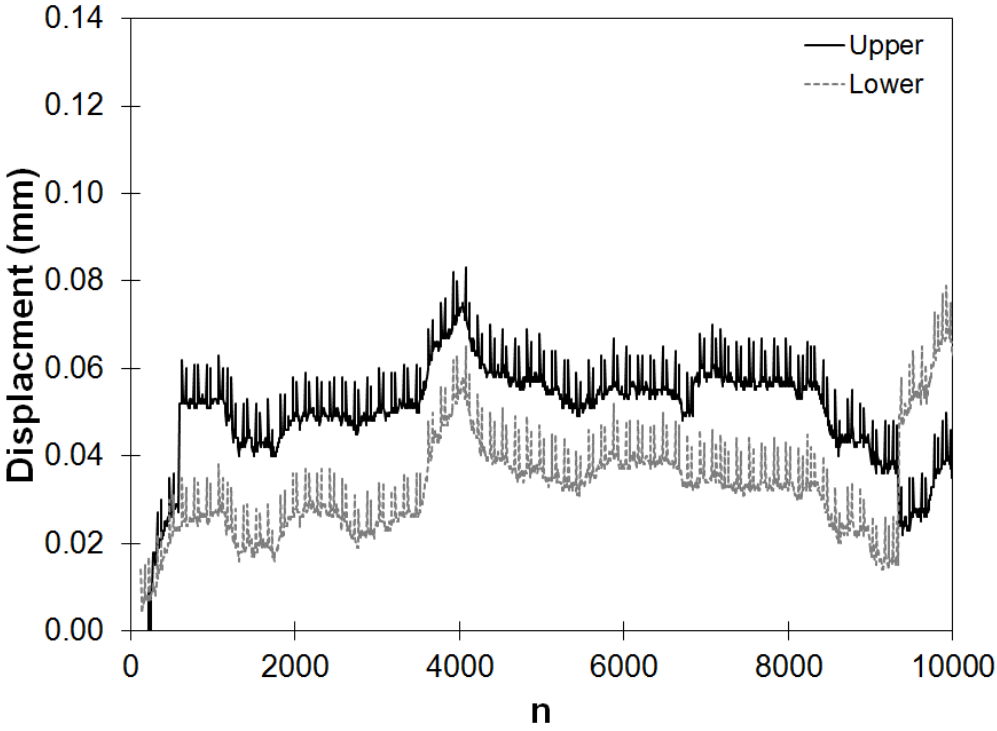

Fig. 6.22: LVDT readings for pile with D_p = 6 m under cyclic loads.

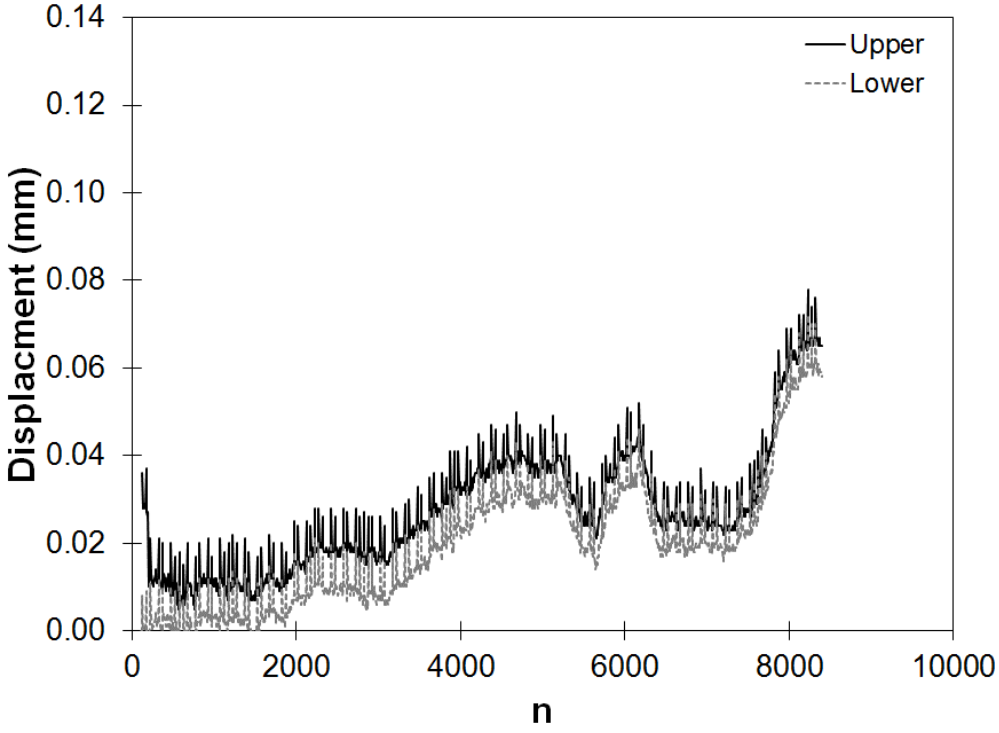

Fig. 6.23: LVDT readings for hybrid foundation system under cyclic loads.

The readings of the LVDTs are used to calculate the variation of the cumulative rotation and corresponding stiffness (as indicated in Fig. 6.20) with the number of load cycles and the results are presented in Figure 6.24 for the different foundation systems. **Figure 6.24** shows that as the number of cycles increased, the general trend is that calculated stiffness initially either remained the same or decreased slightly, followed by an increase at an almost constant slope and then remained almost constant afterwards. This is clearly demonstrated by the straight lines fitted to the cyclic test data. These observations confirm that there was no degradation in the tangential stiffness. Leblanc *et al.* (2010) observed similar behaviour through cyclic load testing of very stiff piles installed in cohesionless material. Their analysis of the test results demonstrated that the slope of a straight line fitted to the test data will not change (i.e. no stiffness degradation) with the number

of loading cycles or soil state (i.e. loose or dense soil). However, the pile stiffness at the first cycle (k_0) may change.

It can also be noted from Fig. 6.24 that the initial increase in stiffness was highest for the pile with D_p = 6 m compared to both the monopile with D_p = 4m and the hybrid foundation with D_{pl} = 16 m. However, it was observed that the hybrid foundation system reached a plateau after a fewer load cycles, i.e., it offered stable behaviour faster. This is attributed to the soil densification below the plate. This may be an important favourable feature for a foundation system supporting wind turbines that experience large number of load cycles (n) throughout the wind turbine life.

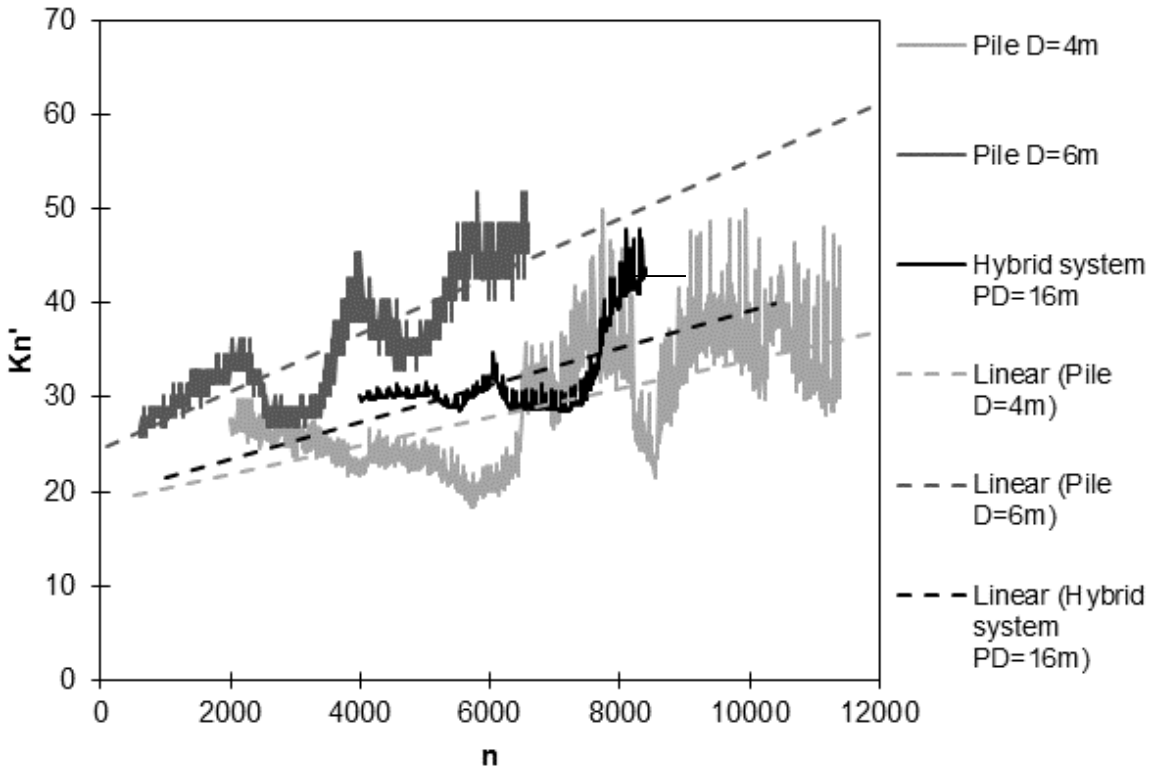

Fig. 6.24: Variation of stiffness with number of cycles n for different foundation systems.

From Figure 6.25, it can be noted that the trends of accumulated rotation of the different foundation systems were similar to their lateral displacements. It can also be noted from Figure 6.25 that as the number of load cycles increased, the accumulated rotation initially either remained the same or decreased slightly, followed by an increase at an almost constant slope and then remained almost constant afterwards. Furthermore, the slope of the stiffness of the hybrid system had increased with smaller value than that of the pile with D_p = 6 m, meaning that its rotational response tends to stabilise sooner than the monopile. LeBlanc et al. (2010) showed that although the rotation of the very stiff pile varies with the soil relative density and load amplitude but the slope of the trend line representing the variation of rotation with number of load cycles remains almost the same, i.e. no degradation. This same behaviour is observed in the current study.

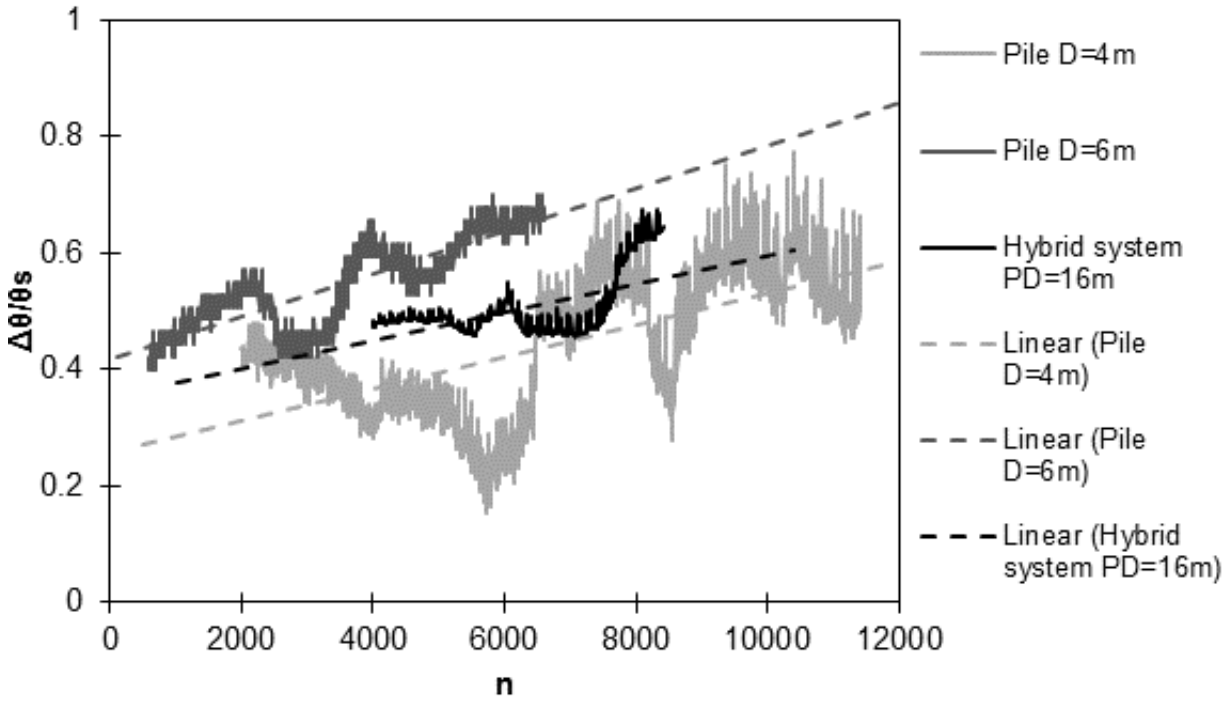

Fig. 6.25: **Variation of a**ccumulated dimensionless rotation with number of cycles (*n*) for different foundation systems.

6.9. NUMERICAL MODELING

To verify the validity of the scaled physical model results, three dimensional finite element models of the tested foundation systems were established using the commercial software ABAQUS (Hibbitt, 2009). Only the monotonic loading phase was considered in the analysis. The numerical model verification was performed for the cases of a monopile with diameter 0.08 m (i.e. which is equivalent to a pile with 4.0 m diameter in the actual size) and a hybrid foundation system with plate 0.32 m diameter (which is equivalent to 16.0 m in prototype). The overall models of these two systems are shown schematically in **Fig. 6.26**.

6.9.1. Numerical model meshing

A sensitivity analysis was conducted to determine the suitable dimensions for the size of elements. The vertical boundary was cylindrical representing the steel soil chamber used to enclose the soil in the scaled physical model tests. The horizontal boundary at the bottom of the model was placed at the bottom of the test cylinder. The mesh was developed using the automatic sweep meshing technique and the medial axis algorithm, which is available in the Abaqus software (2009). The approximate global size of the element was in the range of 0.1-0.5 m.

6.9.2. Boundary Conditions

Fixed translations in X, Y and Z directions were applied at the bottom boundary of the soil model. Fixed translations in both X, Y directions were applied at the vertical boundaries on the soil external surfaces. Interaction surfaces were applied at the interfaces between the elements representing the pile and adjacent soil that allow pile slippage and separation, which can properly

simulate the tangential and normal behaviour. Both monopile (D_p=4) and hybrid foundation system were analyzed considering the static loading phase of the laboratory tests.

6.9.3. Model Description

A 1.72 m long steel pile with diameter, D_p = 0.08 m and wall thickness of 0.005 m was considered in the analysis similar to the monopile tested in the laboratory. The hybrid foundation system with a 1.72 m long steel pile with diameter, D_p = 0.08 m, wall thickness of 0.005 m and plate diameter of 0.32 m. The monopile and hybrid foundation system were installed in sand soil with an average friction angle, $\phi = 36°$ and unit weight of $\gamma = 14.41$ kN/m^3. The 3D numerical model was used to analyze the response of the monopile and hybrid foundation system under horizontal force of 21 kg at the pile head. The steel pipe, steel pile and steel plate were assigned the following properties: yield strength, f_y = 240 MPa, Young's Modulus, E_s = 200 GPa and Poisson's ratio, $\nu = 0.3$. The calculated lateral displacement at top of steel pipe will be compared with the measured response to verify the validity of the observed responses of the foundation system.

6.9.4. Foundation and Soil Modeling

A three dimensional (3D) nonlinear finite element model of the foundation system and soil was established employing the ABAQUS program (Hibbitt, 2009). The soil and components of foundation system were modeled using 3D deformable solid elements with different material models. The sand soil was simulated with the Mohr-Coulomb failure criterion. Interaction properties was considered between different materials to ensure the actual simulation including tangential and normal behavior. The elements were primarily hex shaped and the mesh was developed using the automatic sweep meshing technique and the medial axis algorithm which is available in ABAQUS. The approximate global size of the element was in range 0.1-0.5 m. The

steel pipe, steel pile and steel plate were modeled as elastic-perfectly plastic material with the following properties: yield strength, $f_y = 240$ MPa, Young's Modulus, $E_s = 200$ GPa and Poisson's ratio, $\nu = 0.3$.

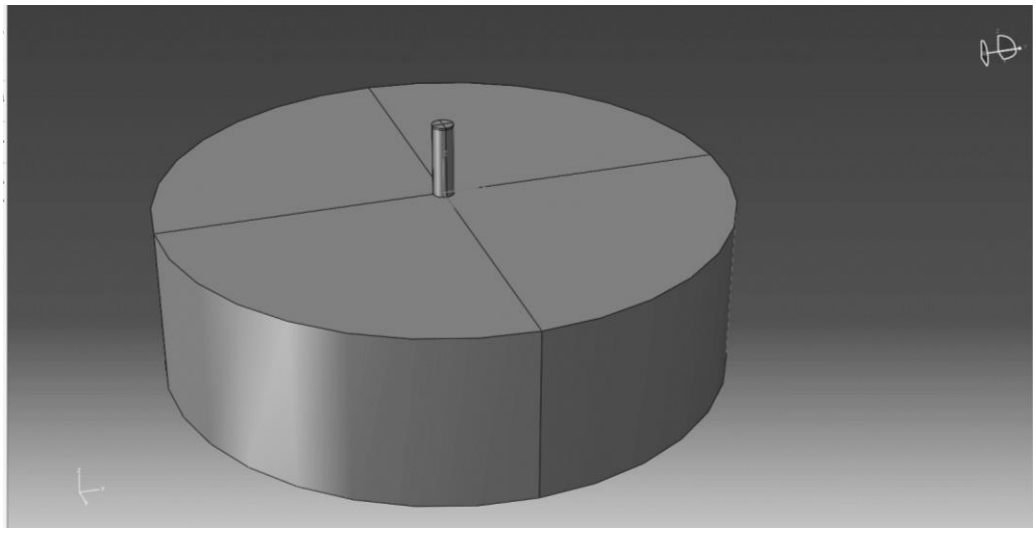

a)

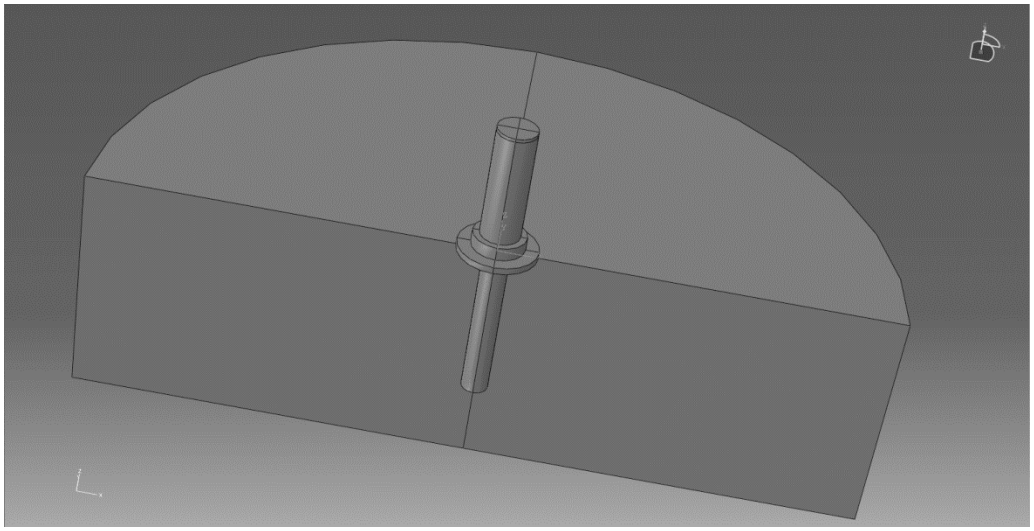

b)

Fig. 6.26: ABAQUS models of examined foundations: a) monopole; b) hybrid foundation system.

6.9.5. Results of Numerical Models

The analyzed foundation systems including monopole, D_p=0.08m and hybrid system with D_{pl} = 0.32 m were modeled considering the same static loads during the experimental study. The calculated responses are compared with the measured responses in **Fig. 6.27**. Generally, there is a good agreement between the calculated and measured responses for both foundation systems as shown in **Fig. 6.27**. In case of the monopile, the agreement between the calculated and measured responses is excellent along the entire static load test data. In the case of hybrid foundation system, the laboratory response curve exhibited stiffer initial response compared to the calculated response, which can be attributed to the lateral soil resistance along the plate wall due to the partial embedment of the plate thickness in the soil during installation in the tank.

These results further confirm the validity of the experimental observations. In addition, the results confirm the superior performance of the hybrid foundation system in terms of initial stiffness (which is important for performance of supported wind turbines) and lateral capacity (which increases the factor of safety of the foundation against excessive lateral displacement).

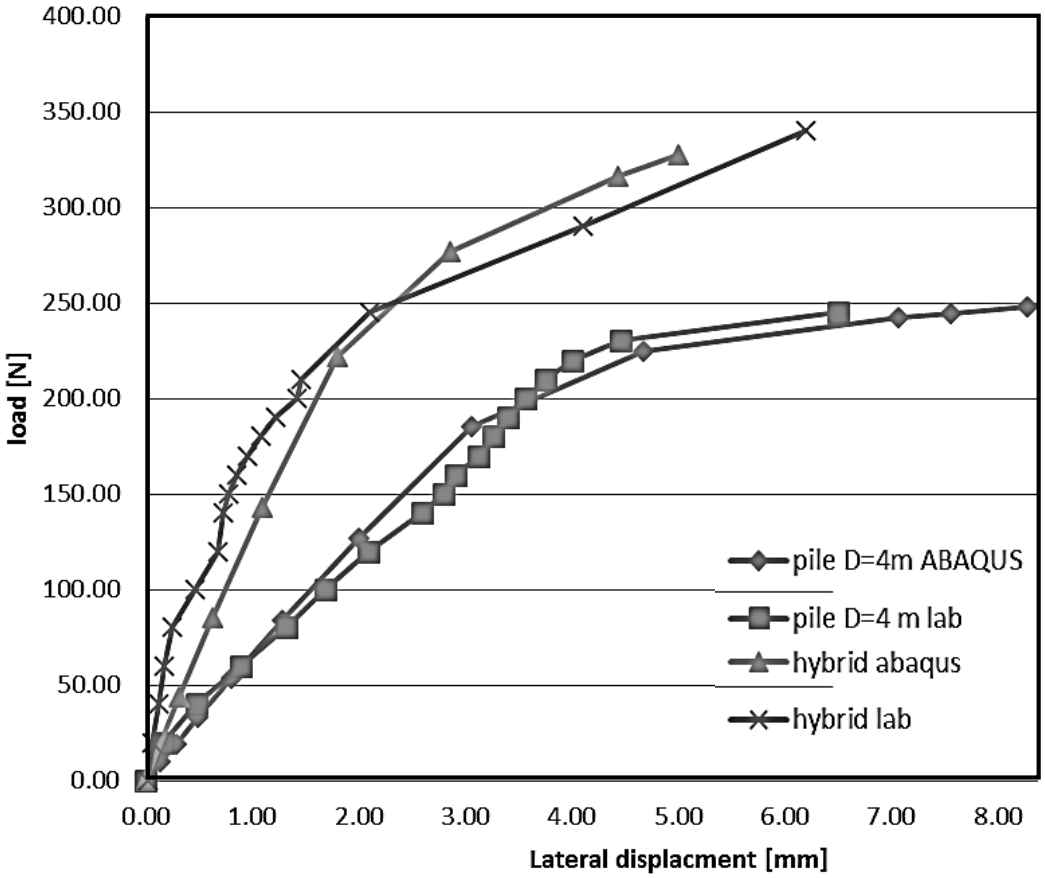

Fig. 6.27: Comparison between the lab and ABAQUS results.

6.10. SUMMARY AND CONCLUSIONS

The long term performance of the hybrid foundation system, which combines a monopile and concrete plate, as well as the conventional monopoles, subjected to cyclic loading was evaluated. A scaled-down non-dimensional framework of stiff foundation models installed in sand was used to conduct a series of static and cyclic loading tests under 1-g. Four main model foundations were tested. In addition, three dimensional nonlinear analyses were conducted to further confirm the validity of the test observations. The results from the physical and numerical modeling confirmed the superior performance of the hybrid foundation system in terms of increased lateral and rotational stiffnesses, which is important for performance of supported wind turbines, as well as lateral capacity, which increases

the factor of safety against excessive lateral displacement. Furthermore, the results obtained from the tests were employed to develop an equation to predict the stiffness of the proposed hybrid foundation system.

6.11. REFERENCES

Altaee, A., and Fellenius, B. H. (1994). Physical modelling in sand. Canadian Geotechnical Journal, Vol. 31, No. 3, pp. 431-443.

Byrne, B.W. and Houlsby, G.T. (2003). Foundations for offshore wind turbines", Philosophical Transactions of the Royal Society of London, Vol. (361), pp. 2909-2930.

Allotey, N. and El Naggar, M.H. (2008a). Generalized dynamic Winkler model for nonlinear soil-structure interaction analysis, Canadian Geotechnical Journal, Vol. 45, No. 4, pp. 560-573.

Allotey, N. and El Naggar, M.H. (2008b). A numerical study into lateral cyclic nonlinear soil-pile response, Canadian Geotechnical Journal, Vol. 45, No. 9, pp. 1268-1281.

Aristonous, M., Trochanis, J.B., and Paul, C. (1991). Three dimensional nonlinear study of piles, Journal of Geotechnical Engineering, Vol.117, No. 3, pp 429-447.

Bentley, K.J. and El Naggar, M.H. (2000). Numerical analysis of kinematic response of piles. Canadian Geotechnical Journal, Vol. 37, No. 6, pp. 1368-1382.

Bhushan K., and Haley, S. C., (1980). Development of computer program using P-Y data from load test results for lateral load design of drilled piers. Research report prepared for Woodward-Clyde Consultants Professional Development Committee, San Francisco, California.

Bhushan, K., and Askari, S., (1984). Lateral load tests on drilled pier foundations for solar plant heliostats. Laterally Loaded Piles, ASTM STP 835, James A. Langer, Ed., American Society of Testing and Materials, pp. 141-155.

Bhushan, K., Lee, L. J., and Grime, D. B., (1981). Lateral load tests on drilled piers in sand. Proceedings of a Session on Drilled Piers and Caissons, sponsored by the Geotechnical Engineering Division at the ASCE National Convention, St. Louis, Missouri, pp. 131-143.

Bhushan, K., Haley, S. C., and Fong, P. T., (1979). "Lateral load tests on drilled piers in stiff clays. Journal of the Geotechnical Engineering Division, ASCE, Vol. 105, No. GT8, Proc. Paper 14789, pp. 969-985.

Budhu, M., and Davies, T. G. (1987). Nonlinear analysis of laterally loaded piles in cohesionless soils. Canadian Geotechnical Journal, Vol. 24, No. 4, pp. 289-296.

DNV-OS-J101, Offshore Standard, (2011). Design of offshore wind turbine structures, Electronic Version available at http://www.dnv.com/ (On Jan. 25, 2013).

El-Marassi, M., Newson, T., El Naggar, M.H. and Stone, K. (2008). Numerical modelling of the performance of a hybrid monopiled-footing foundation. Proceedings of 61st Canadian Geotechnical Conference, Edmonton, pp. 97-104.

Hellmigk, K., (2012). Development of a 1g model pile test facility for offshore wind turbines. Master thesis, University of Rhode Island.

Kelly, R. B., Houlsby, G. T. & Byrne, B. W. (2006). A comparison of field and laboratory tests of caisson foundations in sand and clay. Geotechnique, Vol. 56, No. 9, pp. 617–626.

LeBlanc, C., Byrne, B. W. & Houlsby, G. T. (2010). Response of stiff piles to random two-way lateral loading. Geotechnique, *Vol.* 60, No. 9, pp. 715–721.

Reese, L.C. and Welch, R.C. (1975).Lateral loading of deep foundations in stiff clay, Journal of Geotechnical Engineering, ASCE, Vol. 101, No. 7, pp. 633-649.

Lee, J et al (2012). A cyclic lateral system for measuring lateral behaviour for offshore wind energy foundations. European Wind Energy Conference, Copenhagen, Denmark. Volume 3.

Lin, S. S. & Liao, J. C. (1999). Permanent strains of piles in sand due to cyclic lateral loads. Journal of Geotechnical and Geoenvironmental Engineering, Vol. 125, No. 9, pp. 798–802.

Long, J. and Vanneste, G. (1994). Effects of cyclic lateral loads on piles in sand. Journal of Geotechnical Engineering, ASCE, Vol. 120, No. 1, 225–244.

Maheshwari, B.K., Truman, K.Z., El Naggar, M.H. and Gould, P.L. 2004. 3D nonlinear analysis for seismic soil-pile-structure interaction. Soil Dynamics and Earthquake Engineering, Vol. 24, No. 4, pp. 343-356.

Soliman, A., and Nehdi, M. (2010). Effect of drying conditions on autogenous shrinkage in ulta-high performance concrete at early-age. Material and Structures, Vol. 44, pp. 879-899.

Reese, L. and Matlock, H. (1956). Nondimensional solutions for laterally loaded piles with soil modulus assumed proportional to depth. Proceedings of 8th Conference on Soil Mechanics and Foundation Engineering, Austin, TX.

Reese, L. C., Cox, W. R., and Koop, F. D., (1974). Analysis of laterally loaded piles in sand. Proceedings of 6th Annual Offshore Technology Conference, Houston, Texas, Vol. 2, Paper No. OTC 2080, pp.473-483.

Robertson, P. K., Davies, M. P., and Campanella, R. G., (1989). Design of laterally loaded driven piles using the flat dilatometer. ASTM Geotechnical Testing Journal, Vol. 12, No. 1, pp. 30-38.

McClelland, B. and Focht, J. (1958). Soil modulus for laterally loaded piles. Transaction of soil Mechanics, ASCE, Vol. 84, pp. 1049–1086.

Poulos, H. and Hull, T. (1989). The role of analytical geomechanics n foundation engineering. In Foundation engineering: Current principles and practices, ASCE, Reston, VA, Vol. 2, pp. 1578–1606.

Wroth, C. P., Randolph, M. F., Houlsby, G. T. and Fahey, M. (1979). A review of the engineering properties of soils with particular reference to the shear modulus, University of Cambridge, Report CUED/D-SOILS TR75.

CHAPTER SEVEN

CONCLUSIONS AND RECOMMENDATIONS

7.1 Introduction

In this thesis, numerical and experimental investigations have been carried out to evaluate the capacity and performance of an innovative foundation system for offshore wind turbines, namely the hybrid foundation system. The hybrid system is composed of a steel pile and a concrete plate to increase its stiffness and capacity. The proposed system is capable of satisfying the serviceability and capacity requirements with economically viable cost.

Wind tunnel test were conducted on a scaled down model based on a 5 MW NREL (National Renewable Engineering Laboratory) at the Boundary Layer Wind Tunnel Laboratory at Western University, Canada. A 1:150 model was tested under different blade positions and wind angles of attack. Six components of load were measured at the base of the wind turbine model and their values were calculated by using force balance technique. The loading results were compared with limited NREL loading results, which were achieved by performing analysis using the FAST (Fatigue, Aerodynamics, Structures, and Turbulence) program.

A series of three-dimensional finite element analysis was carried out employing the finite element analysis programme, ABAQUS, considering different foundation systems including: monopile with diameter of 4m, monopile with diameter of 6 m, hybrid foundation system with and without ribs with different plate diameter. All foundation systems were analyzed considering piles with

varying length from 16 to and 36 m. The displacement of the different foundation systems at main sea level and at mud level as well as their rotations were calculated under different load combinations. The axial and horizontal capacities of each system were also evaluated to investigate the increase in each system capacity compared to the monopole and asses its relative advantage.

Furthermore, monotonic and cyclic load tests were conducted on scaled down foundation models under 1g. Both static and up to 12000 load cycles were applied to the foundation models in order to investigate the long term effects of the loading on both rotation and stiffness of the system. An equation was proposed to account for the plate effect on the hybrid system stiffness.

The measurable objectives associated with the investigation program were as follows:

- Prove the system concept and its ability to function as an effective foundation system for wind turbines.
- Provide guidelines for wind loads acting on the foundations of wind turbines.
- Evaluate the proposed hybrid system performance under different load combinations.
- Develop design guidelines for the axial capacity of hybrid system and for evaluating its lateral stiffness.

7.2 Main findings

This study confirmed that the hybrid foundation system is suitable for supporting offshore wind turbines and it can help in reduction the high cost of wind turbine foundations. The following represents the main conclusions drawn from the study.

7.2.1 Main finding chapter 3: FOUNDATION DESIGN LOADS FOR 5 MW NREL OFFSHORE WIND TURBINE

- The overall base loads were obtained experimentally using the force balance technique and a rigid model of the turbine-tower structure.
- Reference load based on 5 MW NREL wind tunnel are now available to be used in any future analysis.

7.2.2 Main finding chapter 4: PERFORMANCE OF HYBRID FOUNDATION SYSTEM FOR OFFSHORE WIND TURBINES

- By adding the precast concrete plate, the lateral resistance of the monopile with D_p=4m increased sufficiently to provide comparable performance of monopole with D_p = 6m.
- The hybrid system was shown to meet the response requirements of the offshore wind turbine foundations according to DNV-OS-J101 (2011).
- The analysis for different load combinations demonstrated that the conventional approach, which considers only two components (horizontal load and rocking moment) can grossly underestimate the response of the wind turbine system.

7.2.3 Main finding chapter 5: CAPACITY OF HYBRID FOUNDATION SYSTEM FOR WIND TURBINES

- The hybrid system provides a significant increase over that of the 4 m-diameter monopole (up to 550 % of its capacity).
- The lateral capacity of the HSNR D_{plate} =16m is 180% of the capacity of monopole with D_p = 4 m, and is only 10% less than the capacity of the monopile with D_p = 6 m. As the

hybrid system satisfies the requirements of the DNV-OS-J101 (2011), it can be used to support the 5 MW NREL wind turbine instead of the larger monopile with 6m diameter, which can result in significant savings.

7.2.4 Main findings Chapter 6: EFFET OF LONG TERM CYCLIC LOADING ON STIFFNESS AND CAPACITY OF HYBRID FOUNDATION

- An equation was provided to scale down the hybrid system under 1g accounting for the effect of the plate.

- Long term cyclic loading effect on system stiffness and rotation was evaluated and was demonstrated that the hybrid foundation system provided superior performance to the conventional monopile.

7.3 Recommendations for future research

This study investigates a hybrid system that can meet the requirements for offshore wind turbine foundations with lower cost. It can also be used to upgrade the stiffness and capacity of existing system. To further evaluate the system and provide guidance for its application in wind turbine foundation design, the following is recommended:

- In the current study, the wind turbine model used in the wind tunnel test was assumed to be fully fixed and the forces were calculated accordingly. This leads to a conservative estimate of the foundation loads. Future back analysis should be conducted accounting for effect of system flexibility.

- The soil considered in the analysis and the experimental program was sand. Future investigations should consider performance of hybrid systems installed in clay to provide wider understanding of the system behaviour.

- A wider range of plate dimensions relative to pile length should be considered in future research.

- The loading time history established from the wind tunnel tests should be used in the laboratory scaled down testing to evaluate the effect of the load variation in comparison with cyclic loading with constant amplitude.

Ahmed Abdelkader, PhD candidate, Msc

RELEVANT EXPERIENCE

University of Western Ontario-London, ON 2010-Present

Research and Teaching Assistant

- Executed research projects related to foundations of wind turbine.
- wind tunnel test for a scaled down model of 5 MW NREL wind turbine at Boundary Layer Wind Tunnel.
- Lab test of scaled down model under 1 g.
- Tutored 3 undergrad level courses in CEE.
- Attended certified courses in "Teaching in the Canadian class rooms), (The Language of Advanced Discussions) and (Communications in Canadian Classrooms) at Western Teaching support center.

Port-Said University-Port Said, Egypt 2006-2010

Research and Teaching Assistant

- Worked as Assistant Lecturer at Civil Engineering Department, Port Said University for 6 undergrad courses.

El Araby Consultant Office-Port Said, Egypt 2006-2009

Design Engineer-Part Time

- Designed concrete structures and foundations.

OTHER WORK EXPERIENCE

Educational Program Innovations Center (EPIC)-Mississauga, ON 2014 - Present

Instructor

- Instructor for online-course, (Environmental and Geotechnical Engineering)

EDUCATIONAL

University of Western Ontario-London, ON 2010-Present

Doctor of Philosophy Candidate, Civil and Environmental Engineering Department

- PhD. Thesis udder title of (Investigation of Hybrid Offshore Wind Turbine Foundation system).

Port-Said University-Port Said, Egypt 2006-2009

Master of Applied Science, Civil Engineering Department.

- MASc Thesis: Optimization of Reinforced Concrete Piled Raft.

Port-Said University-Port Said, Egypt 2000-2005

Bachelor of Applied Science

- Accumulated grade: 86.7 % (Excellent with Degree of Honour)

AWARDS

- Full scholarship from Egyptian Government for PhD